USGS
science for a changing world

National Water-Quality Program

Spatially Referenced Models of Streamflow and Nitrogen, Phosphorus, and Suspended-Sediment Loads in Streams in the Southeastern United States

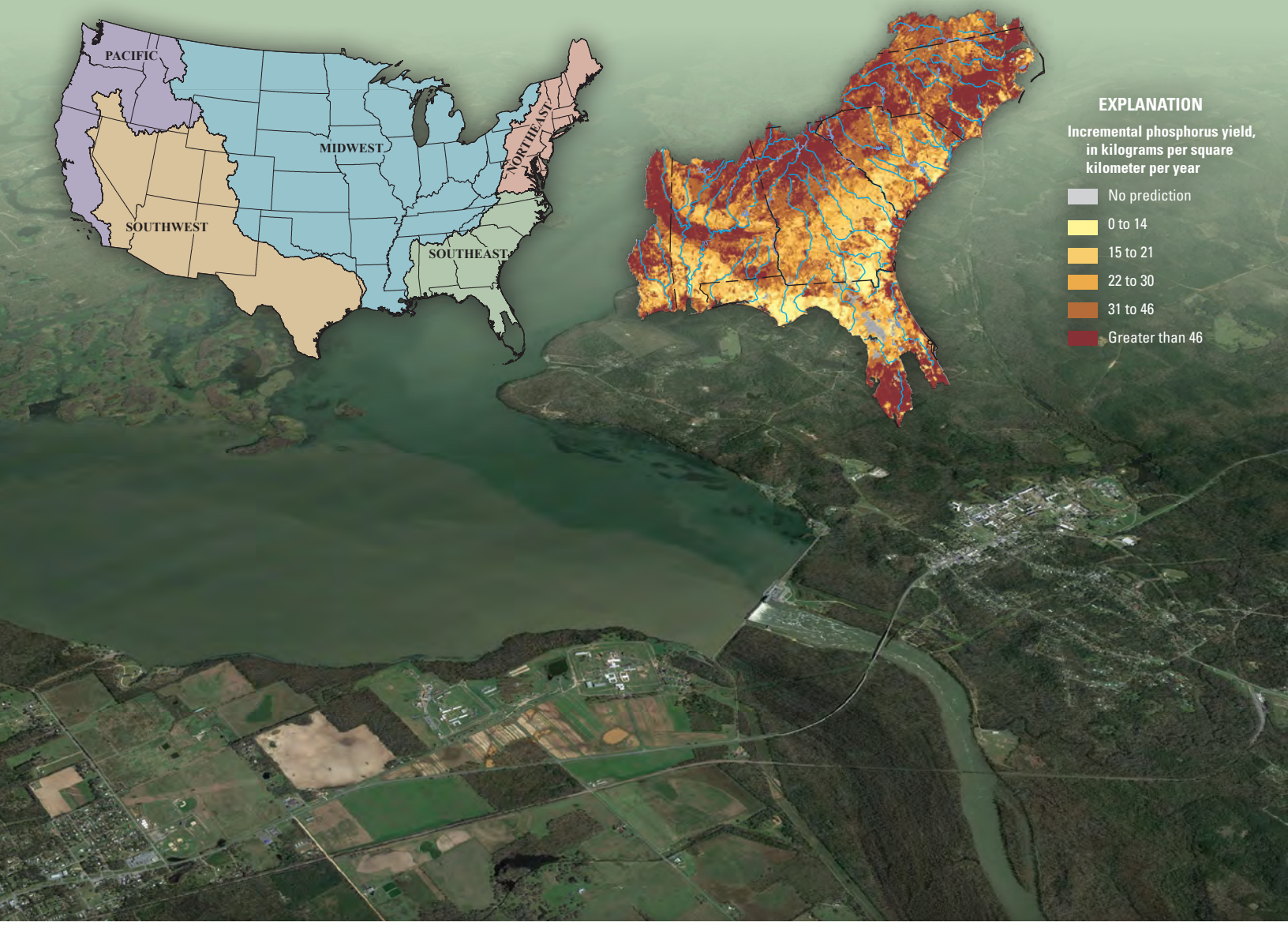

Scientific Investigations Report 2019–5135

U.S. Department of the Interior
U.S. Geological Survey

Cover: Upper left: SPAtially Referenced Regression On Watershed attributes (SPARROW) modeling regions of the conterminous United States. Upper right: SPARROW simulated total phosphorus incremental yield, in kilograms per square kilometer per year. Lower center: Lake Seminole and the Apalachicola River near Chattahoochee, Florida. Credit: Satellite image courtesy of Google Earth.

Back cover: Major streams of the United States in the Southeast modeling region. Credit: U.S. Geological Survey digital data, 2006–14.

Spatially Referenced Models of Streamflow and Nitrogen, Phosphorus, and Suspended-Sediment Loads in Streams in the Southeastern United States

By Anne B. Hoos and Victor L. Roland II

National Water-Quality Program

Scientific Investigations Report 2019–5135

U.S. Department of the Interior
U.S. Geological Survey

U.S. Department of the Interior
DAVID BERNHARDT, Secretary

U.S. Geological Survey
James F. Reilly II, Director

U.S. Geological Survey, Reston, Virginia: 2019

Suggested citation:
Hoos, A.B., and Roland, V.L. II, 2019, Spatially referenced models of streamflow and nitrogen, phosphorus, and suspended-sediment loads in the Southeastern United States: U.S. Geological Survey Scientific Investigations Report 2019–5135, 87 p., https://doi.org/10.3133/sir20195135.

Associated data for this publication:
Roland, V.L. II, and Hoos, A.B., 2019, SPARROW model inputs and simulated streamflow, nutrient and suspended-sediment loads in streams of the Southeastern United States, 2012 base year: U.S. Geological Survey data release, https://doi.org/10.5066/P9A682GW.

ISSN 2328-0328 (online)

Foreword

Sustaining the quality of the Nation's water resources and the health of our diverse ecosystems depends on the availability of sound water-resources data and information to develop effective, science-based policies. Effective management of water resources also brings more certainty and efficiency to important economic sectors. Taken together, these actions lead to immediate and long-term economic, social, and environmental benefits that make a difference to the lives of the almost 400 million people projected to live in the United States by 2050.

In 1991, Congress established the National Water-Quality Assessment (NAWQA) to address where, when, why, and how the Nation's water quality has changed, or is likely to change in the future, in response to human activities and natural factors. Since then, NAWQA has been a leading source of scientific data and knowledge used by national, regional, state, and local agencies to develop science-based policies and management strategies to improve and protect water resources used for drinking water, recreation, irrigation, energy development, and ecosystem needs (https://water.usgs.gov/nawqa/applications/). Plans for the third decade of NAWQA (2013–21) address priority water-quality issues and science needs identified by NAWQA stakeholders, such as the Advisory Committee on Water Information and the National Research Council and are designed to meet increasing challenges related to population growth, increasing needs for clean water, and changing land-use and weather patterns.

Federal, State, and local agencies have invested billions of dollars to reduce the amount of pollution entering rivers and streams that millions of Americans rely on for a variety of water needs and biota rely on for habitat. Understanding the sources and transport of pollution is crucial for designing strategies to improve water quality. The U.S. Geological Survey's (USGS) SPAtially Referenced Regression On Watershed attributes (SPARROW) model was developed to aid in the understanding of sources and transport of pollution across large spatial scales. The SPARROW model is calibrated by statistically relating watershed sources and transport-related properties to monitoring-based water-quality load estimates. This report describes the methods and results of SPARROW models developed to estimate streamflow, and total nitrogen, total phosphorus and suspended-sediment transport in streams of the southeastern United States. The model results are expected to provide useful information for understanding the hydrology and water quality of streams in the southeast. They are also expected to provide useful information for understanding anthropogenic influences on surface-water resources and for managing those resources to ensure adequate water supply for human needs and to ensure ecological integrity for fish and other aquatic life.

We hope this publication will provide you with insights and information to meet your water-resource needs and will foster increased citizen awareness and involvement in the protection and restoration of our Nation's waters. The information in this report is intended primarily for those interested or involved in resource management and protection, conservation, regulation, and policymaking at the regional and national levels.

Dr. Donald W. Cline
Associate Director for Water
U.S. Geological Survey

Acknowledgments

The authors acknowledge the many Federal, State, regional, local, and private sampling agencies and organizations that contributed water-quality data used to estimate stream loads. Several individuals made special efforts to provide geospatial data for this analysis: Steven Perakis of the U.S. Geological Survey Forest and Rangeland Ecosystem Science Center, Jesse Bash of the U.S. Environmental Protection Agency Atmospheric Modeling and Analysis Division, and Andy Woeber of the Florida Department of Environmental Protection. The work of Craig Johnston, a dedicated geographer who made many contributions to the hydrography dataset used in this report through his skill in digital stream network analysis, is gratefully acknowledged. This work also benefited from review comments and suggestions from Dale Robertson and Olivia Miller, U.S. Geological Survey.

Contents

Figures

Tables

Conversion Factors

International System of Units to U.S. customary units

Multiply	By	To obtain
	Length	
millimeter (mm)	0.03937	inch (in.)
meter (m)	3.281	foot (ft)
kilometer (km)	0.6214	mile (mi)
	Area	
square meter (m^2)	0.0002471	acre
square kilometer (km^2)	247.1	Acre
square kilometer (km^2)	0.3861	square mile (mi^2)
	Flow rate	
meter per second (m/s)	3.281	foot per second (ft/s)
meter per day (m/d)	3.281	foot per day (ft/d)
meter per year (m/yr)	3.281	foot per year ft/yr)
cubic meter per second (m^3/s)	35.31	cubic foot per second (ft^3/s)
millimeter per year (mm/yr)	0.03937	inch per year (in/yr)
	Mass	
kilogram (kg)	2.205	pound avoirdupois (lb)
metric ton (t)	0.9842	ton, long [2,240 lb]
	Density	
kilogram per cubic meter (kg/m^3)	0.06242	pound per cubic foot (lb/ft^3)
	Application rate	
kilogram per square kilometer per year ([kg/km^2]/yr)	0.008921	pound per acre per year ([lb/acre]/yr)

Temperature in degrees Celsius (°C) may be converted to degrees Fahrenheit (°F) as follows:

$$F = (1.8 \times °C) + 32.$$

Abbreviations

5pK	Five-parameter regression with Kalman smoothing
AET	actual evapotanspiration
BRE	Beale ratio-estimator
CI90	90-percent confidence interval
CMAQ	Community Multiscale Air Quality
d/m	days per meter
DEM	digital elevation model
df	degrees of freedom
e2NHDPlusv2_us	Revised National Hydrography dataset plus version 2 for the United States
EPA	U.S. Environmental Protection Agency
ET	evapotranspiration
HUC	Hydrologic Unit Code

Joules/s	Joules per second
$kg*m^2/s^3$	kilograms square meter per cubic second
kg/yr	kilograms per year
lnRMSE	natural log Root Mean Square Error
m*d	product of meters and days
m/s^2	meters per square second
MAFlowUcfs	Mean annual streamflow, in cubic feet per second
mg/L	milligrams per liter
Mgal/d	million gallons per day
t	metric tons
t/km^2	metric tons per square kilometer
$t/km^2/yr$	metric tons per square kilometer per year
N	nitrogen
NAWQA	National Water Quality Assessment Project
NHDPlusv1	National Hydrography Dataset Plus Version 1
NHDPlusv2	National Hydrography Dataset Plus Version 2
NID	National Inventory of Dams
NLCD	National Land Cover Database
NLLS	Nonlinear least-squares
NPDES	National Pollution Discharge Elimination System
NWIS	National Water Information System
P	phosphorus
pctRMSE	percent error
PET	mean annual potential evapotranspiration
PPT	precipitation
PPT–AET	difference of precipitation and actual evapotranspiration
PredQ_SESpar	SPARROW predicted streamflow in each reach (including upstream contributions)
Q	streamflow in cubic feet per second
QReach	mean annual streamflow through a stream reach or lake/reservoir reach
QWithdr_	mean annual amount of water withdrawn from a stream reach or lake/reservoir reach for consumptive use at power plants, groundwater withdrawal, or surface-water withdrawal
R^2	coefficient of determinantion
RMSE	Root Mean Squared Error
S	channel slope
SPARROW	SPAtially Referenced Regression On Watershed attributes
SS	suspended sediment
SSC	suspended-sediment concentration
StrmPwrChange_frac	Stream power change across a stream reach, expressed as fraction of stream power at the end (upstream or downstream) with highest stream power
tinv()	returns 0.95th quantile from Student's *t* distribution with *n* degrees freedom
TN	total nitrogen
TP	total phosphorus
TPC	Typical Pollutant Concentration

TSS	total suspended solids
U.S.	United States
USGS	U.S. Geologcial Survey
WSA	Waterbody Surface Area
WWTP	Wastewater Treatment Plant
yr/m	years per meter
α	Source coefficient

Spatially Referenced Models of Streamflow and Nitrogen, Phosphorus, and Suspended-Sediment Loads in Streams in the Southeastern United States

By Anne B. Hoos and Victor L. Roland II

Abstract

Spatially Referenced Regression On Watershed attributes (SPARROW) models were applied to describe and estimate mean-annual streamflow and transport of total nitrogen (TN), total phosphorus (TP), and suspended-sediment (SS) in streams and delivered to coastal waters of the southeastern United States on the basis of inputs and management practices centered near 2012, the base year of the model. Previously published TN and TP models for 2002 served as a starting point and reference for comparison. The datasets developed for the 2012 models not only represent updates of previous conditions but also incorporate new approaches for characterizing sources and transport processes that were not available for previous models.

Variability in streamflow across the southeastern United States was explained as a function of precipitation adjusted for evapotranspiration, spring discharge, and municipal and domestic wastewater discharges to streams. Results from the streamflow model were used as input to the water-quality SPARROW models, and areas with large streamflow prediction errors—urban areas and karst areas—were used to provide guidance on where additional data are needed to improve routing of flow.

Variability in TN transport in Southeast streams was explained by the following five sources in order of decreasing mass contribution to streams: atmospheric deposition, agricultural fertilizer, municipal wastewater, manure from livestock, and urban land. Variable rates of TN delivery from source to stream were attributed to variation among catchments in climate, soil texture, and vegetative cover, including the extent of cover crops in the watershed. Variability in TP transport in Southeast streams was explained by the following six sources in order of decreasing mass contribution to streams: parent-rock minerals, urban land, manure from livestock, municipal wastewater, agricultural fertilizer, and phosphate mining. Varying rates of TP delivery were attributed to variation in climate, soil erodibility, depth to water table, and the extent of conservation tillage practices in the watershed.

Variability in SS transport in Southeast streams was explained by variable sediment export rates for different combinations of land cover and geologic setting (for upland sources of sediment) and by gains in stream power caused by longitudinal changes in channel hydraulics (for channel sources of sediment). Sediment yields for the transitional land cover (shrub, scrub, herbaceous, and barren) varied widely depending on geologic setting and on agricultural land cover. Varying rates of SS delivery, like those for TP, were attributed to variation in climate, soil erodibility, and the extent of conservation tillage practices in the watershed, as well as to areal extent of canopy land cover in the 100-meter buffer along the channel. Relatively large uncertainty, compared to the other three models, for almost all the SS source coefficients indicates the need for caution when interpreting the results from the sediment model.

TN, TP, and SS inputs to streams from sources were balanced in the models with losses from physical processes in streams and reservoirs and with water withdrawals. The losses in streams and reservoirs along with withdrawals removed 35, 44, and 65 percent of the TN, TP, and SS load, respectively, that entered streams before reaching coastal waters.

Introduction

Mobilization of nutrients and sediment to surface waters as a result of human activities has impaired water quality and beneficial uses of many streams, lakes, and estuaries throughout the United States (U.S.). Nutrients were identified as the primary cause of impairment for 17 percent of impaired streams and 36 percent of impaired lakes in the U.S., and sediment was identified as the primary cause of impairment for 11 percent of impaired streams and 7 percent of impaired lakes during the period from 2002 to 2012 (U.S. Environmental Protection Agency, 2016). In the southeastern U.S., nutrients were identified as the primary cause of impairment for 22 and 67 percent of impaired streams and lakes, respectively, and sediment was identified as the primary cause of impairment for 6 and 3 percent of impaired streams and lakes, respectively (from data provided by U.S. Environmental Protection Agency, 2016).

Regulatory and management actions to reduce nutrient and sediment loading to receiving waterbodies are costly to implement. The multiple sources of nutrients and sediment pose a challenge in identifying and accounting for the dominant sources within a watershed. Because nutrients are reactive and transform during transit, the location of a nutrient source on the landscape influences its effect on the delivery to a downstream receiving waterbody.

Watershed models provide a framework for improved understanding of nutrient and sediment sources and how they move through the landscape and stream network and for designing and targeting water-quality management programs. The watershed model SPAtially Referenced Regression On Watershed attributes (SPARROW; Schwarz and others, 2006; Preston and others, 2009) is a hybrid statistical and process-based mass-balance model that typically uses nonlinear least-squares (NLLS) regression to relate observations of stream load of a constituent to predictor variables such as constituent sources and watershed or channel features that affect the rate of constituent delivery to receiving waters. SPARROW models describing stream transport of total nitrogen (TN) and total phosphorus (TP) were developed previously for large regions of the conterminous U.S. (Smith and others, 1997; Preston and others, 2011) as part of the U.S. Geological Survey (USGS) National Water Quality Assessment (NAWQA) Project. Previously published SPARROW models for the southeastern U.S. described TN and TP transport for 2002 and were based on a 1:500,000-scale stream network dataset (Hoos and McMahon, 2009; Garcia and others, 2011) as well as on a finer, 1:100,000-scale stream network (Hoos and others, 2013). A SPARROW model describing suspended-sediment (SS) transport for 1992 was developed for the conterminous U.S. (Schwarz, 2008) and based on the 1:500,000 stream network.

To build on the SPARROW modeling work done previously for the southeastern U.S., the USGS developed new models with substantial improvements over the previous models. The new models are based on inputs and management practices centered near 2012, the base year of the model, and on hydrologic data collected from 2000 to 2014. The predictions from these models represent loads and yields that would have been observed from 2000 to 2014 given the hydrologic conditions throughout that period and given inputs and management practices that were similar to those occurring in 2012. The set of water-quality constituents for which regional models were developed was expanded from TN and TP to also include streamflow and SS. These additional constituents not only are of value in themselves but also are related to nutrient loads; therefore, they provide a broader basis of information for understanding the factors that affect nutrient loads and concentrations in waterbodies.

Some of the gaps or limitations in the model input data that were identified during or following the development of the 2002 TN and TP models can now be addressed. A few of the major improvements include datasets describing the effects of agricultural best-management practices on TN, TP, and SS transport; improved estimates of wastewater-effluent quality and location of small wastewater dischargers; reduced bias in estimates of stream TN and TP loads used to calibrate the model; and evaluation of datasets representing TN contribution from sources not included in previous models, such as springs, forested areas, and septic systems. Limitations noted by Schwarz (2008) for the previous sediment SPARROW model that are addressed in the new SS SPARROW model include inadequate representation by the coarse 1:500,000-scale stream network of headwater streams, which are typically considered to be the most important channel sources of sediment (Bull, 1979), and the need to characterize sediment-trapping properties of streams and their associated floodplains.

Mean-annual streamflow has not been a subject for regional SPARROW modeling prior to this study. The clusters of larger than average prediction errors from the 2002 TN and TP models in urban areas and in parts of central Florida indicate that improved accounting of hydrologic modifications (water additions to or withdrawals from streams) and discharges from regional groundwater to streams may improve modeling of TN and TP transport. In this study, we evaluate whether inclusion of withdrawals and additions as input terms in the calibration of a streamflow SPARROW model helps to adjust flow routing to more closely predict actual conditions, and whether these routing adjustments in turn can be used in the TN, TP, and SS models to improve routing of constituent flux.

This report documents SPARROW models developed to predict mean-annual streamflow and transport of TN, TP, and SS in streams of the southeastern U.S. The Southeast area is one of five regions for which models were developed as part of a national modeling effort by the USGS (fig. 1). The other four areas are the Northeast, Midwest, Southwest, and Pacific regions of the U.S. All of the new models are based on 1:100,000-scale hydrography and on inputs and management practices centered near 2012. The TN and TP models differ from the previously published 2002 models in substantive ways, including but not limited to (1) improved model calibration methods, (2) changes in load estimation methods to address accuracy issues, and (3) introduction of new model terms that were not considered for the 2002 model. The report describes, for each of the four SPARROW models, the sources and methods used for all model inputs, model calibration results, and summaries of model predictions.

Study Area Description

The area of the southeastern U.S., hereafter referred to as the "Southeast," includes the drainages to the South Atlantic coast of the U.S. and to the eastern half of the Gulf of Mexico coast of the U.S. (fig. 2*A*). This area includes all tributaries draining to the U.S. coast between and including the Chowan-Roanoke River Basin in Virginia and North Carolina and the Pascagoula River Basin in Mississippi, excluding

Figure 1. Spatial extent of the Southeast SPARROW (SPAtially Referenced Regression On Watershed attributes) model region.

drainages in South Florida. The area covers 628,000 square kilometers (km^2) and includes all or parts of eight states.

For streams affected by substantial diversions of water and constituent mass between surface-water basins, streamflow and transport of TN, TP, and SS may not reflect source and transport conditions in the topographic watershed. Inclusion of such streams in a SPARROW modeling approach without sufficient data to describe the flux across watershed divides may be inappropriate. For this reason, stream basins in South Florida and the Withlacoochee River downstream from the Tsala Apopka chain of lakes in central Florida (fig. 2*A*) were excluded from the Southeast SPARROW models.

Land cover affects the sources and transport of TN, TP, and SS to streams. Forested land covers 39 percent of the Southeast model area, whereas agricultural land, urban (developed) land, water and wetlands, and other land (shrub, scrub, herbaceous, and barren) represent 17, 10, 20, and 14 percent, respectively (fig. 3). Row-crop agriculture is most intense in the Coastal Plain (boundary shown in fig. 2*B*) of eastern North Carolina, South Carolina, southern and southeastern Georgia, and in northeastern Mississippi; pasture and hay agricultural land is distributed throughout the area.

The primary source of water for streamflow, and an important factor for transport of TN, TP, and SS to streams, is the volume of water from precipitation that is available for direct runoff from a catchment to the adjacent stream or for infiltration to the subsurface. This term is calculated from climatic data as the difference between precipitation (PPT) and actual evapotranspiration (AET), hereafter referred to as "PPT–AET." PPT–AET is generally highest (greater than 400 millimeters [mm]) in the western part of the model domain and in the southern Appalachian Mountains, and lowest (less than 250 mm) in central South Carolina, southeastern Georgia, and central Florida (fig. 4).

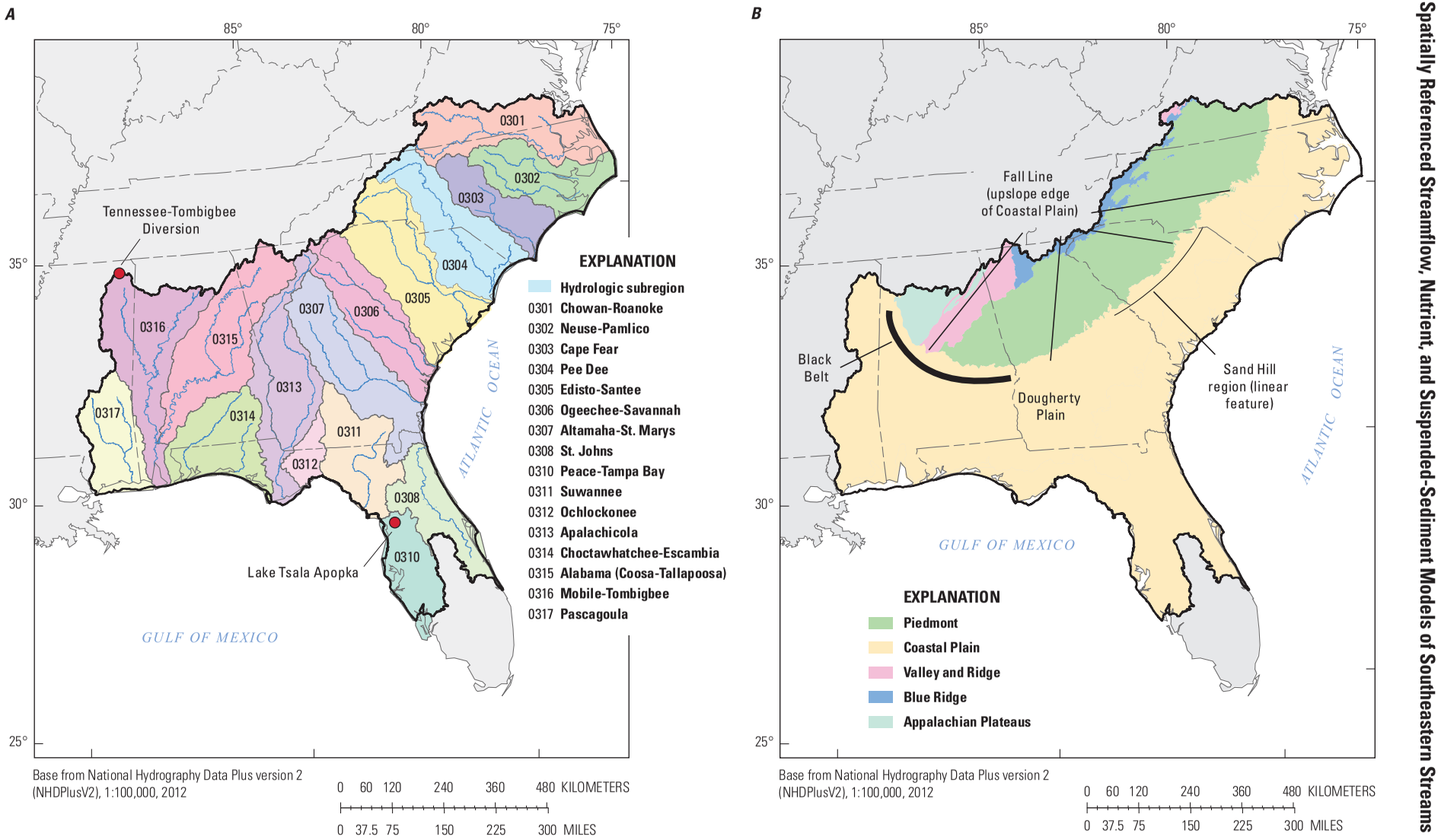

Figure 2. *A.* Hydrologic units and *B.* physiographic provinces in the Southeast region of the United States.

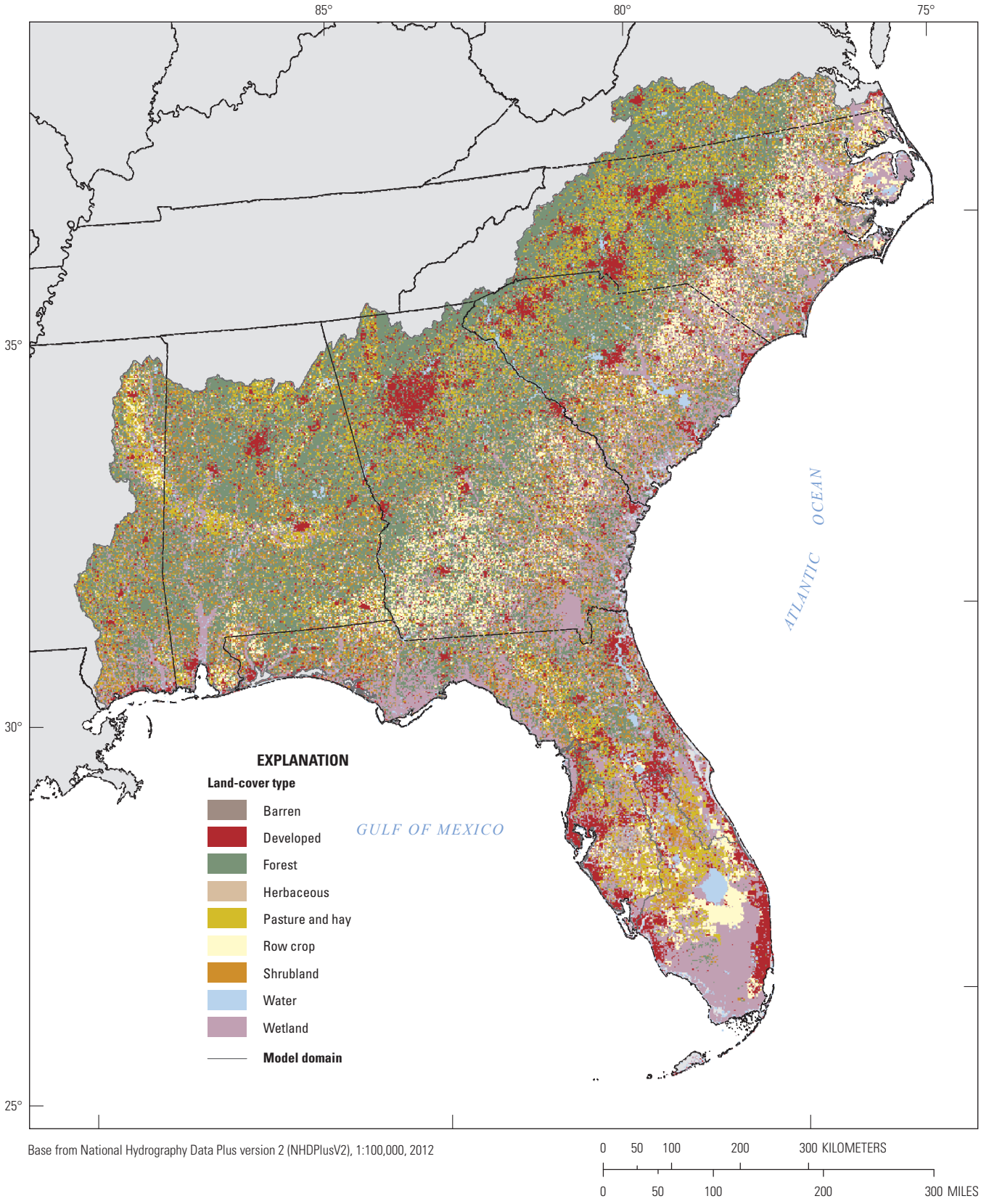

Figure 3. Land cover in the Southeast region of the United States, 2011 (Homer and others, 2015; Wieczorek and others, 2019).

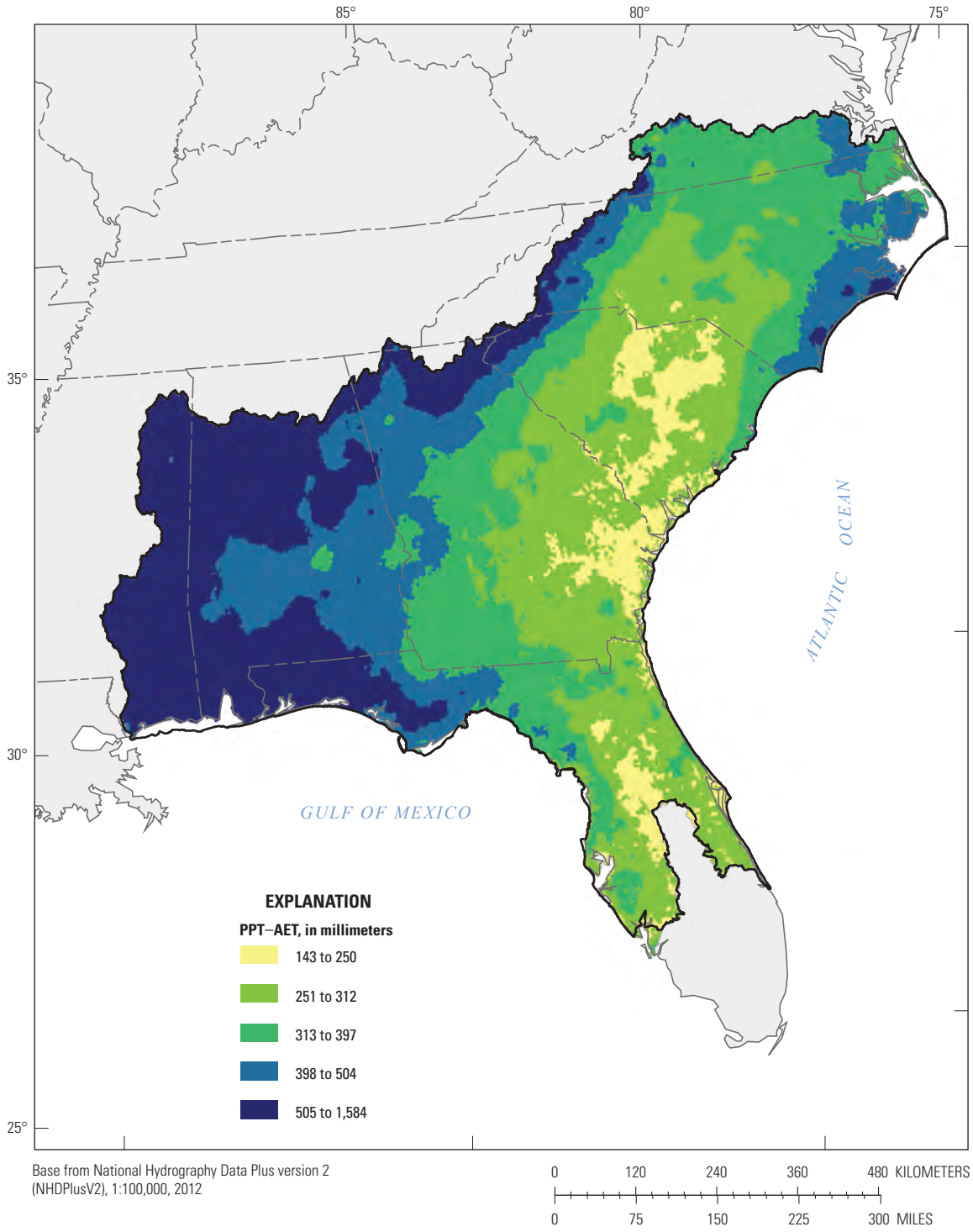

Figure 4. Mean-annual precipitation minus actual evapotranspiration (PPT–AET) in the Southeast region, 2000–14 (Wolock and McCabe, 2018; Wieczorek and others, 2019).

Methods

The SPARROW Modeling Approach

The SPARROW model is a hybrid statistical and mechanistic model typically used to estimate the movement of mass through the landscape under long-term, steady-state conditions (Schwarz and others, 2006). The model infrastructure consists of a detailed digital representation of a stream-reach network and digital elevation model (DEM)-delineated areas (referred to as "catchments") associated with the stream-reach segments (see Glossary for more information on the terms "reach" and "catchment"). The model uses data describing catchment attributes—for example, sources of constituent mass, landscape characteristics, and stream- and waterbody properties—to explain the spatial variation in monitored mean-annual flux throughout the model domain. In the SPARROW models described in this report, the term "mean-annual flux" refers to either streamflow (in cubic feet per second) or TN, TP, or SS loads (in kilograms or metric tons per year). The monitored mean-annual streamflow or load is the dependent variable (the calibration dataset) in the model and the watershed attributes are the explanatory variables. SPARROW can simulate the net effect of landscape properties (such as land cover, climate, soil properties, geology, and hydrology) on the delivery of water, sediment, and nutrients from land to streams, as well as the processes that lead to permanent loss within free-flowing streams and within lakes and reservoirs. A calibrated SPARROW model can be used to estimate streamflow and water-quality conditions throughout a stream network, including areas where no monitoring data are available.

Concepts and Procedures for Model Calibration

The SPARROW NLLS regression calibration technique uses an iterative process to estimate coefficients for the user-specified set of explanatory variables and evaluate the statistical significance of those variables. Beginning in the headwater reaches, SPARROW uses initial values of model coefficients to estimate the streamflow or constituent load generated within the incremental catchment for each stream reach and the permanent loss in free-flowing streams and impoundments (lakes or reservoirs). The mathematical equation providing the framework for the SPARROW model is described briefly in appendix 1. The simulated incremental streamflows or constituent loads are accumulated moving downstream through the surface-water drainage network until a calibration station is reached, at which point the accumulated streamflow or constituent load is adjusted to match the monitored values at the calibration station. The accumulation process then continues downstream after the calibration-station adjustment and continues until a terminal reach (such as an estuary or internal drainage) is encountered. The calibration procedure then adjusts the coefficients in the model on the basis of the differences between the estimated and monitored streamflow or constituent load at the model-calibration stations, reestimates the accumulated streamflow or constituent load by using the revised coefficients, and repeats the entire calibration process several times until the differences between the estimated and monitored values are minimized. A calibrated SPARROW model can estimate streamflow or constituent load and associated uncertainty throughout the stream network, including areas where no water-quality data exist.

The watershed attributes evaluated in a SPARROW model represent processes that are expected to add water, nutrients, or sediment to the watershed (sources) or enhance or mitigate their delivery from the watershed to the stream (land-to-water delivery terms). In this context, the terms "enhancing" or "mitigating" respectively refer to increasing or decreasing delivery to the stream relative to the average delivery rate for the model area. Stream-channel characteristics and lake or reservoir characteristics expected to cause permanent reductions in constituent load are also evaluated in the calibration process (aquatic-loss terms). The final set of explanatory variables for each model includes statistically significant or otherwise important attributes. The significance of the coefficients for the source terms and aquatic-loss terms in the models was determined by using a one-sided *t*-test and a significance level of 0.10 (the one-sided *t*-test was appropriate because the coefficients for the source terms and aquatic-loss terms can reasonably only be positive). In contrast, the significance of the coefficients for the land-to-water delivery terms was determined by using a two-sided *t*-test and a significance level of 0.05 (coefficients for land-to-water delivery terms can be positive or negative).

Final model specifications are typically selected by comparing coefficient of determination (R^2) of yield values and root mean squared error (RMSE) values between successive runs and selecting the model with lowest RMSE, statistically significant and physically interpretable coefficient values, and minimal spatial structure of residuals. Spatial structure of residuals for calibration stations within the same large watershed or ecoregion is examined qualitatively through visual inspection of maps of residual values and is quantified by using the Moran's *I* statistic (Cliff and Ord, 1973).

Uncertainty in the NLLS regression-estimated model coefficients is assessed at 90-percent confidence intervals (CI_{90}); these are computed as:

$$CI_{90} = \text{NLLS-estimated value} +/- \text{NLLS-estimated standard deviation} * \text{tinv}(0.95,\text{df}) \quad (1)$$

where

df is degrees of freedom of the NLLS regression, andtinv

tinv() is returns the 0.95th quantile from the Student's t distribution with degrees of freedom df—that is, the quantile for which the probability is 0.95 that an observation from a t distribution is less than or equal to that quantile.

Uncertainty in the predicted flux for each stream reach was evaluated by using a parametric bootstrap method (Schwarz and others, 2006) that generates successive iterations of coefficients based on the assumption that the coefficients are normally distributed with mean and covariance matrix given by the parametric model results. A mean value (the parametric bootstrap estimate) and standard error were then estimated for each flux estimate.

Guidelines for Interpreting Model-Estimated Values of Coefficients

The coefficients estimated by using the SPARROW model provide insight into the important properties and processes that control water, nutrient, and sediment movement through a watershed. Statistical significance of the coefficient for a predictor variable is interpreted to mean that the predictor variable influences the dependent variable (streamflow, nutrient or sediment load). Lack of significance of the coefficient for a predictor variable does not necessarily mean it does not affect the dependent variables. It may mean that the effect is small relative to model noise, or it may indicate limitations (for example, lack of spatial resolution) in the input data or spatial collinearity with another variable in the specification.

The model coefficients are interpreted in the Calibration sections of this report to quantify the effect of the associated predictor variable on streamflow or constituent transport. The coefficients quantify the effects of the predictor variable; the coefficients fall short of quantifying their effect on actual transport when the model is inadequately specified (for example, missing an important source variable) or in the case of interactions between variables. For example, the coefficient for delivery variable A may be positive only because of the spatial covariation of delivery variables A and B, rather than because of its effect on transport processes. The interpretations offered throughout this report regarding interpretation of coefficient values therefore need to be considered with caution.

The model-estimated source coefficient, α, describes the land-to-water delivery ratio:

$$\alpha = [\text{streamflow or mass of constituent delivered to the adjacent stream channel}] / [\text{measured input to the catchment}] \quad (2)$$

The value of α for the land-applied sources (that is, sources not discharged directly to the stream) represents the delivery ratio estimated for an average catchment in the model domain; the delivery ratio is actually simulated as varying among catchments to account for the spatially varying physical characteristics, such as vegetation or soil properties, that affect water delivery. The value of α, therefore, represents the average effect, averaged for the model domain, of all model-specified processes of water or constituent losses during land-to-water transport.

Land-to-water delivery variables evaluated in the model are considered to represent factors that enhance or mitigate, relative to the average α, delivery of flow or constituent mass from land to streams. The sign and magnitude of the coefficient for land-to-water delivery variables define the effect of each variable on the delivery ratio. Delivery variables with positive coefficients are positively correlated with delivery ratio; that is, as the variable increases in value, the delivery of constituent to the stream, per unit of constituent input to the catchment, also increases. A negative coefficient indicates that as the variable increases in value, the delivery to the stream decreases.

The magnitude of the coefficient for a delivery variable indicates the sensitivity of the delivery ratio to changes in the delivery variable. For delivery variables that are log transformed, the interpretation of sensitivity can be quantified as follows: a coefficient value of x means that a 1-percent difference between catchments in the value of the delivery variable causes an x-percent difference between catchments in the delivery ratio. If all delivery variables are log transformed, the variables with the larger (positive or negative) coefficient are those to which the delivery ratio is more sensitive.

The coefficients for the stream and reservoir loss terms, when multiplied by the values for those terms, represent the ratio between the amount of water, sediment, or nutrients entering a stream or reservoir that is discharged from that waterbody. The complement of this ratio is, therefore, the estimated fraction of water, sediment, or nutrients lost from transport in the waterbody. In a steady-state model, such as SPARROW, loss during transport refers to permanent removal. Permanent removal can occur as a result of evaporation, particle settling, or denitrification by benthic bacteria. Transient loss or gain of mass in transport resulting from the seasonal cycling (for example the cycling of growth and decay of aquatic plants) is not characterized in the calibration data (mean-annual loads); therefore, transient losses and gains are not reflected in the analysis.

Changes in the Model Calibration Procedures from Previous SPARROW Applications

Reducing Bias in the Mean-Annual Load Estimates Used to Calibrate the SPARROW Models.

Previous SPARROW models have been calibrated with mean-annual TN and TP loads estimated by using regression techniques that were later shown to be potentially biased (Stenback and others, 2011; Richards and others, 2012). To minimize this problem, mean-annual loads used in calibration in this study were estimated with the Beale ratio-estimator (BRE, Beale, 1962) technique provided there was no significant trend in load over time. The BRE method was implemented in stratified form as described in Cochran (1977). This approach was used because it was shown to have less bias in estimates of long-term mean-annual loads than most regression approaches (Lee and others, 2016). When statistically significant trends in the mean-annual load for a site and

constituent were present, loads were estimated and detrended to 2012 by using five-parameter regression with Kalman smoothing (5pK) methods. Prior to use, all loads were evaluated for accuracy and bias. The approaches used to estimate loading using the BRE technique and 5pK techniques and assess their accuracy are described in detail by Saad and others (2019).

Accounting for the Effects of Nested Monitoring Sites

The phrase "nested monitoring sites" refers to the situation in which one monitoring site is located downstream from another site. In SPARROW calibration, the load estimate for the upstream site of the nested pair is used to determine the load at the downstream station; that is, the load estimated for the stream reach with the upstream site is reset to the monitored load so that load estimates downstream reflect (are conditioned on) the monitored information. Use of the conditioned load estimate at the downstream site during model calibration minimizes error and reduces the correlation of errors between nested basins (Schwarz and others, 2006). Calibration conducted by using conditioned load estimates can, however, result in bias (underestimation) in residuals at the downstream sites of nested pairs, particularly for pairs where the intervening drainage area between the two sites is small relative to the total upstream drainage area of the downstream site; this underestimation in turn reduces the potential effect of these sites on the estimation of coefficients (Wellen and others, 2014). Calibration conducted by using conditioned load estimates may also result in spatial correlation in residuals of nested pairs (Qian and others, 2005).

To address the potential unequal effect of the nested basins during model calibration, a statistical algorithm was developed in which weights are computed for each monitoring site on the basis of the fraction of the upstream drainage area that is downstream from other monitoring sites (termed the "nested area share"), and these weights are used in a subsequent reestimation of the model done by using weighted nonlinear least squares regression (Schwarz and others., 2006, eq. 1.55). Placing greater weight on the residuals from downstream stations with small nested area share corrects for the otherwise unequal influence of nested basins during calibration. To obtain the weights for each monitored-load estimate, the SPARROW model is first calibrated with equal weighting applied to all monitoring sites. The squared values of these residuals are then regressed on the nested area share. The inverse of the predicted values from this regression then serves as weights in a subsequent reestimation (recalibration) of the SPARROW model. If the coefficient associated with the nested area share from this regression has a significant positive value, the recalibrated (with weights) SPARROW model calibration is selected as the final model.

Evaluating Model Error by Using Unconditioned Load Estimates and Percentage Error

The RMSE of the regression is the primary statistical evaluation criteria in most SPARROW applications. RMSE is typically calculated from the difference in the monitored loads and the conditioned model-estimated loads computed during calibration (all terms in natural log space), but this approach can underestimate the RMSE compared to when full model predictions are made without conditioning. To provide a fair assessment of model accuracy in prediction mode—for example, model accuracy for a reach lacking any upstream monitoring information—the unconditioned RMSE was also computed for each final model on the basis of the differences between the monitored loads and full unconditioned model predictions.

Conditioned and unconditioned RMSE are reported in natural logarithm space (*ln*RMSE) as well as in real space—that is, as percent error of predicted load or yield in units of mass or mass per unit area. The formula for calculating percent RMSE, $100\sqrt{\exp(lnRMSE^2 - 1}$, is described in more detail in appendix 2.

Combining Load Estimates Based on Concentration Data from Different Sampling and Analytical Techniques to Calibrate a Single SPARROW Model

Water-quality data used to calibrate SPARROW models were typically collected by various agencies that used different field collection and laboratory techniques. Two analytical techniques have commonly been used for measuring sediment in the water column: the suspended-sediment concentration (SSC) method (American Society for Testing and Materials, 2006) typically used by the USGS, and the total suspended solids (TSS) method (American Public Health Association, American Water Works Association, and Water Pollution Control Federation, 2012) used by most other agencies. SSC is the mass of all the sediment within a known volume of a water-sediment mixture collected directly in the sample (Guy, 1969). In contrast, TSS concentration is the mass of suspended material within a subsample of a water-sediment sample. Such subsampling can introduce negative bias and increase variability, especially when the percentage of sandsize sediment is high (because of sediment settling during subsampling; Gray and others, 2000). In addition, samples collected for SSC analysis are generally collected by using cross-sectionally integrated and flow-integrated techniques, whereas samples collected for TSS analysis are generally collected by using grab techniques. Values determined by using these methods generally are not interchangeable (Gray and others, 2000).

Because the number of monitoring stations with load estimates based on SSC data was not sufficient for SPARROW model development, both the SSC-based load estimates and the TSS-based load estimates were included in the model. To account for the systematic differences between the two sets of load estimates, an additional variable, *CONVERT*, assigned a value of 1.0 when the monitored-load estimate for a reach was for TSS (that is, based on TSS data) and a value of 0.0 when the monitored-load estimate was for SS (that is, based on SSC data), is included in the SS model. The model-estimated coefficient *bCONVERT* associated with this variable can be

interpreted as a scaling factor for converting between the two groups of data, given by:

$$\text{Load of suspended-sediment} = \text{Load of total suspended solids} * [1/\exp(bCONVERT)] \quad (3)$$

Evaluating and Addressing Spatial Structure in Model Residuals

The spatial pattern of model residuals should be examined prior to finalizing model specification to determine whether the residuals are spatially autocorrelated, as autocorrelation may introduce bias into the model parameterization. Spatial autocorrelation can be either positive (meaning the residual values at nearby sites are typically of similar sign) or negative (meaning the residual values of nearby sites are typically of opposite sign). Autocorrelation in the calibration residuals was evaluated for three types of spatial structures or patterns, which correspond to three different types of modeling or measurement error. The results from these evaluations were then used to make corrections to the model input and calibration station set, as appropriate.

1. Significant spatial correlation among loose clusters of calibration sites (sites greater than 5 kilometers (km) apart)—for example, those located within the same large watershed or ecoregion—was evaluated by using the Moran's *I* statistic (Cliff and Ord, 1973). A significant positive value for the Moran's *I* statistic indicates that residuals near each other are generally positively correlated, which indicates that important watershed processes or sources are not included in the model. Ideally, this type of spatial correlation is addressed by including additional predictor variables in the model; the patterns in the residuals may help identify which predictor variables should be added. Datasets representing those variables, if available, were then added to the model specification.
2. Significant spatial correlation among nested site pairs in close proximity (less than 5 km apart) with similar drainage areas (within a factor of 2) was evaluated by using the Pearson correlation coefficient. A significant negative Pearson coefficient indicates error in the streamflow or load estimate at the upstream site in many of these proximal nested pairs. This type of spatial correlation was addressed by removing the upstream site in each pair from the calibration dataset.
3. Significant spatial correlation among nested monitoring site pairs in close proximity but with dissimilar drainage areas (not within a factor of 2) and among nonnested monitoring site pairs in close proximity was evaluated by using the Pearson correlation coefficient. A significant negative Pearson coefficient indicates that the spatial scale of a predictor variable was coarser than the spatial scale of the catchment network. This type of spatial correlation was addressed by randomly selecting one site in each pair and removing it from the calibration dataset.

Data Compilation

Four types of data are used to build, develop, and calibrate SPARROW models: (1) stream network information to define the stream reaches and catchments, and instream/reservoir loss; (2) estimates of long-term mean-annual flux (streamflow or constituent load)—the dependent variable—for monitoring sites throughout the model area; (3) information describing all of the sources of the constituent being modeled (explanatory variables); and (4) information describing variability in the environmental characteristics of the study area that affects land-to-water delivery or losses in the stream network during transport of the constituent (additional explanatory variables). The methods used to compile these four types of data for the Southeast SPARROW models are described in this section. The complete datasets and their associated metadata are reported in Schwarz (2019), Wieczorek and others (2019), Saad and others (2019), and in Roland and Hoos (2019). A complete list of all variables tested in each model is also provided in appendix 3.

Surface-Water Drainage Network

The surface-water drainage network used for this study is based on the NHD Plus Version 2 dataset (NHDPlusv2; Horizon Systems, 2013; Brakebill and others, in press), with some corrections and modifications documented in Schwarz (2019). NHDPlusv2 is a comprehensive set of digital spatial data that includes attributes for surface-water features such as streams, lakes, ponds, and artificial reservoirs (Simley and Carswell, 2009). The surface-water features represented in NHDPlusv2 largely correspond to the features included in 1:100,000-scale USGS topographic maps. Each reach in NHDPlusv2 begins at a point of channel initiation or a tributary junction and ends at the next tributary junction. NHDPlusv2 identifies the incremental watershed for each reach, which is defined as the area that drains directly to a reach without passing through another reach. The NHDPlusv2 network in the Southeast SPARROW model domain is composed of 380,000 stream reaches that vary in size from small intermittent streams (mean-annual streamflow less than 0.1 cubic foot per second [ft^3/s] (3.0 x 10^{-3} cubic meters per second [m^3/s]) to the Mobile River near where it enters the Gulf of Mexico (mean-annual streamflow 68,580 ft^3/s [1,942 m^3/s]).

The NHDPlusv2 stream network incorporates several revisions and improvements to stream routing compared to the NHDPlus Version 1 (NHDPlusv1, U.S. Environmental Protection Agency and U.S. Geological Survey, 2010) stream network used in previous SPARROW models for the Southeast. Many of the improvements since NHDPlusv1 were made for streams in Florida, where artificial canals, natural lakes,

and low surface relief create complex stream routing. Following additional evaluation of routing and catchment delineation in the NHDPlusv2 stream network in preparation for use in SPARROW modeling, further revisions to the network were made and are documented in Schwarz (2019). The revised network, e2NHDPlusv2_us, is the framework for the Southeast SPARROW models.

Mean-Annual Streamflow and Constituent Load Information

As a steady-state, mass-balance model, SPARROW relies on the assumption that the dependent and explanatory variables reflect conditions for comparable time periods (Schwarz and others, 2006). Use of a similar period of record (or closely comparable periods of record) to estimate all variables removes the confounding effect of temporal variability from the SPARROW spatial analysis. For the streamflow model, comparability among estimates of the dependent variable was achieved by using the mean-annual value for a common 15-year period (water years 2000–14) for all stations based on continuous daily streamflow records. A water year is the period from October 1 to September 30; it is designated by the calendar year in which it ends. Sites missing more than 2 years of record during this period were excluded from the calibration dataset; additional site-selection criteria are described in Saad and others (2019). Comparability between dependent and explanatory variables for the streamflow SPARROW model was achieved by using mean values for 2000–14 for PPT–AET, which was expected to be the primary source of streamflow across the study domain.

For the TN, TP, and SS models, however, comparability of conditions cannot be guaranteed by using mean values for 2000–14 for dependent variables and explanatory variables, for two reasons (Schwarz and others, 2006):

1. Because the water-quality monitoring data may not be available for the entire 2000–14 period, the data used to estimate loads may represent different periods of record, sample size, and hydrologic conditions at different sites, or may be affected by long-term trends in water quality.
2. Information for some important explanatory variables was not available for the entire 2000–14 period; therefore, it is not possible to compute long-term averages over the same period used to summarize the dependent variable. For example, estimates of source inputs from fertilizer and wastewater discharge made by using the improved estimation methods described in this report were available only for 2012.

To compensate for these limitations, estimates for the dependent variable, constituent load, were normalized to the selected base year; that is, they were estimated to represent average load that would have been observed during the period 2000–14 if the dynamic factors causing trend in load were held constant throughout that period, equal to their values in the base year (Schwarz and others, 2006). The base year selected for the Southeast SPARROW models was water year 2012. For monitoring sites for which no significant trends in water quality were observed during 2000–14, the mean-annual load for the period is used to represent the base year (2012) load. For monitoring sites with significant trends during 2000–14, the load used for model development was estimated by detrending the average constituent load to 2012, as explained below. The watershed attributes used as explanatory variables (for example, source inputs, climatic data, and land-management practices) in these models were estimated to represent 2012 conditions or conditions as close to 2012 as possible. These variables were detrended to 2012, where possible, prior to use in the constituent models. The predictions from the TN, TP, and SS models, therefore, represent conditions that would have been observed from 2000 to 2014 given the range of hydrologic conditions throughout that period and given source inputs and management practices similar to the ones that occurred in 2012.

The loads used for calibration of the Southeast SPARROW TN, TP, and SS models were computed from water-quality data (concentration data from intermittent sample collection) and continuous streamflow data. The water-quality data were retrieved from several Federal and State data bases, described in Saad and others (2019): a total of 25 Federal, State, regional, local, and private sampling agencies and organizations contributed water-quality data to estimate TN, TP, and SS loads in the Southeast (table 1). The streamflow data were retrieved from the USGS National Water Information System (NWIS; U.S. Geological Survey, 2015). Load-estimation procedures are described in detail in Saad and others (2019). A summary of methods is included here:

- fixed monitoring stations having sufficient water-quality data, sufficiency criteria as described in Saad and others (2019), were matched to a nearby streamflow-gaging station having mostly continuous records for water years 2000 through 2014;
- mean-annual loads were then estimated for each monitoring site using BRE (Beale, 1962; Cochran, 1977) as applied by Lee and others (2016) and a 5pK analysis that included detrending to the 2012 base year (U.S. Geological Survey Fluxmaster program; Schwarz and others, 2006);
- the BRE estimate was favored over the 5pK estimate unless a significant trend in load was detected during 2000–14;
- load estimates with a standard error greater than 50 percent were removed from consideration regardless of which estimation method was used.

Matching a water-quality site with a streamgage involved initially selecting the gage with characteristics that best represented those at the water-quality monitoring site. Load calculations are ideally performed for sites with collocated

Table 1. Sources of water-quality data used to estimate calibration loads for total nitrogen, total phosphorus, suspended-sediment, and total suspended solids used in the Southeast SPARROW models.

[SPARROW, SPAtially Referenced Regression On Watershed attributes]

Federal and State agencies		Regional and local agencies	
Agency	**Number of stations**	**Agency**	**Number of stations**
U.S. Geological Survey	151	City of Cape Coral	4
Alabama Department of Environmental Management	54	Collier County Pollution Control	1
Florida Department of Environmental Protection	83	Hillsborough County Environmental	61
Georgia Department of Natural Resources	65	Leon County Public Works	3
Mississippi Department of Environmental Quality	23	Lake County Water Resource Management	2
North Carolina Department of Environment and Natural Resources	223	Florida Lakewatch	3
South Carolina Department of Health and Environmental Control	87	Manatee County Environmental Management Department	19
Virginia Department of Environmental Quality	74	McGlynn Laboratories Incorporated	1
		Northwest Florida Water Management District	8
		Orange County Environmental Protection	12
		Pinellas County Department of Environmental Management	30
		Seminole County	7
		South Florida Water Management District	3
		Saint Johns Water Management District	50
		Suwannee River Water Management District	22
		Southwest Florida Water Management District	48
		Volusia County Environmental Health Lab	6

water-quality and streamflow data; however, use of a nearby streamgage is a common approach when the data are not collocated. Where collocation was not possible, specific criteria were used to identify suitable nearby gages for a water-quality site. In general, nearby gages had to meet the following requirements: a ratio of watershed area between the water-quality site and flow site between 0.75 and 1.33; if the watershed area of the water-quality site was greater than 130 km^2, then the gage had to be on the same flow path; and the gage had to be within areal distance of 40 km from the water-quality site. If multiple suitable gages were near a potential load site, priority for selection was given to gages with a longer period of data overlap, watershed-area ratios closer to 1, and a shorter distance to the water-quality site (the screening and matching processes are described in more detail by Saad and others [2019]).

The number of sites considered for inclusion in the Southeast SPARROW models was much smaller than the number of sites with data (table 2). For the streamflow SPARROW model for the Southeast, 22 percent of original streamflow sites (687 of 3,121) passed the site-selection protocols and were considered for use as calibration targets. Eighteen percent (569 of 3,121) of the original streamflow sites were used in the final model. Fewer than 3 percent of original sites

Table 2. Number of sites throughout the data compilation and selection process for Southeast SPARROW models.

[SPARROW, SPAtially Referenced Regression On Watershed attributes; –, Note reported separately for this variable]

SPARROW model variable	Number of sites with data	Number of potential sites for consideration in SPARROW models	Sites used in final SPARROW models
Streamflow	3,121	687	569
Nutrients	47,746	1,649	1,197
Total nitrogen	–	834	603
Total phosphorus	–	815	594
Sediment	32,016	635	421
Suspended solids	–	588	412
Suspended sediment	–	47	9

with nutrient data (1,197 of 47,746) were used in the final Southeast nutrient models. Fewer than 2 percent of original sites with sediment data (635 of 32,016) were considered for use as calibration targets and only 1 percent of the original sites (421 of 32,016) were used in the final Southeast sediment model. Even with the elimination of sites, the distribution of the final calibration sites generally covered most of the Southeast area for the streamflow TN, TP, and SS SPARROW models. The density of sites for all models was generally lowest in the western parts and highest in the eastern parts of the Southeast area.

Source Variables

Most source-variable datasets have been updated and refined from those used in previous SPARROW models. In this section, all sources tested for statistical significance in explaining streamflow or constituent transport are described regardless of whether they were retained for the final models. The datasets representing sources in the streamflow SPARROW model describe mean-annual inputs for the period 2000–14, whereas the datasets representing sources in the TN, TP, and SS SPARROW models describe inputs for a time period as close to 2012 as possible.

Sources of Water

Precipitation Minus Actual Evapotranspiration

The primary source of water to catchments in the Southeast is precipitation, PPT. PPT is the only external or "new" source of water to Southeast streams except the transfer of water from the Tennessee River to the Tombigbee River (fig. 2*A*). The difference between inputs from PPT and losses from actual evapotranspiration (AET), referred to as PPT–AET, represents the net amount of PPT to each catchment that is available, after losses from AET, to generate runoff to streams and recharge to groundwater in the catchment. If there are no losses in direct runoff, and no losses to or gains from deeper groundwater—that is, if recharge to groundwater within the catchment equals discharge to streams from groundwater within the catchment—then mean-annual streamflow generated from the catchment will exactly equal mean-annual PPT–AET.

Annual estimates of PPT and evapotranspiration (both potential and actual—PET and AET, respectively) for the Southeast for water years 2000–14 were obtained from Wolock and McCabe (2018). AET was assumed to equal PET unless PET exceeded PPT, in which case AET was set to equal PPT. The difference term PPT–AET was computed from mean-annual PPT and mean-annual AET for 2000–14 and expressed in cubic feet per second as the source term in the streamflow model.

Municipal Use

Water discharged to the stream from municipal wastewater treatment plants (WWTPs) represents internal transfers between stream reaches of water that is ultimately derived from precipitation inputs, rather than an external or "new" source. WWTP discharge may appear as net input to a catchment or watershed, however, depending on the relative location of the balancing municipal withdrawal. If the balancing withdrawal is within the same local catchment, then no net input to the local catchment would be apparent. If the balancing municipal withdrawal is from groundwater or from a distant location, then it may appear in the context of model calibration as a source of streamflow. WWTP discharge to streams and municipal withdrawals are therefore included as separate predictor variables in the streamflow SPARROW model: WWTP discharge as a source variable (described in this section) and municipal withdrawals as a removal variable (described in the section Delivery, Loss, and Removal Variables).

Estimates of 2012 WWTP effluent flow (in ft^3/s) were compiled by Skinner and Maupin (2019) and then assigned to individual NHDPlusv2 reach segments on the basis of outfall location coordinates. Assignments were altered—moved to the next reach segment downstream—in cases where the outfall shared a reach assignment with and was downstream from a streamflow gage (Roland and Hoos, 2019). Estimates of effluent flow were then summed for each reach segment and tested as a source variable in the streamflow model. Estimates of water diversion or transfer associated with withdrawals for public supply were also compiled and included in the model not as source variables but as corrections to flow-routing information in the surface drainage network for the model. Estimates of these diversions for public water supply and transfers (in ft^3/s) were available for specific stream reaches

in NHDPlusv2 (Horizon Systems, 2013), with revisions in Schwarz (2019).

Groundwater Discharge from Large Springs

Groundwater moving along long (regional-scale) flow paths before discharging to streams may effectively represent trans-basin diversion and therefore a potential additional source of streamflow in the watershed. Groundwater discharged from relatively short, shallow flow paths, on the other hand, is considered to be derived from precipitation within the local area; therefore, it would already be included in the primary source term (PPT–AET) in the model.

To represent potential additions to streamflow from groundwater from regional-scale flow paths, discharge data from 207 large springs (mean-annual discharge greater than 10 ft^3/s, equivalent to first- and second-order magnitude springs) in the Southeast were compiled from the NWIS database (U.S. Geological Survey, 2015) and from other sources (Scott and others, 2004; Callahan, 1964). For 30 large springs with daily flow data, the average flow was computed from mean daily flows for the 2000–14 period. For the 177 large springs without daily flow data, intermittent-spring flow measurements for the period from 1970 to recent were used to compute an average value for flow. Flow values (in ft^3/s) were summed by catchment.

Sources of Nitrogen and Phosphorus

Nitrogen (N) and phosphorus (P) in surface water originate from both natural and anthropogenic sources. Natural sources of N include fixation by naturally occurring organisms that convert N from its inert-gas form into molecular N, which is then released to the environment and transported to streams as organic and inorganic N. Other natural sources of N include weathering of N-containing minerals and fixation of N gas by lightning strikes. Weathering and erosion of P-containing minerals in soil and parent rock is the only natural source of reactive P entering groundwater or surface water. Anthropogenic sources of N and P are listed in the following paragraphs.

Selection of variables for testing in the SPARROW TN model is based in part on past research on N budgets for watersheds—for example, Howarth and others (1996) and Boyer and others (2002). The variables tested in the SPARROW TN model represent six general classes of N inputs to the watershed:

- natural sources (represented in model testing by estimates of fixation in forest lands, and a component of atmospheric N deposition),
- agricultural fertilizers (represented by estimates of agricultural fertilizer use, and a component of atmospheric N deposition),
- fixation in agricultural lands (represented by estimates of fixation by cultivated crops),
- import as animal feed (represented by estimates of manure from livestock production, and a component of atmospheric N deposition),
- import as food (represented by estimates of discharge from municipal WWTP and septic-waste systems), and
- fossil-fuel combustion and other urban activities (represented by estimates of urban land-cover area, and by a component of atmospheric N deposition).

Estimates for each variable are described in more detail in this section. Not all of the tested variables were retained in the final model.

Similarly, the variables tested in the SPARROW TP model represent six general classes of P inputs to the watershed:

- natural sources (represented in model testing by the phosphate mineral content of surficial geologic materials),
- agricultural fertilizer (represented by agricultural fertilizer use),
- import as animal feed (represented by estimates of manure from livestock production),
- import as food (represented by estimates of discharge from municipal WWTP and septic-waste systems),
- accelerated erosion from urbanization (represented by urban land area), and
- mining activities (represented by permitted wastewater discharges and surface runoff from mining operations).

Although other minor N and P sources may exist, they could not be tested in the model because data to represent their spatial distribution were insufficient—for example, legacy P in soil from historical agricultural activities, or accelerated erosion due to deforestation.

Atmospheric Deposition

Estimates of atmospheric deposition of N for 2012 were obtained from output from the U.S. Environmental Protection Agency Community Multiscale Air Quality (CMAQ) modeling system (Appel and others, 2017; Zhang and others, 2019). Estimates of atmospheric deposition of P were not consistently available across the model domain. The estimates of total atmospheric N deposition were summed from six component estimates: bias- and precipitation-adjusted wet deposition of oxidized N, bias- and precipitation-adjusted wet deposition of reduced N, mean dry deposition of total oxidized N, mean dry deposition of total reduced N, mean total deposition of total reduced N, and mean total deposition of total reduced N.

Part of the total atmospheric N depositional flux represents the contribution from natural sources: fixation from lightning and nonagricultural organisms and burning from naturally occurring forest fires. The global proportion of natural to human-produced reactive N in the atmosphere in

2,000 was estimated to be 40 percent natural to 60 percent human-produced, on average (Galloway and others, 2003). The atmospheric N depositional flux from human-produced sources comes from several land-based sources including emissions from vehicles and industry and burning, volatilization of manure from livestock operations, and volatilization of agricultural fertilizers. Nitrogen is therefore transported to the stream from manure, fertilizer, and some urban sources along two separate pathways, a direct pathway (source to land to stream) and an indirect pathway (source to atmosphere to land to stream).

Estimates of inputs for manure and fertilizer contribution through indirect pathway (by way of the atmosphere) were available from special simulations of the CMAQ model (Zhang and others, 2012) and were used to distinguish between the direct-runoff pathway contributions from agricultural fertilizer and manure and the indirect pathway. Specifically, estimates from the atmospheric model of the fraction of 2012 atmospheric nitrogen flux that originated as volatilization from manure (or emissions directly from livestock) and as volatilization of commercial fertilizer (Jesse Bash, U.S. Environmental Protection Agency, written commun., 2019) were used to compute estimates for each catchment of depositional flux from each of three components: animal, fertilizer, and all other sources of atmospheric N (Roland and Hoos, 2019). These estimates were then used as source terms in special simulations of the TN SPARROW model, following the approach used for the 2002 nitrogen SPARROW model (described in detail in Hoos and others, 2013, app. 1) except that 2012 estimates of the individual contribution from sources of oxidized atmospheric N, such as vehicle or industrial emissions, were not available; therefore, any contribution from these other emission sources was reported as a single "Other" category.

Fixation by Forest Species

Nitrogen from fixation by forest trees was represented by the spatial distribution of basal area of six N-fixing forest tree species (Wilson and others, 2013): *Vachellia farnesiana* var *farnesiana, Alnus rubra, Cercocarpus ledifolius, Prosopis velutina, Prosopis pubescens*, and *Robinia pseudoacacia*. Basal area for these six tree species was summed for each catchment. Five additional forest tree species are known N-fixers—*Alnus rhombifolia*, *Alnus oblongifolia, Prosopis glandulosa* var. *Robinia neomexicana*, and *Olneya tesota*—but data describing their spatial distribution were not available.

Phosphate Minerals in Surficial Geologic Materials

Estimates of the P content in soil and parent rock were used to represent natural sources of P in the SPARROW TP model following the approach used by Garcia and others (2011). Four sets of estimates were tested in the model: three were based on geochemical data from soil samples collected from approximately 5,000 sites nationwide (Smith and others, 2014) and extrapolated by using three different methods, and the fourth was based on geochemical data from bed-sediment samples collected from 5,560 small stream sites in pristine settings throughout the Southeast (Terziotti and others, 2009). All four datasets are considered surrogates of upland material P content. The data points for each dataset were extrapolated to a smooth surface of soil or bed-sediment P concentrations by using predefined geologic mapping units and methods described by Nardi (2014) and Terziotti and others (2009).

Agricultural Fertilizer Use

Estimates of 2012 farm fertilizer are from the work by Stewart and others (2019) to relate county-level commercial fertilizer sales data to spatially referenced data on acreage of crop types, climate, and other factors related to fertilizer use. The approach built on earlier efforts that used fertilizer sales data from the Association of American Plant Food Control Officials to provide county-level estimates of N and P fertilizer use (Ruddy and others, 2006). The spatially referenced regression method improves the earlier method by allowing for varying ratios of N to P (rather than fixed ratios for each State) and expanding the set of variables used to allocate county-level sales data to the catchment scale.

Fixation by Cultivated Crops

Nitrogen from fixation by cultivated crops was represented by the land area of N-fixing crops from the 2012 Cropland Data Layer (U.S. Department of Agriculture, 2015). N-fixing crops include alfalfa, chickpea, clover, lentil, peanuts, peas, soybeans, vetch, wild flower, and winter wheat.

Manure from Livestock Production

Inputs of N and P from manure were estimated from 2012 county-level livestock population data from the U.S. Census of Agriculture and species-specific rates of N and P waste production (Gronberg and Arnold, 2017). The county-level estimates were then allocated to SPARROW catchments according to the fraction of the agricultural land within the county that was within each catchment.

Municipal Wastewater Discharge to Streams

As part of a nationwide effort, Skinner and Maupin (2019) compiled estimates of 2012 discharge volume and TN and TP loads from 1,776 National Pollution Discharge Elimination System (NPDES) point-source facilities in the Southeast. Of these facilities, 200 are major industrial-wastewater dischargers, 606 are major municipal-wastewater dischargers, and 970 are minor municipal- or domestic-wastewater dischargers.

Details of the data retrieval and estimation methods are described in Skinner and Maupin (2019). The methods used to estimate 2012 TN and TP loads are summarized below:

1. For each discharger, the effluent flow in million gallons per day for each month was multiplied by the number of days in the month and then by either a measured or surrogate TN or TP effluent concentration in milligrams per liter. A surrogate concentration was used in the monthly load estimate when a measured value was not available. The surrogate concentration was either a seasonal median value for the facility (when sufficient facility-specific measurements were available for 2012) or a "typical pollutant concentration" (TPC) that represented a similar type of facility within the same state, adjacent states, or the conterminous U.S. (in order of preference).
2. The monthly load estimates were then summed to estimate the TN and TP loads for water year 2012. For cases when a facility had less than 12 months of flow data for the year but had flow for at least three seasons in 2012, the seasonal nutrient loads were extrapolated to estimate the TN and TP loads for water year 2012 (with the assumption that the facility likely discharged throughout the year and the flow data were simply missing). If a facility had fewer than three seasons of effluent flow, however, then it was assumed to discharge only intermittently, and the annual loads were set equal to the sum of the available monthly loads.

The TN and TP load estimates from Skinner and Maupin (2019) were assigned to individual NHDPlusv2 reach segments on the basis of the outfall location coordinates. Assignments were altered—moved to the next reach segment downstream—in cases where the facility outfall shared a reach assignment with and was downstream from a water-quality monitoring site (Roland and Hoos, 2019). Load estimates were then summed for each reach segment, with estimates for municipal- and domestic-wastewater facilities (Standard Industrial Classification 4952; classification codes described in U.S. Office of Management and Budget, 2017) summed separately from estimates for industrial-wastewater facilities.

Municipal Wastewater Discharge to Land Surface

Many municipal-wastewater systems in the Southeast and especially in Florida route most or all of their treated effluent to reuse systems that discharge to the land surface or subsurface rather than to streams. The treated wastewater is used to irrigate golf courses, parks, residences, and cropland; to recharge groundwater through infiltration basins and injection; and for industrial uses. Discharge volumes and site locations for wastewater reused for irrigation and infiltration to groundwater in Florida were obtained for 2013 (Florida Department of Environmental Protection Water Reuse Program, 2014) and the volume (in ft^3/s) of municipal wastewater applied to land was estimated for each catchment in Florida (Roland and Hoos, 2019).

Wastewater Discharge to the Subsurface: Septic Waste Systems

Estimates of population served by septic waste systems for each SPARROW catchment were computed from 2010 population data and 1990 data on percent of population on septic systems, the latter based on 1990 census information (Wieczorek and others, 2019). The assumption that 1990 percent of population on septic systems was valid through 2010 may not be reasonable, but more recent data are not available consistently across the Southeast. The estimate of population served is intended as a surrogate for mass of TN or TP input to the watershed from septic waste systems or, more specifically, from failing systems.

Land-Cover Areas

Land-cover classifications (Level 2) from the National Land Cover Database 2011 (Homer and others, 2015) were allocated to the SPARROW stream catchments and then summed to represent area for each of the nine Level 1 land-cover categories (fig. 3). The nine land-cover categories were further generalized into four categories: urban, forested, transitional (shrub, scrub, herbaceous, and barren), and agricultural.

Phosphate Mining

Phosphorus input to streams from mining operations is from point sources (permitted wastewater discharged to streams from phosphate-mining facilities) and nonpoint sources (runoff from mined land). Wastewater-discharge input was represented by TP load estimates from Skinner and Maupin (2019) from facilities with Standard Industrial Classification 1475, 1479, and 2874 (classification codes described in U.S. Office of Management and Budget, 2017). Runoff from mined land was represented by estimates of areal extent of the mined land within each catchment and the level of phosphate enrichment in the mined deposit (Terziotti and others, 2009).

Sources of Sediment

Sediment enters streams in the Southeast through two general processes: erosion of soil in upland areas by water and erosion within stream corridors (Swanson and others, 1982). Erosion from upland areas typically occurs where a sloped and exposed soil surface is exposed to precipitation. Erosion within stream corridors (hereafter referred to as "channel sources") is due to eroding stream banks, resuspension of sediment from channel-bed material, and sediment derived from mass wasting where channels intersect valley sides and terrace walls (Gellis and others, 2016).

Upland Sediment Sources

Two land classification systems—surficial-geology classification and land-use/land-cover classification—were combined to represent upland sediment sources in the SS

SPARROW model. The surficial geologic units were used to represent native erodibility of soil— in other words, natural sources of sediment. The land-use/land-cover classes were used to represent the effect of human activities. The surficial-geology classification system from Soller and others (2009) is composed of 50 surficial-geology classes, 13 of which are found in the Southeast (table 3). To facilitate model development, the 13 surficial-geology classes were generalized into 11 categories that represented texture and type of surficial material (table 3). The NLCD land-cover classification system is composed of nine different land-cover categories (Homer and others, 2015) (fig. 3). The nine land-cover categories were generalized into four categories: urban, forested, transitional (shrub, scrub, herbaceous, and barren), and agricultural.

The 11 categories of generalized surficial materials and 4 categories of land use/land cover were then intersected by using a geographic information system (Wieczorek and others, 2019), producing estimates of the area in each catchment of the 40 (10 x 4) possible surficial-geology and land-use/land-cover combinations of upland sources. Some of these combination sources represent very small areas in the Southeast. To ensure that the area for each of the combined classes was large enough to intersect a sufficient number of monitored basins for model calibration, the categories were further generalized and aggregated. The 11 surficial-geology categories were aggregated to the 4 categories shown in the last column of table 3 for testing in the model: alluvium and residuum in very fine-grained sedimentary rock; residuum in igneous and metamorphic rock; residuum in sedimentary rock (discontinuous); and all other categories. The final set of upland sources for testing in the Southeast SS model, therefore, consists of 16 (4 x 4) different geology/land-use combination sources.

Channel Sediment Sources

Input of SS from stream channels is a function of the erosive power of the stream reach (hydraulics) and the availability of erodible sediment materials in the bed or bank in that stream reach (Bull, 1979). Therefore, characterizing spatial variability of channel inputs requires estimates of erosive power and erodible sediment for each stream reach. Spatial variability in erosive power can be represented by several geomorphic attributes or surrogate variables that can be computed by using available datasets. For the sediment SPARROW model, stream power, change in stream power across a stream reach, and reciprocal of channel sinuosity were tested. Floodplain width, channel incision, and bank-height ratio were also considered but were not available as areally extensive datasets. Spatially explicit information describing accumulation in the channel of erodible materials from historical erosion from upland areas or the natural alluvial condition of the stream was also not available.

Stream power is used extensively in models of landscape evolution and river incision and is calculated by the equation

$$\Omega = \rho\, g\, Q\, S\,, \tag{4}$$

where Ω is the stream power (the rate of energy dissipation against the bed and banks of a stream per unit downstream length, in Joules per second [Joules/s], or kilograms square meter per cubic second [$kg*m^2/s^3$]); ρ and g are physical constants (density of water [1,000 kilograms per cubic meter [kg/m^3]); and acceleration due to gravity (9.8 meters per square second [m/s^2]) respectively; Q is streamflow (cubic meters per second [m^3/s]), and S is the channel slope (Bagnold, 1966). Estimates of stream power for testing in the model were computed from mean-annual streamflow (MAFlowUcfs) and channel slope (SLOPE), which were obtained from the enhanced NHDPlus network (Schwarz, 2019).

Change in stream power across a stream reach was calculated following a procedure by D.W. Anning, (U.S. Geological Survey, written commun., 2017) as:

$$\begin{aligned} \text{StrmPwrChange\_frac} = (\Omega_{\text{FromNode}} - \Omega_{\text{ToNode)}} \,/ \\ \text{Max}_{(}\Omega_{\text{FromNode}} - \Omega_{\text{ToNode)}} * 100 \end{aligned} \tag{5}$$

where StrmPwrChange_frac is expressed as a fraction from 0.0 to 1.0, Ω_{ToNode} is estimated by using Q and S for the reach, and Ω_{FromNode} is computed as the sum of Ω for the ToNodes that are immediately upstream from that reach and deliver water and mass to that reach. Changes in density or gravity across the reach were neglected. Positive values of StrmPwrChange_frac were assigned to populate the variable StrmPwrGain_frac. StrmPwrGain_frac was then tested as a surrogate for stream power and channel sources of sediment.

Stream reaches that have been channelized and straightened and reaches for which sinuosity is naturally small tend to have more energy to dissipate against the bed and banks, and therefore have greater erosive power. The geomorphic metric average sinuosity for each stream reach was computed as the ratio of the length of the reach to the linear distance between the upstream and downstream nodes (Wieczorek and others, 2019). The reciprocal of reach-average sinuosity was tested as a surrogate for stream power and channel sources of sediment.

Delivery, Loss, and Removal Variables

This section provides an overview of the datasets that were evaluated to represent factors that affect the land-to-water delivery and aquatic losses and to represent removal by hydrologic manipulation. Many of these datasets were compiled as part of the national NAWQA effort (Wieczorek and others, 2019). Additional descriptions of each of the delivery, loss, and removal variables are included in the Calibration section for each model and in appendix 3.

The variables representing land-to-water transport and delivery processes are generally physical characteristics of the watershed, such as soil properties or topography, or are climate variables. Aquatic-loss processes refer to the natural processes of loss or decay during transport through the stream network. In the context of the SPARROW steady-state model,

Table 3. Soller surficial geology categories in the Southeast and scheme for aggregating to prepare for testing in the suspended-sediment SPARROW model.

[SPARROW, SPAtially Referenced Regression On Watershed attributes]

Soller category	Area in the Southeast, in square kilometers	Percent of area in the Southeast[1]	Description	Aggregation to 10 categories representing texture and type, use for intersection with land-cover categories	Final aggregation to 4 surficial-geology categories, to ensure area of each intersects a sufficient number of sediment-monitored basins for calibration
11	51,969	8.3	Alluvial sediments thin	alluvial_1	Alluvium, and residuum on very fine-grained sedimentary rock
211	72,675	11.6	Coastal-zone sediments mostly fine-grained	fine_4	All other categories
221	44,102	7.0	Coastal-zone sediments mostly medium-grained	medium_3	All other categories
321	1,402	0.2	Eolian sediments mostly dune sand thin	medium_3	All other categories
610	4,398	0.7	Colluvial sediments (discontinuous)	colluv_6	All other categories
640	1,039	0.2	Colluvial sediments and residual material	colluv_6	All other categories
701	11,145	1.8	Organic-rich muck and peat thin	organic_7	All other categories
910	103,454	16.5	Residual materials developed in igneous and metamorphic rocks	igmet_91	Residuum in igneous and metamorphic rock
920	137,932	21.9	Residual materials developed in sedimentary rocks (discontinuous)	resid_sed_92	Residuum in sedimentary rock (discontinuous)
930	13,244	2.1	Residual materials developed in fine-grained sedimentary rocks	resid_fine_sed_93	All other categories
940	56,706	9.0	Residual materials developed in carbonate rocks (discontinuous)	resid_carb_94	All other categories
950	98,358	15.7	Residual materials developed in alluvial sediments	resid_alluvial_95	All other categories
970	20,635	3.3	Residual materials developed in bedrock (discontinuous)	resid_bedr_9	Residuum in sedimentary rock (discontinuous)

[1]Percentages do not sum to 100 because the Soller data layer does not extend to the edge of the model domain.

loss in the network refers to permanent removal, for example, due to particle settling or denitrification by benthic bacteria.

Aquatic loss of nutrient and sediment mass in free-flowing streams was modeled as a function of mean water depth, mean-annual velocity, and reach length (Schwarz, 2019), where mean water depth of a stream reach was estimated as a continuous function of mean streamflow and other channel attributes including slope, elevation, sinuosity, and urban land cover (estimated by six-parameter regression; Roland and Hoos, 2019). Although channel characteristics other than mean water depth, such as ditching/draining or condition of riparian vegetation, also may affect instream loss rates of N, P, and sediment, these characteristics were not tested in the aquatic-loss function for these models because regionally extensive and consistent datasets were generally unavailable.

Aquatic loss of nutrient and sediment mass in lakes and reservoirs was modeled as a function of areal hydraulic load, defined as the ratio of outflow to surface area of the lake or reservoir. Estimates of surface area and areal hydraulic load were compiled from two sources: NHDPlusv2 (Horizon Systems, 2013) and the National Inventory of Dams (NID; U.S. Army Corps of Engineers, 2011). NHDPlusv2 served as the primary data source of areal hydraulic load for 35,328 reservoirs in the Southeast (8,979 are intermediate to large—that

is, surface area greater than 0.5 km^2). Estimates from the NID provided additional information for 2,320 reservoirs (130 were intermediate to large in size) (Wieczorek and others, 2019). NHDPlusv2 provided segmented values computed separately for individual flowline segments of the lake or reservoir, which were computed as the ratio of outflow from the flowline segment to the water surface area of the segment of lake or reservoir within the catchment segment. The NID data provided only single values for each reservoir, which were computed as the ratio of outflow from the reservoir to the total water surface area of the reservoir. The estimates of areal hydraulic load used in the models are therefore a hybrid dataset of segmented values (for most lakes and reservoirs) and total waterbody values (for 2,320 reservoirs that are missing from the NHDPlusv2 set).

From hydraulic load for waterbodies (lakes and reservoirs), two additional variables were created: areal hydraulic load if the waterbody is in the karst landscape region (mostly in Florida) and areal hydraulic load for all remaining reaches. Separation of karst and non-karst areal hydraulic load was done to determine whether the processes and rates of constituent loss (settling and denitrification for N, settling for P and SS) in these lakes differ from those in the rest of the Southeast because of different morphologic, hydrologic, and hydraulic features of waterbodies in these areas. Many lakes in Florida's karst landscape were formed naturally by solution processes or sinkhole subsidence and collapse (Schiffer, 1998), whereas waterbodies in the rest of the Southeast were either built (reservoirs) or formed naturally in ancient sea depressions (for example, the lakes of the Coastal Plain of North and South Carolina).

Loss of water during transport through lakes and reservoirs was modeled as a function of the product of mean-annual PET (Wieczorek and others, 2019) and waterbody surface area (WSA), divided by mean-annual streamflow through the lake or reservoir (QReach). Estimates of WSA were obtained from NHDPlusv2 and NID. The estimate of QReach was obtained from Schwarz (2019). The term PET*WSA/QReach (unitless), mathematically equivalent to PET*Reciprocal areal hydraulic load, is hereafter referred to as "Lake/reservoir evaporation." The difference term 1–Lake/reservoir evaporation represents the fraction of water that is not evaporated from the lake or reservoir reach and, therefore, it is the amount delivered to the downstream end of the reach. Values less than 0.02 for the term 1–Lake/reservoir evaporation were censored to 0.02. Finally, the variable for testing in the model was computed as $-ln$(1–Lake/reservoir evaporation) to improve interpretability of the estimated model coefficient (*ln* denotes the natural logarithm function). The estimated value represents a scaling factor between the unevaporated (delivered) fraction specified from the input data—1–Lake/reservoir evaporation—and the delivery fraction calculated from the SPARROW mass-balance analysis. An estimated coefficient value of 1 signifies an overall 1:1 correspondence between the delivery fraction calculated from the data and the delivery fraction calculated from the SPARROW mass-balance analysis.

Several variables, termed "removal variables," were used to characterize losses because of human manipulation of streamflow, in contrast to aquatic-loss variables that represented natural attenuation processes in streams, lakes, and reservoirs. These variables were direct estimates of the quantity of mass removed and are, therefore, expressed in the same units as the mass variable (in this case streamflow) to be removed, rather than surrogate variables (such as time of travel or areal hydraulic load) that vary proportionally with loss processes.

Records of consumptive water use at power-generating plants indexed to specific stream reaches (Wieczorek and others, 2019) were used to represent net water withdrawals at power plants. In some cases, the specific stream reach associated with the withdrawal was revised to an adjacent stream reach for which mean-annual streamflow (estimated by NHDPlusv2) better matched and supported the calculated annual withdrawal amount (Roland and Hoos, 2019).

Groundwater pumping has been shown to deplete nearby streamflow (Barlow and Leake, 2012). Estimates of 2010 county-level groundwater withdrawal (Maupin and others, 2014) were used to represent this potential diversion of water from streams. The amount of groundwater withdrawal for each county was evenly distributed among the catchments in the county and scaled proportionally to the catchment area. In most areas in the Southeast where large quantities of groundwater are pumped for irrigation and public supply, flow exchange between stream and aquifer is restricted by a confining unit; the exception is in northwestern Florida, southern Georgia, and southern Alabama, where the upper confining unit of the Floridan surficial aquifer system is thin or absent (Mosner, 2002). The estimates of 2010 groundwater withdrawal amounts were therefore set to 0 for all catchments except those in the areas where the upper confining unit of the Floridan surficial aquifer system is thin or absent (defined by Williams and Dixon, 2015, fig. 55; additional details in Roland and Hoos, 2019).

Surface-water withdrawals for municipal water supply were represented by information on population served by municipal water-supply withdrawals from specific stream reaches (Wieczorek and others, 2019). The estimates of population served were converted to annual water withdrawal amounts (in ft^3/s) by using per capita water-use data (Maupin and others, 2014), and in some cases the specific stream reach associated with the withdrawal was revised to an adjacent stream reach for which mean-annual streamflow matched and supported the calculated annual withdrawal amount (Roland and Hoos, 2019).

The estimates of surface-water withdrawals for power plant consumptive use, groundwater withdrawals from unconfined aquifers, and surface-water withdrawals for municipal water supply described above were transformed to predictor variables for the SPARROW models by computing the ratio of the removal amount (QWithdr_) to the estimate of mean-annual streamflow for that reach, or QReach (Schwarz, 2019), and subtracting the ratio from 1. The term 1–Qwithdr_/

QReach represents the fraction of water that is delivered past the point of withdrawal to the downstream end of the reach and is thus an expression of delivery fraction, calculated directly from the data. Values for this term that were less than 0.02 were censored to 0.02. Finally, the variable for testing in the model was computed as $-ln$(1–QWithdr/QReach) to improve interpretability of the estimated model coefficient. The interpretation of the coefficient value for this variable follows the same logic as described above for the coefficient for aquatic loss of streamflow in lakes and reservoirs.

Diversions also represent removal from the stream network. The NHDPlus dataset (Schwarz, 2019) uses data from discharge records at the transfer intakes or from discharge records above and below the diversions to describe a diversion in flux routing. These data were not used to represent removal in the model specifications; rather, they were accounted for in the digital stream network flux-routing information.

Reporting of Model Predictions

For each stream reach, SPARROW models provide estimates of incremental (originating in the immediate catchment area) and accumulated (originating in the immediate and all upstream catchments) load and yield reaching the stream, volumetrically weighted concentration, and the relative contribution to stream load from different sources, termed "source-shares." In addition, the delivered incremental and accumulated load/yield from each stream reach is computed as that part of the load/yield (delivery fraction) ultimately transported downstream to the basin outlet, in this case the coastline of either the Atlantic Ocean or the Gulf of Mexico, after accounting for downstream removal/attenuation in streams and reservoirs.

Predictions from the Southeast SPARROW models are presented in three ways in this report:

1. as maps of incremental water yield and incremental TN, TP, and SS yield delivered from each of the 380,000 modeled catchments to their respective adjacent streams. Incremental yields were calculated as the amount of streamflow or constituent load generated within each incremental catchment divided by the catchment area. These values are useful for comparing the relative intensity of discharge and load generation within catchments because they are normalized for contributing area;
2. as maps of estimates of the yield from each catchment that is transported downstream to the basin outlet; and
3. as summaries of the TN, TP, and SS load and yield delivered from the catchment to the respective adjacent streams for each of the 16 four-digit Hydrologic Unit Code areas (boundaries adapted from Seaber and others, 1987; hereafter referred to as HUC4 watershed areas) within the study domain (fig. 2).

Datasets of predictions from each model are provided in Roland and Hoos (2019).

Streamflow SPARROW Model

Calibration

Observations of mean-annual streamflow (2000–14) at 569 streamflow-gaging stations in the Southeast (fig. 5*A*) were used to calibrate the streamflow SPARROW model. Values shown are for streamflow normalized by the upstream drainage area, hereafter referred to as "water yield," in millimeters per year (mm/yr). Water yield was greatest (greater than 500 mm/yr) in the northern and northwestern parts of the area and near the Gulf of Mexico coast in Mississippi, Alabama, and the panhandle of Florida. Water yield was smallest (less than 250 mm/yr) for areas draining the Piedmont region (location shown in fig. 2*B*) of North Carolina, South Carolina, and Georgia and in the interior regions of Florida. The net amount of PPT–AET was similar to the monitored flow throughout the study area (fig. 5*B*). Sites for which monitored water yield was smaller, by more than 20 percent of the average PPT–AET in the upstream area (implying loss of water in the upstream area) were clustered in central Florida and in eastern and southeastern Georgia but were otherwise dispersed relatively evenly across most states in the model area. Sites for which monitored water yield was larger, by more than 20 percent of the average PPT–AET in the upstream area (implying sources of water other than PPT–AET in the upstream area) were clustered in central Florida, in the western panhandle of Florida, and near urban centers in Alabama, Georgia, and North Carolina.

Six source terms and 18 land-to-water delivery and aquatic loss or removal factors (table 4) were evaluated as possible predictor variables in the model. The source variable *PPT–AET*, the net amount of precipitation after losses from ET, was expected to and did explain the largest part of the variability in monitored water yield. The departures (fig. 5*B*) were explained by the additional sources and the transport factors included in the streamflow model. Two additional source variables, *Spring (1st and 2nd magnitude) discharge to streams* and *Municipal/domestic wastewater discharge to streams,* were significant in explaining variation of streamflow (table 5). A fourth source variable, *Transfer of water from outside model domain (one case, from Tennessee River to a tributary of the Tombigbee River),* was assigned a coefficient value of 1 (not included in the statistical estimation) to account for the transfer of flow from outside the model domain. The variables developed to describe water inputs to the watershed from land application of municipal wastewater and irrigated agriculture (table 4) were not significant and therefore were not included in the final model. These sources may not have been significant in explaining streamflow at this

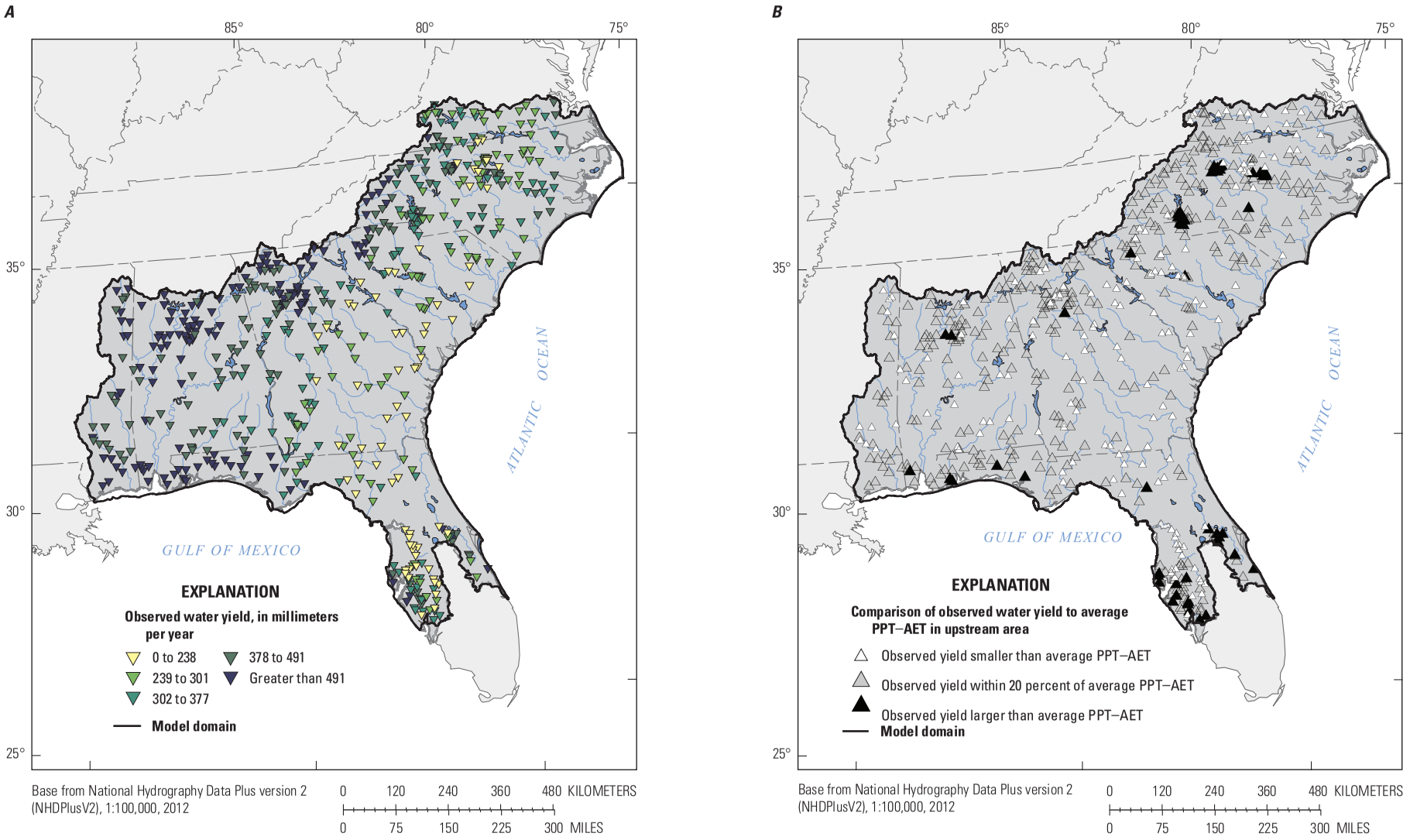

Figure 5. Mean-annual water yield for the period 2000–14 *A.* estimated from daily record from 569 streamflow gaging stations in the Southeast and *B.* compared to the average value of precipitation minus actual evapotranspiration (PPT–AET) in the area upstream from the gaging station.

Table 4. Source, delivery, loss, and removal variables evaluated in the streamflow SPARROW model for the Southeast.

[SPARROW, SPAtially Referenced Regression On Watershed attributes; Variables retained in the final specification of the model are denoted with an asterisk (*); variables tested but not retained are denoted with grey-shading; additional information (publication references, links for downloading) for each variable is provided in appendix 3; Log, natural logarithm; PPT−AET, Precipitation minus Actual Evapotranspiration; MAFlowUcfs, Mean-annual streamflow in the reach, estimate from enhanced National Hydrography Dataset Plus (NHDPlus) version 2; ft^3/s, cubic feet per second; m^3/yr, cubic meters per year; km^2, cubic meter per year; square kilometer; km, kilometer; log, natural logarithm; mm/yr, millimeter per year]

Source variable	
*	PPT−AET from water balance model, ft^3/s, mean of 2000–14
*	Spring (first and second magnitude) discharge to streams, ft^3/s
*	Municipal/domestic wastewater discharge to streams, ft^3/s, 2012
*	Transfer of water from outside model domain (one case, from Tennessee River to a tributary of the Tombigbee River), ft^3/s
	Municipal wastewater applied to land (irrigation, infiltration basin), ft^3/s, 2013
	Area of land in irrigated agriculture, km^2, 2012
Land-to-water delivery variable	
*	Log of annual mean Enhanced Vegetation Index (EVI), 2012
*	Log of percent clay
*	Log of average travel distance across catchment to stream, km
*	Log of wetland evaporation deficit (percent of catchment in wetland area conditioned by the difference term potential evapotranspiration minus actual evapotranspiration), mm/yr
*	Log of percent agricultural land, 2011
*	Log of percent urban land, 2011
	Log of impervious surface area, 2011
	Log of percent irrigated agriculture, 2012
	Log of percent tile drains, 1992
	Log of soil permeability, inches per hour
	Log of air temperature from water balance model, degrees Celsius, mean of 2000–14
	Curve number, calculated by using empirical formula for hydrologic soil group B
	Log of percent of catchment in each hydrologic soil group
Aquatic-loss variables	
*	Lake/reservoir evaporation, expressed as −log[1−(product of reciprocal areal hydraulic load and potential evapotranspiration)], unitless, mean of 2000–14
	Lake/reservoir and wetland evaporation (surface area of open waterbodies and wetlands conditioned by potential evapotranspiration), m^3/yr, mean of 2000–14
Water-removal variable	
*	Consumptive use at power plants, 2010, expressed as -log(1-fraction of unremoved streamflow)
*	Groundwater withdrawal (county level) from unconfined aquifer, 2010, expressed as −log(1−fraction of unremoved streamflow)
*	Surface-water withdrawal for municipal water supply based on popn served, 2013, expressed as −log(1−fraction of unremoved streamflow)

Table 5. Model-estimated coefficients and diagnostics for the streamflow SPARROW model for the Southeast.

[SPARROW, SPAtially Referenced Regression On Watershed attributes; additional information (publication references, links for downloading) for each variable is provided in appendix 2; --, not estimated because coefficient was fully constrained; proximal, site pairs that are within 5 kilometers distance; PPT−AET, precipitation minus actual evapotranspiration; ft^3/s, cubic feet per second; mm/yr, millimeter per year; RMSE, of the set of residuals for monitored reaches; Log, natural logarithm; R^2, coefficient of determination; *p*-value, probability value; *t*-value, *t*-statistic; <, less than]

Variable	Variable unit	Coefficient unit	Model coefficient value	90-percent confidence interval for the model coefficient		Standard error of the model coefficient	*p*-value	*t*-value	Variance inflation factor
				Lower	Upper				
Source (model coefficient = α)									
PPT−AET from water-balance model	ft^3/s	Fraction	0.923	0.880	0.966	0.033	<0.0001	27.597	13.606
Spring (first and second magnitude) discharge to streams	ft^3/s	Fraction	0.727	0.549	0.905	0.139	<0.0001	5.235	1.021
Municipal/domestic wastewater discharge to streams	ft^3/s	Fraction	0.983	0.743	1.223	0.187	<0.0001	5.256	1.096
Transfer of water from Tennessee River to a tributary of the Tombigbee River	ft^3/s	Fraction	Constrained to equal 1	--	--	--	--	--	--
Land-to-water delivery									
Log of annual mean Enhanced Vegetation Index	Unitless	Unitless	–0.772	–0.984	–0.560	0.129	<0.0001	–5.995	3.307
Log of percent clay	Unitless	Unitless	–0.223	–0.265	–0.182	0.025	<0.0001	–8.879	2.931
Log of average travel distance across catchment to stream in kilometers	Unitless	Unitless	–0.073	–0.112	–0.034	0.024	0.0023	–3.065	8.426
Log of wetland evaporation, in mm/yr	Unitless	Unitless	–0.028	–0.045	–0.011	0.010	0.0057	–2.776	2.886
Log of percent urban land	Unitless	Unitless	0.069	0.050	0.088	0.012	<0.0001	5.878	7.165
Instream loss									
Lake and reservoir evaporation, −log[1− (product of reciprocal areal hydraulic load and potential evapotranspiration)]	Unitless	Unitless	1.547	1.126	1.969	0.328	<0.0001	4.713	1.459
Removal as water withdrawals									
Consumptive use at power plants, −log(1−fraction of unremoved streamflow)	Unitless	Unitless	1.282	0.734	1.829	0.427	0.0014	3.004	1.207
Groundwater withdrawal from an unconfined aquifer, −log(1−fraction of unremoved streamflow)	Unitless	Unitless	1.209	0.930	1.488	0.218	<0.0001	5.555	1.599

Table 5. Model-estimated coefficients and diagnostics for the streamflow SPARROW model for the Southeast.—Continued

[SPARROW, SPAtially Referenced Regression on Watershed attributes; additional information (publication references, links for downloading) for each variable is provided in appendix 2; --, not estimated because coefficient was fully constrained; proximal, site pairs that are within 5 kilometers distance; PPT−AET, precipitation minus actual evapotranspiration; ft^3/s, cubic feet per second; mm/yr, millimeter per year; RMSE, of the set of residuals for monitored reaches; Log, natural logarithm; R^2, coefficient of determination; *p*-value, probability value; *t*-value, *t*-statistic; <, less than]

Variable	Variable unit	Coefficient unit	Model coefficient value	90-percent confidence interval for the model coefficient		Standard error of the model coefficient	*p*-value	*t*-value	Variance inflation factor
				Lower	Upper				
Surface-water withdrawal for municipal water supply, −log(1−fraction of unremoved streamflow)	Unitless	Unitless	1.057	0.844	1.269	0.166	<0.0001	6.384	1.065

Spatial test	Number of sites/ site pairs	Test statistic	*p*-value
Spatial autocorrelation of residuals from nonproximal sites (Moran's *I* test statistic)	569 sites	0.2608	<0.0001
Spatial autocorrelation of residuals from nonnested proximal site[a] (Pearson's *r* test statistic)	33 site pairs	0.3058	0.084
Spatial autocorrelation of residuals from nested proximal sites (Pearson's *r* test statistic	8 site pairs	0.4629	0.248
Weights—Coefficient for log of nested area share[b]	569 sites	0.758	<0.0001

Model summary statistics				
Conditioned RMSE[c]	In logarithmic space	0.17	In percent[d]	17
Unconditioned RMSE[e]	In logarithmic space	0.18	In percent[d]	18
Mean exponentiated weighted error		1.02		
R^2 of dependent variable (streamflow)		0.99		
R^2 of yield		0.81		
Number of sites used to calibrate the model		569		

[a]Also including nested stations with dissimilar drainage area.

[b]The fraction of the upstream drainage area that is downstream from other streamflow-gaging stations.

[c]Conditioned RMSE: the residuals are calculated as the difference between natural log of monitored streamflow and natural log of predicted streamflow, where the prediction has been conditioned on monitored streamflow at the closest upstream station(s).

[d]RMSE in terms of percent in real space units was computed as: $100 \times (\exp[RMSE^2]-1)^{0.5}$; RMSE in this equation is in natural log space.

[e]Unconditioned RMSE: same as conditioned RMSE except the prediction is not conditioned on monitored streamflow for upstream station(s).

scale of analysis, or their contributions may be substantial but accounted for by one or more of the final source terms that covary spatially with these sources.

The model-estimated coefficient for *PPT–AET* was 0.923 (table 5), which means that for a catchment with average properties of land-to-water delivery, 0.923 ft^3/s (0.026 m^3/s) of water is delivered to the adjacent stream channel for every 1 ft^3/s (0.028m^3/s) of *PPT–AET* applied to the catchment (explained in Guidelines for Interpreting Model-Estimated Values of Coefficients in the Methods section). Significant coefficients for *Spring (1st and 2nd magnitude) discharge to streams* and *Municipal/domestic wastewater discharge to streams* are interpreted to mean that these variables help explain streamflow variability in areas where streamflow yield was substantially larger than average values of *PPT–AET* in the upstream area (fig. 5B), for example in urban areas and in central Florida. In general, coefficient values of 1 would be expected for both these sources because source inputs were monitored at the point of discharge to the stream. The coefficient of 0.727 (table 5) for *Spring (1st and 2nd magnitude) discharge to streams* indicates that spring-discharge inputs to the model were likely overestimated (for example, were not monitored at the exact point of discharge to the stream network) and the model-calibration process compensated by estimating a coefficient lower than expected. The coefficient of 0.983 (table 5) for *Municipal/domestic wastewater discharge to streams* indicates that the estimates of wastewater discharge likely had very little bias.

Thirteen variables (table 4) were evaluated as possible land-to-water delivery variables—that is, as factors that enhance or mitigate, relative to the average delivery ratio (α), water delivery to streams from the source *PPT–AET*. The five land-to-water delivery variables were included in the final model and their estimated coefficients are listed in table 5. The larger (more different from 0) coefficient values for *Log of Enhanced Vegetation Index* and *Log of percent clay* mean that the delivery ratio for the source *PPT–AET* was most sensitive to these variables in the sense that a unit percent change in these variables will yield a larger percent change in delivery ratio than a unit percent change in the other delivery variables.

The negative coefficient (–0.772) associated with *Log of Enhanced Vegetation Index* may be explained by high rates of plant uptake leading to high values of evapotranspiration losses that were not fully accounted for in the water-balance calculations of AET used to derive PPT–AET. The negative coefficient (–0.223) associated with *Log of percent clay* is counterintuitive given the tendency of clay soils to increase yield of direct runoff to streams compared to sandy soils by reducing the proportion of PPT–AET that infiltrates to the subsurface and groundwater and returns to the stream as base flow. The negative coefficient for this variable in the SPARROW model may be explained by the negative spatial correlation of clay soils with areas of groundwater discharge from regional aquifer systems, for example where the upper confining unit of the Floridan aquifer is thin or absent (northwestern Florida, southern Georgia, and southern Alabama). Negative correlation may also be caused by interaction or collinear effects with other land-to-water delivery variables. To test these hypotheses, the model was calibrated with *Log of percent clay* as the only land-to-water delivery variable and using only the calibration sites outside the areas of groundwater discharge from the Floridan aquifer (spatial extent shown in Williams and Dixon, 2015, fig. 55); the estimated coefficient was positive and not significant. As noted in the section Guidelines for Interpreting Model-Estimated Values of Coefficients in the Methods section, the sign (positive or negative) of a delivery variable coefficient may result from spatial covariation with other delivery variables rather than indicating that it directly affects transport processes.

The negative coefficients (–0.073 and –0.028, respectively) for the delivery variables *Log of travel distance across catchment to stream* and *Log of wetland evaporation deficit* can be explained by higher evaporative losses during overland transport along longer flow paths and higher evaporative losses for both runoff and groundwater discharge intercepted by wetland areas within the catchment.

The positive coefficient (0.069) for *Log of percent urban land* may reflect the combined effect of paved surfaces increasing yield of direct runoff to streams compared to pervious surfaces, and the shorter travel times of direct runoff in urban streams altered for efficient stormwater conveyance, decreasing loss of water to evaporation. The positive coefficient also may represent some hydrologic manipulations in urban areas that are not accounted for by the source variable *Municipal/domestic wastewater discharge to streams*. For example, wastewater discharge to streams from industrial facilities and combined wastewater/stormwater discharge to streams, neither of which is accounted for in the source variable *Municipal/domestic wastewater discharge to streams,* may increase streamflow in urban areas where they represent a water transfer from one watershed to another.

A single variable, *Lake/reservoir evaporation* (5), was evaluated to characterize the loss of water during transport through lakes and reservoirs. The estimated coefficient, 1.547, for the first-order reservoir decay function implies that a 1-percent increase in the term (1–Lake/reservoir evaporation) causes a 1.547-percent decrease in the delivery fraction for a reach. That the coefficient is greater than 1.0 indicates that the estimates for *Lake/reservoir evaporation* likely underestimate evaporative losses from the waterbody.

All three removal variables tested in the streamflow model to represent direct or indirect withdrawals from the stream were significant (table 5). The estimated coefficient values 1.282, 1.209, and 1.057 for the variables *Consumptive use at power plants*, *Groundwater withdrawal from an unconfined aquifer*, and *Surface-water withdrawal for municipal water supply,* respectively, are rate coefficients for a first-order decay function and have the same meaning as the coefficient for *Lake/reservoir evaporation*. A coefficient close to 1 implies a 1:1 correspondence between the term (1–Qwithdrawal/Qreach) computed from the input data, and the delivery fraction for the reach. A coefficient value substantially larger or

smaller than 1 indicates that the estimates of Qwithdrawal are biased high or low, respectively, compared to the amount of flow actually removed from the stream.

Goodness of fit between the monitored values of streamflow and the values predicted with the streamflow SPARROW model is quantified in the calibration statistics reported in table 5 and illustrated by graphs and maps of model error at calibration stations (figs. 6 and 7). The RMSEs of conditioned and unconditioned residuals, 0.17 and 0.18, respectively (table 5), are equivalent to mean error of 17 and 18 percent, respectively. The R^2 of yield for the streamflow model, 0.81 (table 5), measures the fraction of variance in the monitored water yield (in log space) that is accounted for by the model; therefore, the streamflow model explains 81 percent of the variance in log-transformed monitored water yield.

The tight clustering of observations around the 1:1 line for predicted against actual streamflow (fig. 6*A*, *B*) illustrates the small error compared to the range of values. The residuals were essentially homoscedastic, with only a slight tendency toward larger residuals for smaller predicted values of streamflow (see figure 6*C*). Heteroscedasticity was slightly more pronounced in the residuals of yield, illustrated in figure 6*D*, but overall the model fit was very good.

Most of the 30 sites with extreme over- or underprediction of water yield were in urban areas in North Carolina or Florida. Extreme over- or underprediction is defined here as unconditioned residual values outside the interval prescribed by -2*RMSE to 2*RMSE, which for this model corresponds to -0.34 to 0.34 (or about 35 percent error). These extreme cases are depicted in figure 7*A* as the darkest color triangles. The large errors in urban areas indicate that the predictor variables in the final streamflow model probably do not sufficiently characterize the hydrologic manipulations that effectively divert water between urban watersheds (despite inclusion of information on withdrawals for municipal water supply, irrigation, and power generation). The large errors for many sites in Florida indicate the need for improved characterization of diversions and for information about the substantial contributions to or losses from streams related to regional groundwater in this karst landscape.

The distribution of overprediction as opposed to underprediction among sites (fig. 7) has a distinct spatial structure or bias: the model tends to underpredict in some areas (most sites in North Carolina) and overpredict in other areas (most sites in Georgia and Mississippi). The statistical test Moran's *I* (Cliff and Ord, 1973) provides a quantitative estimate of spatial autocorrelation. The test statistic of 0.26 with an associated *p*-value less than 0.0001 (table 5) confirms positive and statistically significant spatial autocorrelation, which indicates the likelihood of potential shortcomings in the model specification, such as omission of an important source or delivery term or spatial bias in one or more input variables. These conditions may have caused bias in estimation of the model coefficients.

Residuals of site pairs in close proximity (less than 5 km apart) were tested for significant and negative autocorrelation. The site pairs were divided into two groups for testing, according to their nested status and in correspondence with two possible causes of spatial dependency (described in the Methods section). The residuals in both groups were spatially independent, with *p*-values for the two tests of 0.084 and 0.248 (table 5). A finding of significant correlation would have implied that observations used to calibrate the model were not independent and could have resulted in bias in estimation (underestimation) of the standard error of coefficients. Therefore, none of the sites from the proximal site pairs was removed from the calibration set.

The positive value (0.758) and *p*-value less than 0.0001 for the coefficient for nested area share (table 5) indicates that calibrating the model without accounting for the effects of nested basins would have underestimated residuals and discounted the effect of downstream sites in the model calibration. The final calibrated model reported in table 5 therefore incorporated a recalibration step in which weighted regression was used to address the unequal effects of nested basins in calibration (described in the Methods section).

Predictions

The streamflow SPARROW model was used to predict mean-annual streamflow and water yield for streams throughout the Southeast for the period 2000–14 (fig. 8). The pattern of model-predicted water yield is nearly identical to the pattern of monitored water yield (fig. 5*A*): largest (greater than 500 mm/yr) in northern Georgia, Alabama, and Mississippi and near the Gulf of Mexico coast in Mississippi, Alabama, and the panhandle of Florida, and near the coast of North Carolina. The broad band that extends from northwestern Mississippi through central Alabama with predicted yield smaller than 400 mm/year matches the pattern of monitored water yield but departs from the pattern for PPT–AET. This difference corresponds to the presence of soil with higher clay content in the Black Belt region (location shown in figure 2*B*) and results from the finding that greater clay content of soil is associated with lower delivery to streams. The thin band of higher water-yielding catchments that extends northeastward through central Georgia and South Carolina corresponds with presence of soil with high sand content, referred to in North and South Carolina as the Sand Hill region (location shown in figure 2*B*).

The almost identical pattern of predicted water yield from catchment to adjacent stream and predicted water yield from catchment to the basin outlet at coastal waters (comparing figures 8*A* and *B*) for most of the model domain illustrates that losses of water during transport through the channel network to the coast are relatively insignificant. Differences between figures 8*A* and 8*B* in certain areas, for example small tributaries in north Georgia, correspond with withdrawals/diversions for municipal water supply, irrigation, and power generation, or with evaporation from reservoirs.

Predicted variables from the streamflow SPARROW model were linked with the three constituent models

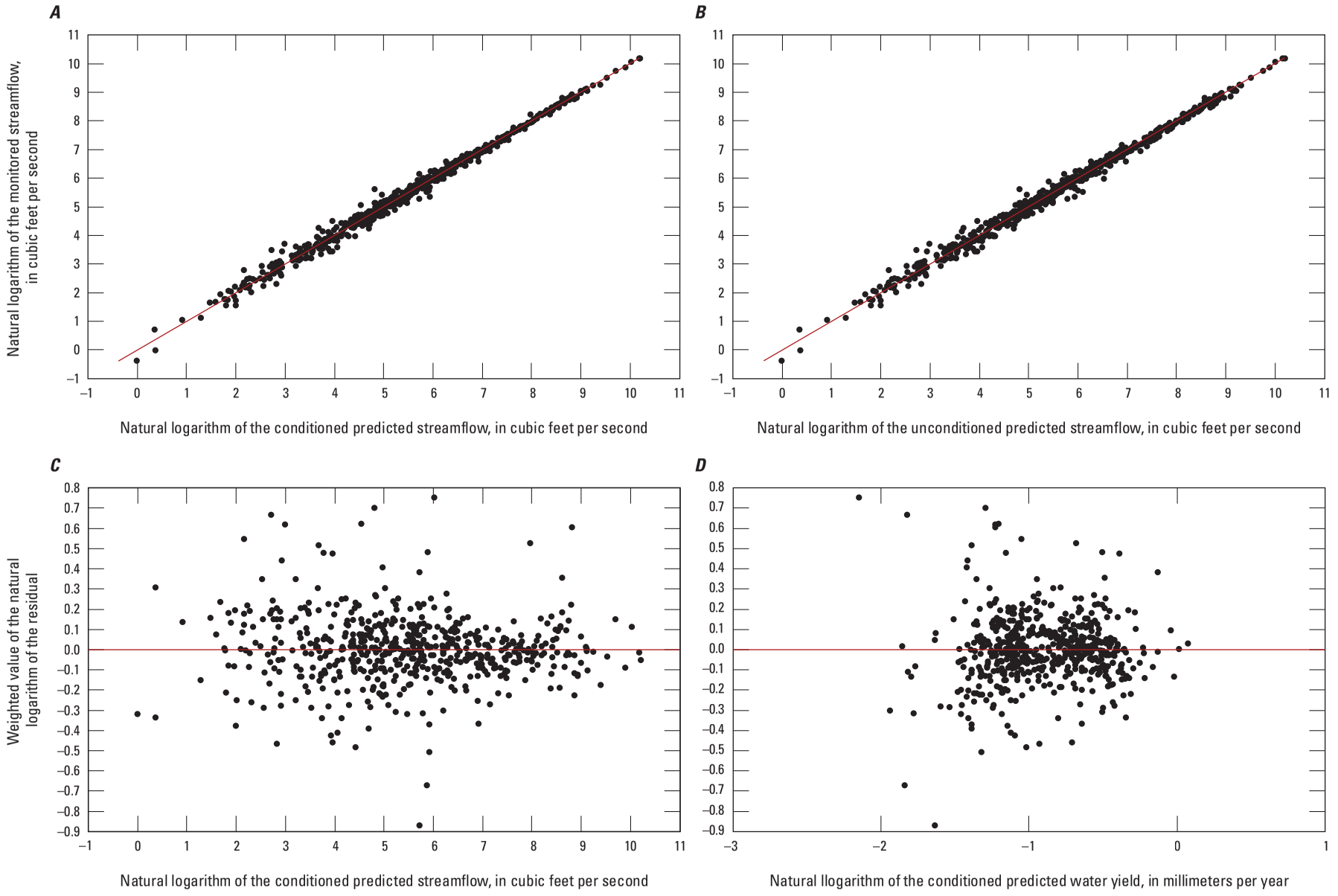

Figure 6. Diagnostic plots for the streamflow SPARROW (SPAtially Referenced Regression On Watershed attributes) model for the Southeast: *A*. monitored streamflow versus conditioned predicted streamflow, *B*. monitored streamflow versus unconditioned predicted streamflow, *C*. weighted residuals versus predicted streamflow, and *D*. weighted residuals versus predicted yield, for 569 calibration stations. Conditioned predicted streamflow means that the prediction is conditioned on monitored streamflow for the closest upstream station(s). Unconditioned predicted streamflow means that the prediction is not conditioned on monitored streamflow for upstream station(s).

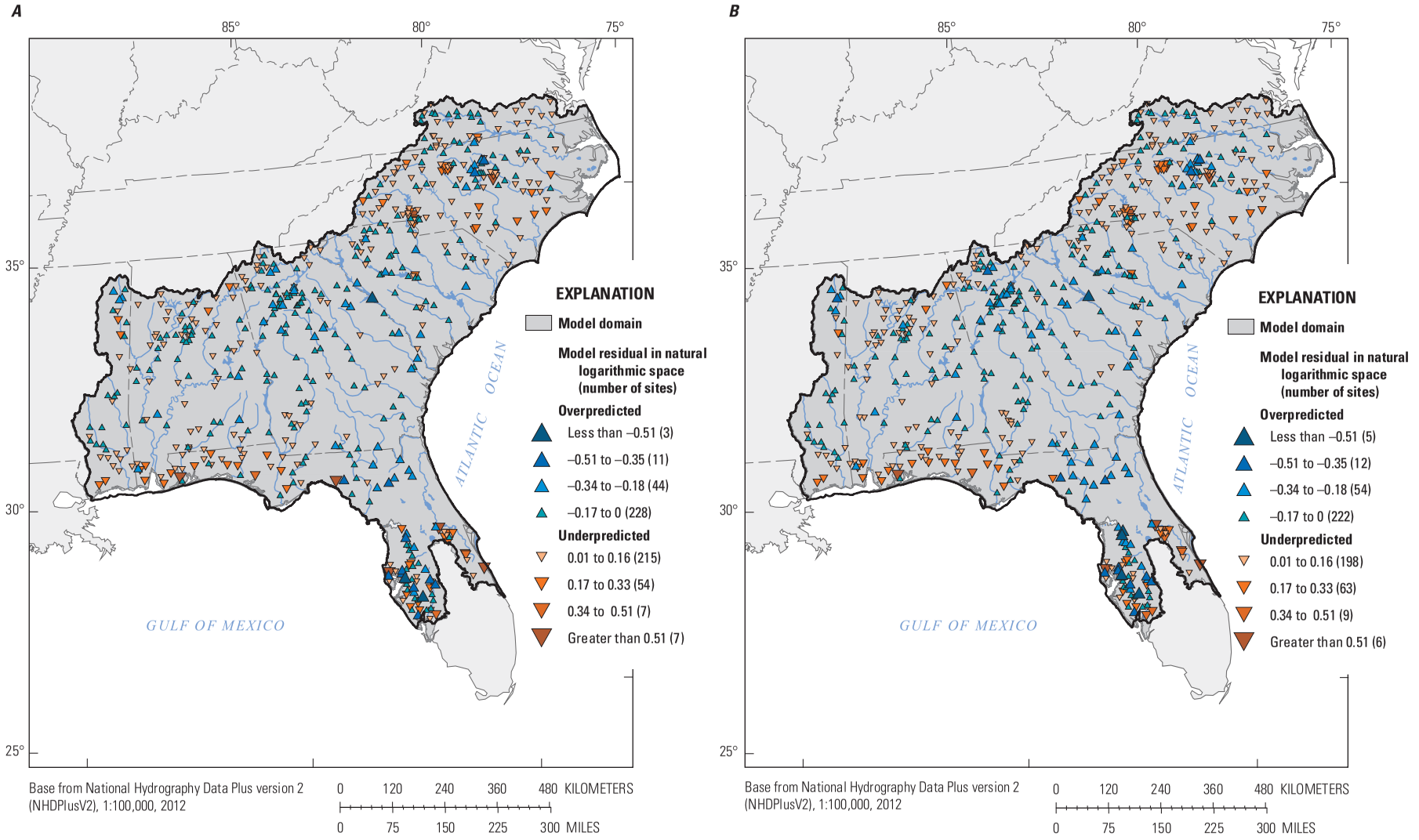

Figure 7. Spatial distribution of *A*. conditioned residuals and *B*. unconditioned residuals from the streamflow SPARROW (SPAtially Referenced Regression On Watershed attributes) model for the Southeast. Conditioned residuals are calculated as the difference between natural log of monitored streamflow and natural log of predicted streamflow, where the prediction has been conditioned on the monitored streamflow at the closest upstream station(s). For unconditioned residuals the prediction is not conditioned on monitored streamflow for upstream streamflow-gaging station(s).

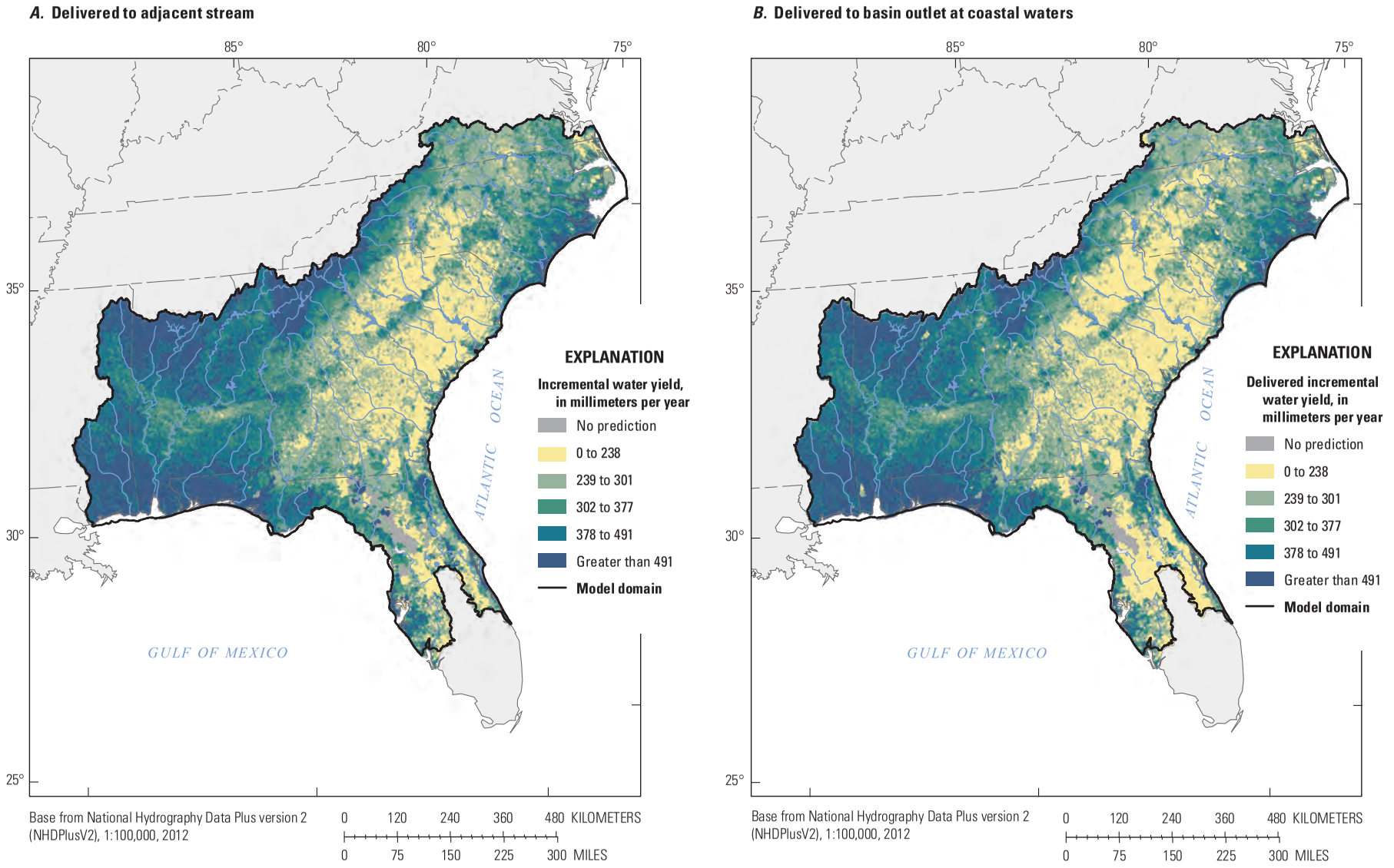

Figure 8. Mean-annual incremental yield of water *A.* delivered to the adjacent stream, and *B.* delivered to the basin outlet at coastal waters, predicted from the streamflow SPARROW (SPAtially Referenced Regression On Watershed attributes) model for the Southeast.

(TN, TP, and SS). The SPARROW-predicted *Incremental flow from catchment* was tested in each constituent model as a land-to-water delivery variable and its performance was compared with the variable *PPT–AET*. The SPARROW-predicted streamflow in each reach (including upstream contributions), referred to as the variable *PredQ_SESpar*, was also used in computations of the predictor variables evaluated as aquatic-loss variables and in computed mean-annual flow-weighted concentration for each reach. Compared to the estimate of streamflow in NHDPlusv2, the SPARROW prediction of streamflow has the advantage of accounting for the identical set of water removals specified in the streamflow model.

Total Nitrogen SPARROW Model

Calibration

Observations of TN load at 603 monitoring sites in the Southeast (illustrated as yields in figure 9) were used to calibrate the TN SPARROW model. Nitrogen yields were smallest, less than 200 kilograms per square kilometer per year ([kg/km²]/yr), for sites in southern Virginia, northern North Carolina, South Carolina, and isolated areas in Georgia and Florida. Nitrogen yields exceeding 423 (kg/km²)/yr were observed throughout the Southeast and were especially prevalent in the Piedmont region of Georgia and North Carolina, in the Coastal Plain region of North Carolina, and in many parts of Florida (locations of Piedmont and Coastal Plain regions are shown in figure 2*B*).

The source terms and transport and delivery factors tested in the TN model are listed in table 6. Of the 16 attributes tested as source variables, two variables represent natural sources of N: *Density of N-fixing tree species* and a component of *Atmospheric deposition of TN*. Only a part of the atmospheric deposition source term represents natural sources, however, because emissions from anthropogenic activities contribute substantially to atmospheric N in many areas of the Southeast. The remaining 15 variables tested as sources in the TN model represent the spatial distribution of anthropogenic sources.

Five source terms were significant in explaining variation of TN loads (table 7): *Atmospheric deposition of TN*, *Municipal/domestic wastewater TN discharged to streams*, *Urban land cover*, *Fertilizer TN applied to agricultural land*, and *Manure TN from livestock production*. The variables developed to describe N inputs to the watershed from N fixation by cropland or trees, land application of municipal wastewater, septic systems, industrial wastewater, and spring discharge were not significant and therefore were not included in the final model. These sources may not have been significant in explaining TN loads at the scale of this analysis, or their contributions may be substantial but accounted for by one or more of the final source terms that covary spatially with these sources.

The model-estimated value of 0.947 (table 7) for *Municipal/domestic wastewater TN discharged to streams* indicates that the input estimates of TN load in municipal/domestic wastewater were relatively unbiased and (or) that all of the TN in the effluent from these facilities is accounted for in the monitored stream loads. The other significant N sources were applied to the land surface rather than discharged directly to the stream; therefore, they were subject to processes of N transformation and attenuation during land-to-water delivery. The coefficients for the land-applied sources represent the mass delivery ratio for a catchment with average land-to-water delivery properties. For example, the coefficient estimate of 0.085 associated with *Agricultural fertilizer* may be interpreted as indicating that 8.0 percent of the N applied as fertilizer is delivered to adjacent stream reaches, if average delivery properties for the catchment are assumed.

The delivery ratio for land-applied sources was simulated as varying among catchments according to all the model-specified processes of N transformation and attenuation during land-to-water delivery for that source category. Such processes include denitrification in soil, losses during subsurface transport to streams, or processes that extend the residence time in soil or subsurface transport compared to surface transport. Twelve watershed characteristics were evaluated as possible land-to-water delivery variables (table 6). The four land-to-water delivery variables in the final model and their associated coefficients and statistics are presented in table 7.

The larger coefficient values for *Log of summer Enhanced Vegetation Index* and *Log of PPT–AET* mean that TN delivery was most sensitive to these variables. The positive coefficient (0.554) associated with *Log of PPT–AET* may be explained by higher rates of water transport through the catchment and therefore shorter travel times, allowing less opportunity for immobilization and exposure to anaerobic conditions and denitrification. The negative coefficient (-0.775) associated with *Log of summer Enhanced Vegetation Index* may be explained by high rates of plant uptake leading to relatively high denitrification or immobilization on the landscape.

The positive coefficient (0.117) associated with the variable *Soil organic matter content* may result from the association between organic-matter content and saturated hydric soils of riverine and palustrine wetlands. Hoos and others (2013) found that wetland systems were associated with enhanced land-to-water delivery of N (lower than average removal efficiency) and indicate that this effect may be caused by conversion of bioavailable N to refractory organic N (for example, see Wiegner and Seitzinger, 2004) and thus higher TN loading through the stream channel. The negative coefficient (-0.166) associated with *Percent cover crops* may be caused by increased rates of plant uptake and harvest of residual fertilizer from the cultivated field or by increased denitrification or immobilization of N associated with reduced direct runoff from cover-cropped fields. The agricultural best management

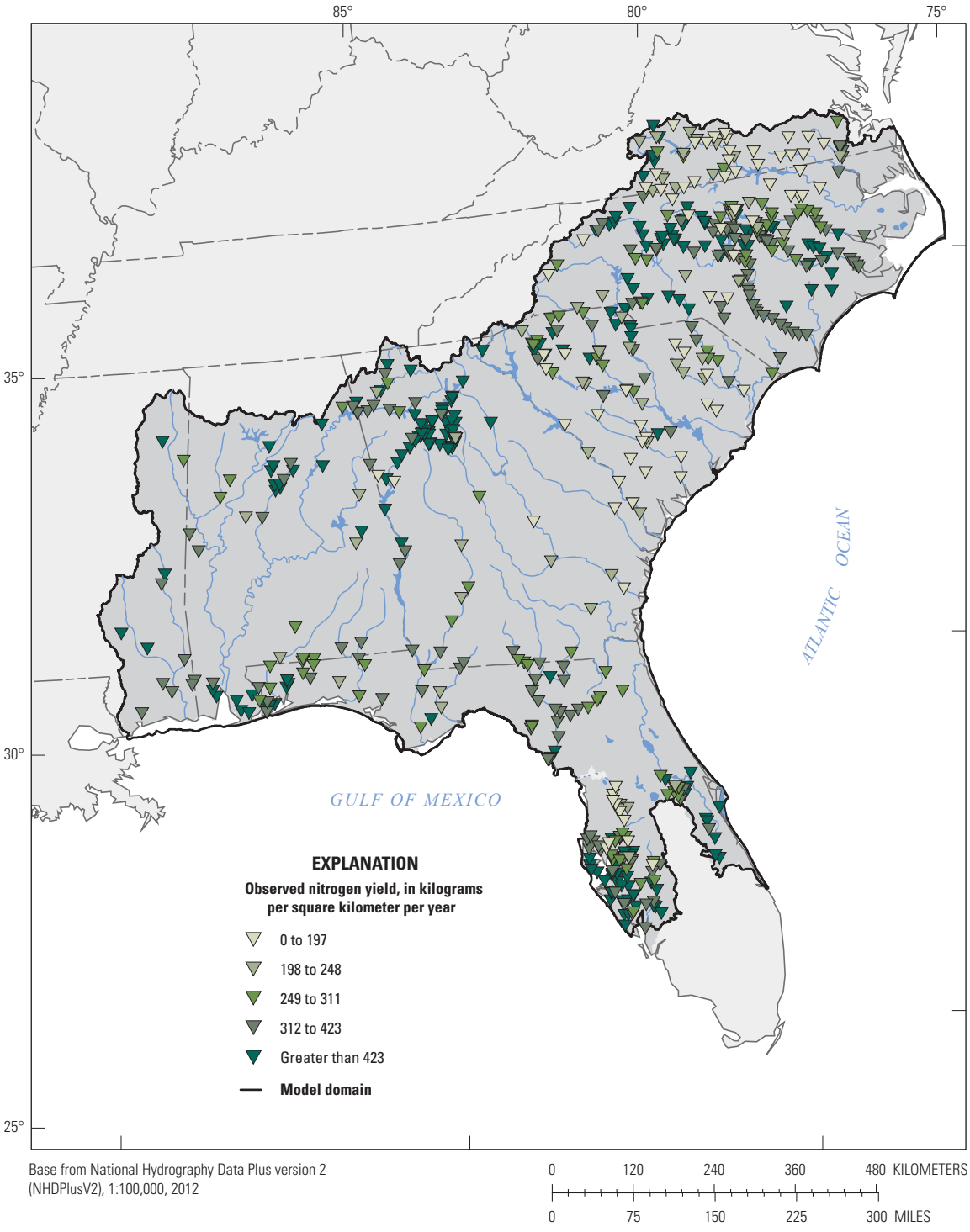

Figure 9. Total nitrogen yield estimated for the base year 2012 from stream monitoring data from 603 sites in the Southeast.

Table 6. Source, delivery, loss, and removal variables evaluated in the total nitrogen SPARROW model for the Southeast.

[SPARROW, SPAtially Referenced Regression On Watershed attributes; variables retained in the final specification of the model are denoted with an asterisk (*); variables tested but not retained are denoted with grey-shading; additional information (publication references, links for downloading) for each variable is provided in appendix 3; Log, natural logarithm; TN, total nitrogen; N, nitrogen; PPT−AET, precipitation minus actual evapotranspiration; PredQ_SESpar, mean-annual streamflow in the reach, 2000–14, estimated from conditioned predictions of the streamflow SPARROW model; NHD, National Hydrography Dataset; NID, National Inventory of Dams; MAFlowUcfs, mean-annual streamflow in the reach, estimate from enhanced National Hydrography Dataset Plus (NHDPlus) version 2; kg/yr, kilograms per year; km^2, square kilometers; ft^3/s, cubic foot per second; mm/yr, millimeter per year; <, less than; >, greater than]

	Source variables
*	Atmospheric deposition of TN, kg/yr, mean of 2010–12
*	Municipal/domestic wastewater TN discharge to streams, kg/yr, 2012
*	Urban land cover, km^2, 2011
*	Fertilizer TN applied to agricultural land, kg/yr (national weighted), kg/yr, 2012
*	Manure TN from livestock production, kg/yr, 2012
	Density of N-fixing tree species, 2010
	Cropland area of N-fixing cultivated crops, km^2, 2012
	Municipal wastewater applied to land (irrigation, infiltration basin), ft^3/s, 2013
	Population on septic system, 2010 (estimated by using 1990 percent of population served by septic system)
	Industrial wastewater TN discharged to streams, kg/yr, 2012
	Fertilizer TN applied to agricultural land (state weighted), kg/yr, 2012
	Fertilizer TN applied to agricultural land (unconditioned), kg/yr, 2012
	Fertilizer TN applied to agricultural land (Kalman conditioned), kg/yr, 2012
	Spring (first and second magnitude) discharge to streams, ft^3/s
	Spring (first magnitude) TN discharge to streams, kg/yr
	Spring (first and second magnitude) TN discharge to streams, kg/yr
	Land-to-water delivery variables
*	Log of PPT−AET, mm/yr, detrended to base year 2012; in contrast to PPT-AET used as source term in the streamflow model, this term is normalized by the area of the catchment
*	Log of summer mean Enhanced Vegetation Index (EVI), 2012
*	Log of soil organic-matter content
*	Log of percent of catchment in cover crops, 2012
	Log of incremental flow from catchment to stream (streamflow SPARROW model), mean of 2000–14
	Log of air temperature from water-balance model), celsius, mean of 2000–14
	Log of annual mean EVI, 2012
	Log of soil permeability, inches per hour
	Log of percent clay
	Log of depth to bedrock, inches
	Log of percent of catchment in no till or conservation tillage, 2012
	Log of percent of catchment in conservation easement, 2012
	Aquatic-loss variables
*	Reach time of travel (days) per meter of stream depth, where depth is estimated as a continuous function of stream discharge PredQ_SESpar and other channel characteristics (using the six-parameter regional regression equation)
*	Reciprocal areal hydraulic load for waterbodies in karst landscape (mostly in Florida), calculated by using surface area from NHD or NID and stream discharge PredQ_SESpar
*	Reciprocal areal hydraulic load for waterbodies not in karst landscape, calculated by using surface area from NHD or NID and stream discharge PredQ_SESpar
	Reach time of travel per meter of stream depth, where depth is estimated as a continuous function of stream discharge PredQ_SESpar according to the simple power law formula: depth (meters) = 0.06356 * PredQ_SESpar (ft^3/s) ^ 0.3966
	Time of travel in small streams (stream discharge <30 ft^3/s)
	Time of travel in intermediate streams (stream discharge 31–100 ft^3/s, or 0.849–2.83 m^3/s
	Time of travel in large streams (stream discharge > 100 ft^3/s, or > 2.83 m^3/s)
	Water-removal variables
*	Consumptive use at power plants, 2010, expressed as −log(1−fraction of unremoved streamflow)
*	Groundwater withdrawal (county level) from unconfined aquifer, 2010, expressed as, −log(1−fraction of unremoved streamflow)
*	Surface-water withdrawal for municipal water supply based on popn served, 2013, expressed as −log(1−fraction of unremoved streamflow)

Table 7. Model-estimated coefficients and diagnostics for the total nitrogen SPARROW model for the Southeast.

[SPARROW, SPAtially Referenced Regression On Watershed attributes; additional information (publication references, links for downloading) for each variable is provided in appendix 2; TN, total nitrogen; kg/yr, kilogram per year; km2, square kilometer PPT−AET, precipitation minus actual evapotranspiration; not sign., coefficient for reservoirs and lakes in karst landsape is statistically indistinguishable from zero but is retained in order to complete the description of TN removal across across all lakes and reservoirs in the Southeast; --, not estimated because coefficient was fully constrained; RMSE, root mean squared error; Log, natural logarithm; R^2, coefficient of determination; proximal, site pairs that are within 5 kilometers distance; d/m, day per meter; yr/m, year per meter; kg/km^2/yr; kilogram per square kilometer per year; m/d, meter per day; m/yr, meter per year; *p*-value, probability value; *t*-value, *t*-statistic <, less than]

Variable	Variable unit	Coefficient unit	Model coefficient value	90-percent confidence interval for the model coefficient		Standard error of the model coefficient	*p*-value	*t*-value	Variance inflation factor
				Lower	Upper				
Source (model coefficient = α)									
Atmospheric deposition of TN	kg/yr	Fraction	0.338	0.295	0.380	0.033	<0.0001	10.115	8.090
Municipal/domestic wastewater TN discharged to streams	kg/yr	Fraction	0.947	0.828	1.066	0.093	<0.0001	10.230	1.138
Urban land cover	km^2	kg/km^2/yr	292.595	201.541	383.649	70.970	<0.0001	4.123	3.262
Fertilizer TN applied to agricultural land, national weighted	kg/yr	Fraction	0.085	0.067	0.103	0.014	<0.0001	6.058	2.397
Manure TN from livestock production	kg/yr	Fraction	0.047	0.026	0.068	0.016	0.0020	2.893	2.639
Land-to-water delivery									
Log of PPT−AET, in mm/yr	Unitless	Unitless	0.554	0.408	0.699	0.088	<0.0001	6.278	1.555
Log of summer Enhanced Vegetation Index (EVI)	Unitless	Unitless	–0.775	–1.081	–0.470	0.185	<0.0001	–4.182	2.425
Log of soil organic-matter content, in percent	Unitless	Unitless	0.117	0.054	0.181	0.038	0.0024	3.054	1.267
Log of cover crops area, in percent of catchment	Unitless	Unitless	–0.166	–0.213	–0.119	0.029	<0.0001	–5.818	1.090
Aquatic loss									
Streams and rivers—Reach time of travel per meter of stream depth	d/m	m/d	0.083	0.052	0.114	0.024	0.0003	3.462	4.670
Reservoirs and lakes—Reciprocal of areal hydraulic load (excludes waterbodies in karst landscape)	yr/m	m/yr	5.036	3.561	6.512	1.150	<0.0001	4.378	1.257
Reservoirs and lakes—Reciprocal of areal hydraulic load (waterbodies in karst landscape)	yr/m	m/yr	0.827 (not sign.)	0.000	2.109	0.999	0.2041	0.828	1.127
Removal as water withdrawals									
Consumptive use at power plants, fraction of instream flow	log(1−fraction of unremoved streamflow)	Unitless	1.282	--	--	--	--	--	--
Groundwater withdrawal from an unconfined aquifer, fraction of instream flow	log(1−fraction of unremoved streamflow)	Unitless	1.209	--	--	--	--	--	--

Table 7. Model-estimated coefficients and diagnostics for the total nitrogen SPARROW model for the Southeast.—Continued

[SPARROW, SPAtially Referenced Regression On Watershed attributes; additional information (publication references, links for downloading) for each variable is provided in appendix 2; TN, total nitrogen; kg/yr, kilogram per year; km2, square kilometer PPT−AET, precipitation minus actual evapotranspiration; not sign., coefficient for reservoirs and lakes in karst landsape is statistically indistinguishable from zero but is retained in order to complete the description of TN removal across across all lakes and reservoirs in the Southeast; --, not estimated because coefficient was fully constrained; RMSE, root mean squared error; Log, natural logarithm; R^2, coefficient of determination; proximal, site pairs that are within 5 kilometers distance; d/m, day per meter; yr/m, year per meter; kg/km^2/yr; kilogram per square kilometer per year; m/d, meter per day; m/yr, meter per year; *p*-value, probability value; *t*-value, *t*-statistic <, less than]

Variable	Variable unit	Coefficient unit	Model coefficient value	90-percent confidence interval for the model coefficient		Standard error of the model coefficient	*p*-value	*t*-value	Variance inflation factor
				Lower	Upper				
Surface-water withdrawal for municipal water supply, fraction of instream flow	Ln (1−fraction of unremoved streamflow)	Unitless	1.057	--	--	--	--	--	--

Spatial test	Number of sites/site pairs	Test statistic	*p*-value
Spatial autocorrelation of residuals from nonproximal sites (Moran's *I* test statistic)	598 sites	0.0166	0.429
Spatial autocorrelation of residuals from nonnested proximal site[a] (Pearson's *r* test statistic)	87 site pairs	0.0556	0.179
Spatial autocorrelation of residuals from nested proximal sites (Pearson's *r* test statistic	43 site pairs	–0.1613	0.208
Weights: coefficient for log of nested area share[b]	598 sites	0.814	<0.0001

Model summary statistics				
Conditioned RMSE[c]	In logarithmic space	0.35	In percent[d]	36
Unconditioned RMSE[e]	In logarithmic space	0.36	In percent[d]	38
Mean exponentiated weighted error		1.07		
R^2 of dependent variable (load)		0.97		
R^2 of yield		0.65		
Number of sites used to calibrate the model		598		

[a]Also including nested sites with dissimilar drainage area.

[b]The fraction of the upstream drainage area that is downstream from other monitoring sites.

[c]Conditioned RMSE: the residuals are calculated as the difference between natural log of monitored load and natural log of predicted load, where the prediction has been conditioned on monitored load at the closest upstream site(s).

[d]RMSE in terms of percent in real space units was computed as: $100 \times (\exp[RMSE^2]-1)^{0.5}$; RMSE in this equation is in natural log space.

[e]Unconditioned RMSE: same as conditioned RMSE except the prediction is not conditioned on monitored load for upstream station(s).

practices of no till, conservation tillage, and conservation easements were tested but were not significant.

Ten physical stream-channel, reservoir, and lake attributes characterizing aquatic loss or removal of N during transport through the stream network were evaluated (table 6). The only attribute selected to represent N loss in free-flowing streams was computed as the quotient of mean water travel time and mean water depth in a stream reach, in days per meter (d/m). Nitrogen loss was modeled as a first-order decay function; therefore, its coefficient (0.083 m/d) can be interpreted as the rate of N loss per day of water travel time. Estimated mean water depth for stream reaches in the Southeast mostly ranges between 0.10 and 1.0 meter (5th and 95th percentile); therefore, the model-calculated rate of N loss per day of water travel time typically ranges between 0.83/d (small streams) and 0.083/d (large rivers). This inverse relation between N loss-rate coefficient and stream depth is consistent with the concept that attenuation from denitrification is inversely related to stream depth and directly related to the associated proportion of transported mass in contact with the streambed. The coefficient estimate for the Southeast of 0.083 m/d is within the range of results of experimental studies (Howarth and others, 1996; Mulholland and others, 2004). Comparison of the estimated coefficient to values reported for previous TN SPARROW models for the Southeast is not possible because TN loss rate as a function of stream depth was not specified in previous models. This estimate is about twice the TN loss rate estimated by a previous TN SPARROW model for the Midwest (Robertson and Saad, 2013).

The variable representing loss in lakes and reservoirs, *Reciprocal of areal hydraulic load* (*years per meter* [*yr/m*]), is the ratio of lake or reservoir surface area to outflow, computed for each incremental segment of the waterbody. The estimated coefficient for the first-order reservoir decay function (5.036 for lakes and reservoirs in the Southeast excluding karst landscape) can be interpreted as a hypothetical settling velocity (meters per year) that, when multiplied by the reciprocal of areal hydraulic load (years per meter) and exponentiated, quantifies the proportion of the TN mass transported through the lake or reservoir. The reservoir loss rate coefficient for lakes and reservoirs in Florida was much smaller (0.827) and not significant. The value of 5.036 meters per year (m/yr) for waterbodies excluding Florida compares closely with the estimate (5.8 m/yr) from the 2002 TN SPARROW model for the eastern U.S. (Hoos and others, 2013), which was based on the NHDPlusv1 stream network (U.S. Environmental Protection Agency and U.S. Geological Survey, 2010), and is about half the estimate (13.1 m/yr) from the 2002 TN model for the Southeast (Hoos and McMahon, 2009), which was based on a coarser resolution, 1:500,000-scale stream network. A larger estimate of loss rate coefficient was expected for the coarser resolution network, as it likely compensates for a sparser representation of lakes and reservoirs.

The variables used in the TN model to represent direct or indirect withdrawals from the stream were *Consumptive use at power plants*, *Groundwater withdrawal from unconfined aquifer*, and *Surface-water withdrawal for municipal water supply*. The coefficients for these variables were not estimated in the TN model; rather, they were constrained to equal the estimated coefficient values from the calibrated streamflow SPARROW model. It was assumed that the coefficient values estimated for these three variables by the streamflow SPARROW model (1.282, 1.209, and 1.057, respectively) can properly represent the effects of water withdrawals on TN transport.

Goodness of fit between the monitored values of TN load and yield (fig. 9) and the values predicted by the SPARROW TN model is quantified in the calibration statistics reported in table 7 and illustrated by graphs and maps of model error (figs. 10 and 11). The RMSE of conditioned and unconditioned residuals (see Glossary for definition of these terms), 0.35 and 0.36, respectively (table 7), are equivalent to a mean error of 36 and 38 percent, respectively. The R^2 of yield for the TN model, 0.65 (table 7), indicates the TN model explains 65 percent of the variance in log-transformed monitored TN yield.

Conditioned residuals from the TN model were slightly larger for smaller predicted values of load than for larger predicted values (fig. 10*A*). The difference in variance (heteroscedasticity) over the range in values is slight. and display no structure around any particular values of the log transformed condition TN predictions (fig. 10*C*). Overall, the error structure is acceptable. Heteroscedasticity was more pronounced in the residuals of yield (fig. 10*D*), errors were larger and more variable for sites with smaller TN yields. The spread of observations around the 1:1 line for predicted against monitored TN load was similar for conditioned and unconditioned residuals (compare figures 10*A* and 10*B*).

Aside from a cluster of consistent underpredictions (unconditioned residuals greater than 0.5) throughout the Suwannee River Basin in northern Florida (fig. 2*B*, discussed in the following paragraph), the spatial pattern of unconditioned residuals (fig. 11) is a scattered pattern of over- and underpredictions with no tendency to predominantly over- or underpredict in specific areas. The Moran's *I* test statistic of 0.0166 and associated *p*-value of 0.429 (table 7) confirmed that residuals were not spatially autocorrelated and that there were not potential shortcomings in the model specification.

TN loads in the Suwannee River Basin were consistently underpredicted, in contrast to the consistent overprediction of streamflow by the streamflow SPARROW model (compare figure 10 to figure 7). Most of the errors along the mainstem of the Suwannee River were caused by large underprediction errors at two upstream sites that propagated downstream for unconditioned predictions (compare figure 11*A* to figure 11*B*). Groundwater discharge of TN from the Upper Floridan aquifer to springs is an increasing source of TN in some tributaries of the Suwannee River Basin (Katz and others, 1999; Upchurch and others, 2007). The predictor variable *Spring* (*1st and 2nd magnitude*) *discharge to streams* was tested in the TN SPARROW model to account for groundwater contribution of nitrate but was not significant.

Residuals for close proximity site pairs (nested and non-nested site pairs less than 5 km apart) were tested for significant

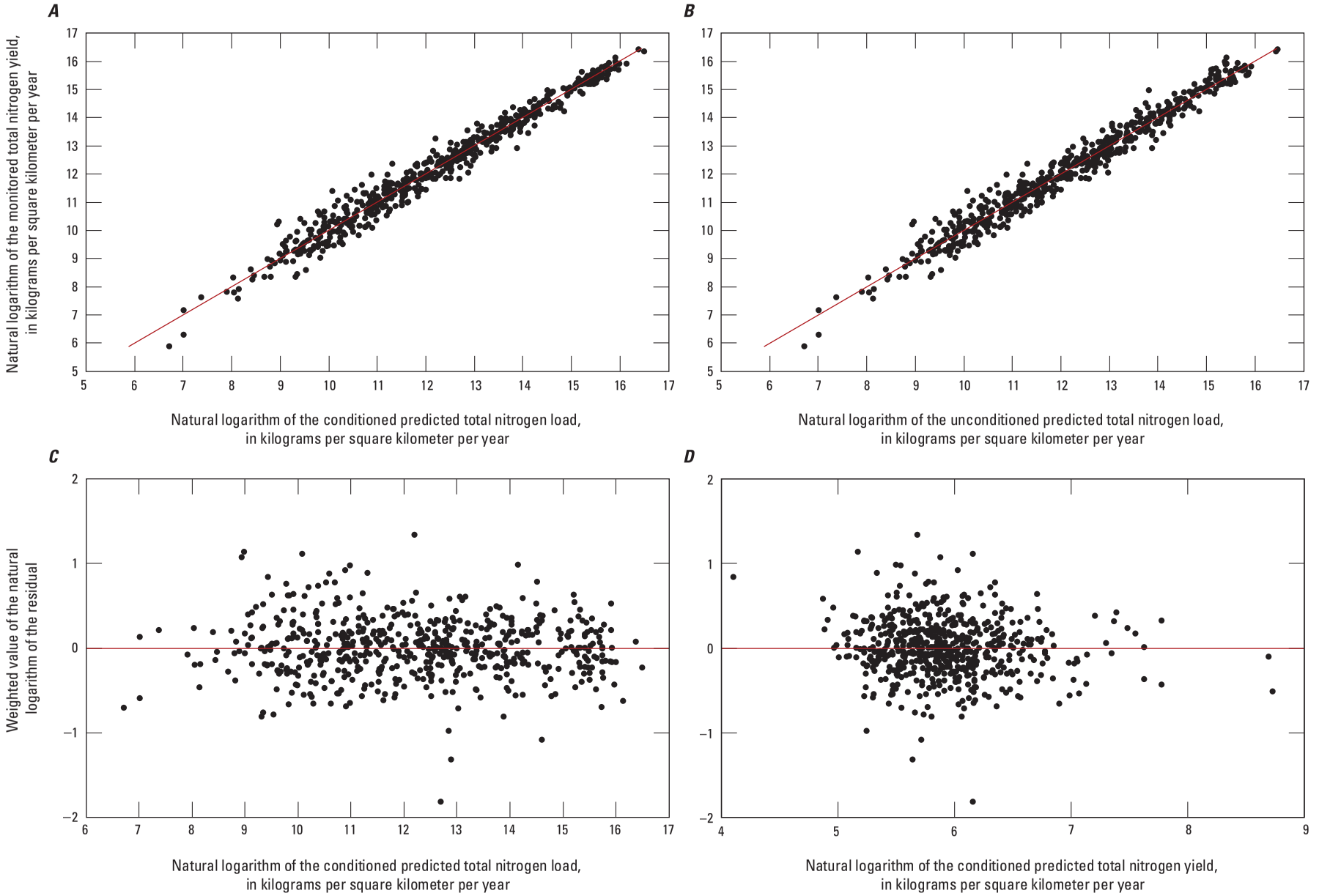

Figure 10. Diagnostic plots for the total nitrogen SPARROW (SPAtially Referenced Regression On Watershed attributes) model for the Southeast: *A*. monitored load versus conditioned predicted load, *B*. monitored load versus unconditioned predicted load, *C*. weighted residuals versus predicted load, and *D*. weighted residuals versus predicted yield, for 603 calibration sites. Conditioned predicted load means that the prediction is conditioned on monitored load for the closest upstream site(s). Unconditioned predicted load means that the prediction is not conditioned on monitored load for upstream site(s).

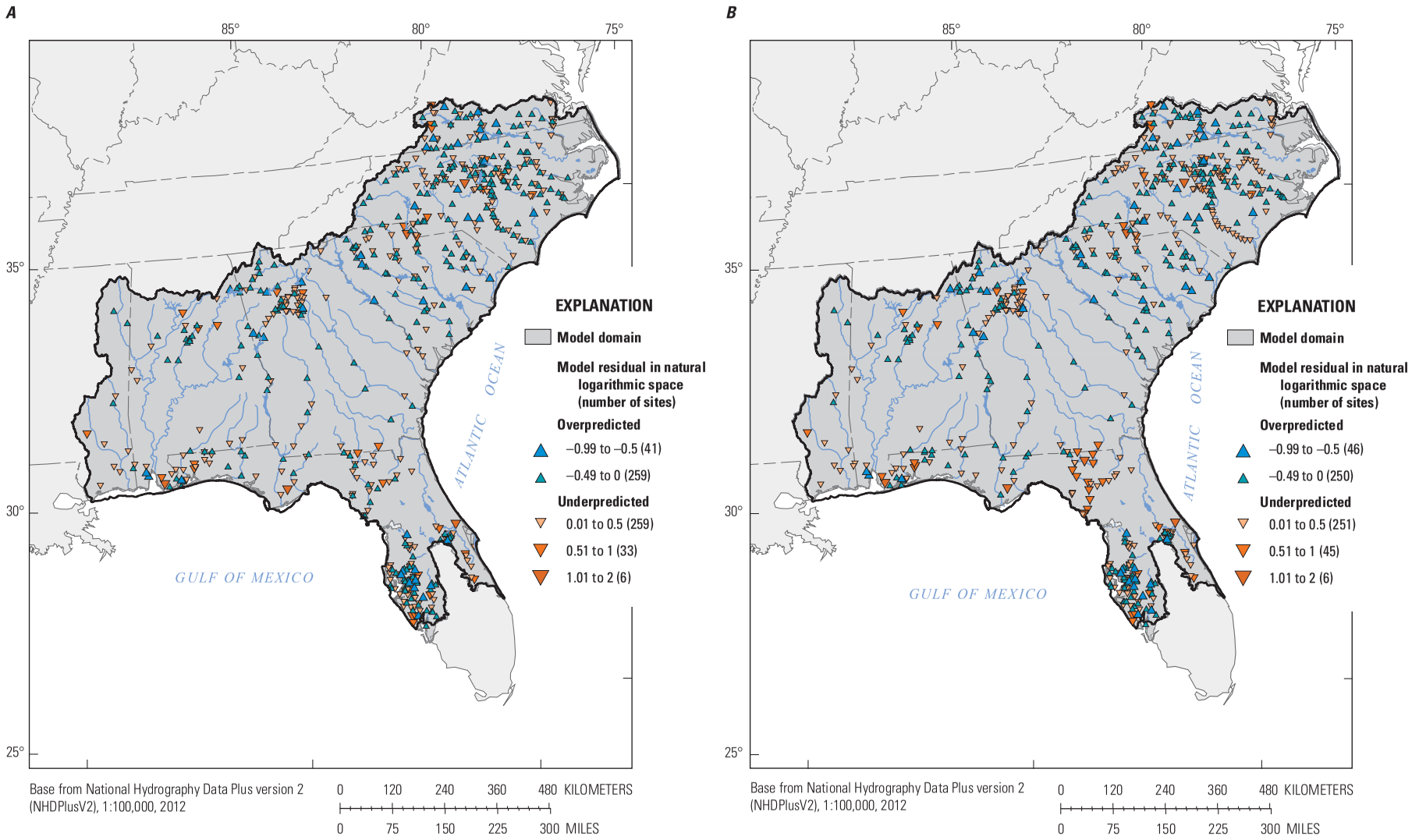

Figure 11. Spatial distribution of *A.* conditioned residuals and *B.* unconditioned residuals from the total nitrogen SPARROW (SPAtially Referenced Regression On Watershed attributes) model for the Southeast. Conditioned residuals are calculated as the difference between natural log of monitored load and natural log of predicted load, where the prediction has been conditioned on the monitored load at the closest upstream site(s). For unconditioned residuals the prediction is not conditioned on monitored load for upstream monitoring site(s).

and negative correlation. The residuals in both groups were not statistically correlated, with *p*-values of 0.208 and 0.179, respectively (table 7). Therefore, none of the sites from the proximal site pairs were removed from the calibration set.

The positive value (0.814) and *p*-value less than 0.0001 for the coefficient for nested area share (table 7) indicates that calibrating the model without accounting for the effects of nested basins would have underestimated residuals and discounted the effect of downstream sites in model calibration. The final calibrated model reported in table 7 incorporated a recalibration step in which weighted regression was used to address the unequal effects of nested basins in calibration.

Predictions

The TN SPARROW model was used to predict TN loads and yields for streams throughout the Southeast (fig. 12). The pattern of model-predicted TN yields delivered from the incremental catchment to the adjacent stream (fig. 12*A*) was similar to the pattern of monitored TN yields (fig. 9): predicted TN yields were smallest (less than 248 [kg/km²]/yr) for catchments in South Carolina, eastern Georgia, and isolated areas in Florida. Predicted TN yields exceed 423 (kg/km²)/yr for catchments in the Piedmont region of Georgia and North Carolina, the Coastal Plain of North Carolina, the Black Belt area of Mississippi and Alabama and Dougherty Plains area of Georgia, and the Tampa Bay and Charlotte Harbor watersheds in Florida (all place locations shown in fig. 2*B*). TN load and yield delivered to adjacent streams from all catchments in the Southeast were 306,921,124 kg/yr and 488 (kg/km²)/yr, respectively (table 8).

The markedly different patterns of model-predicted TN yield from catchments to adjacent streams (fig. 12*A*) as opposed to that from catchments to the basin outlet at coastal waters (fig. 12*B*), especially for catchments far from the coast, results from the substantial losses of TN during transport through the channel network indicated by the model. TN mass lost in the stream network throughout the Southeast was estimated by the model to be 35 percent of the amount delivered from the catchments to adjacent streams.

Model-predicted source shares for loads and yields to adjacent streams are summarized by HUC4 watershed areas in table 8 and illustrated in figure 13. Source shares represent the fraction or percent of the total constituent load and yield originating from each source. Atmospheric deposition was the largest source of TN to streams throughout the Southeast, contributing on average 60.8 percent and as much as 69.7 percent in areas with few other sources (table 8). Municipal wastewater was a significant source in some HUC4 watershed areas, particularly in the Edisto-Santee and Apalachicola HUC4 watershed areas (locations shown in figure 2*A*).

The estimates of nitrogen source share for agricultural fertilizer and manure from livestock are reported in table 8 as two separate components: the share from direct movement of N to the stream from mass applied in the watershed, and the share from indirect transport from source through atmosphere to stream. The share of stream load from manure volatilization/emission to the atmosphere (18.4 percent on average) composes almost one-third, on average, of the atmospheric deposition contribution to stream load (60.8 percent) and is generally about twice the share of manure estimated as moving directly to the stream.

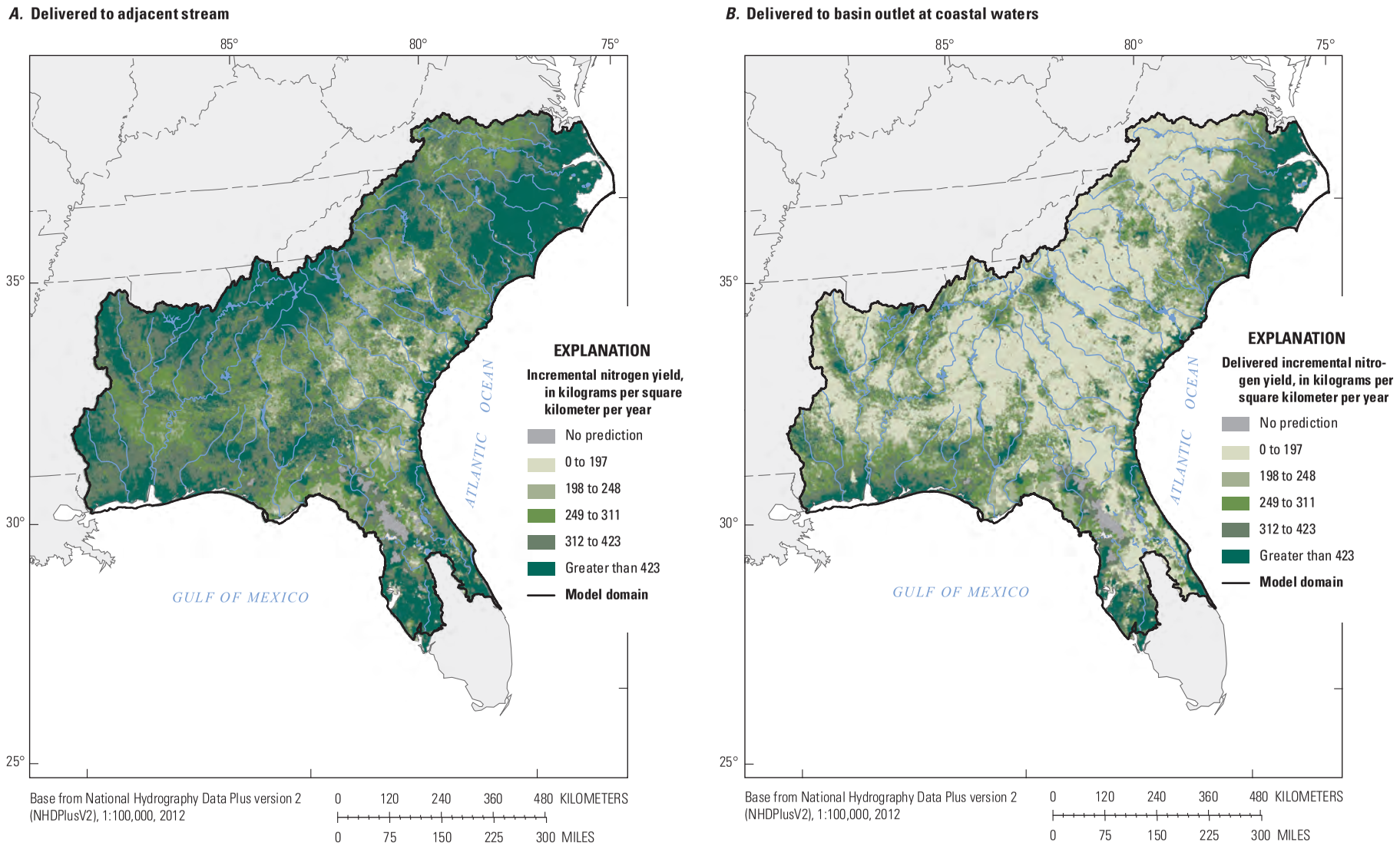

Figure 12. Mean-annual incremental yield of total nitrogen *A*. delivered to the adjacent stream, and *B*. delivered to the basin outlet at coastal waters, predicted from the total nitrogen SPARROW (SPAtially Referenced Regression On Watershed attributes) model for the Southeast.

Table 8. Load, yield, and source shares of total nitrogen delivered from catchment to adjacent stream and summarized by HUC–4 watershed area, estimated from the SPARROW total nitrogen model for the Southeast.

[SPARROW, SPAtially Referenced Regression On Watershed attributes; estimates are based on unconditioned predictions—that is, monitored values are not substituted for simulated values at monitored reaches; National Hydrography Dataset Plus (NHDPlus) version 2; Hydrologic Unit Code–4 (HUC4) watersheds are shown in figure 2; kg/yr, kilograms per year; kg/km^2/yr, kilograms per square kilometer per year]

HUC4 watershed abbreviation[1]	HUC4 watershed name	Basin area, based on NHDPlus network (km^2)	Total nitrogen load delivered to adjacent stream (kg/yr)	Total nitrogen yield delivered to adjacent stream (kg/km^2/yr)	Nitrogen source share (percent of total)					
					Municipal wastewater	Urban land	Agricultural fertilizer[2]	Manure from livestock[3]	Emissions to atmosphere (and subsequent deposition) from power plants, other industry, vehicles, and background	Atmospheric deposition (all components)
Summary for Southeast		**628,346**	**306,921,124**	**488**	**11.7**	**6.0**	**13.4/0.4**	**7.9/18.4**	**41.9**	**60.8**
CH-RO	Chowan-Roanoke	45,675	20,795,787	455	3.2	4.1	22.4/0.5	4.7/21.1	43.8	65.5
NE-PA	Neuse-Pamlico	30,893	23,975,591	776	4.3	4.4	20.9/0.4	6.5/27.7	35.6	63.8
CA-FE	Cape Fear	23,718	16,913,061	713	14.4	4.2	13.3/0.2	17.4/25.6	24.6	50.5
PE-DE	Pee Dee	47,917	24,674,423	515	18.7	4.8	18.5/0.3	9.3/18.2	30.1	48.7
ED-SA	Edisto-Santee	59,748	30,224,283	506	23.3	6.2	8/0.4	4.1/16.2	41.7	58.3
OG-SA	Ogeechee-Savannah	42,891	19,089,763	445	8.7	5.0	7.8/0.4	9.7/20.7	47.5	68.7
AL-SM	Altamaha-St. Marys	53,193	20,380,674	383	10.4	6.7	11.9/0.4	6.5/17.4	46.6	64.4
ST-JO	St. Johns	26,939	13,572,107	504	8.9	11.4	16.8/0.4	3.4/9.1	49.9	59.4
PE-TA	Peace-Tampa Bay	22,004	12,081,410	549	5.9	11.7	29.9/0.2	6.9/8.9	36.4	45.6
SUWA	Suwannee	33,265	10,961,894	330	2.1	4.5	22.8/0.4	7.8/18.5	43.7	62.7
OCHL	Ochlockonee	9,435	3,371,196	357	3.5	6.8	18.2/0.5	4.6/16.7	49.6	66.9
APAL	Apalachicola	52,135	26,393,084	506	25.3	5.9	13.8/0.3	5.4/13.9	35.1	49.5
CH-ES	Choctawhatchee-Escambia	37,119	15,214,357	410	2.3	8.2	9.8/0.5	9.8/18.9	50.2	69.7
ALAB	Alabama	58,891	27,660,206	470	10.3	6.1	6.1/0.4	11.3/18.4	47.3	66.2
MO-TO	Mobile-Tombigbee	55,519	27,097,794	488	10.3	5.4	7.3/0.6	7.7/18.9	49.6	69.2
PASC	Pascagoula	29,004	14,515,495	500	10.4	5.5	4.3/0.4	11.9/17.4	49.9	67.8

[1]HUC4 watershed areas are shown in figure 2 and listed here in north-south order for watersheds (Chowan-Roanoke through St. Johns) draining to the Atlantic Ocean and in east-west order for watersheds (Peace-Tampa Bay through Pascagoula) draining to the Gulf of Mexico.

[2]The estimate for nitrogen source share for "Agricultural fertilizer" is reported as two separate components: share from direct movement of nitrogen to the stream from fertilizer applied in the watershed, and share from indirect transport from source through atmosphere to stream.

[3]The estimate for nitrogen source share for "Manure from livestock" is reported as two separate components: share from direct movement of nitrogen to stream from livestock manure and direct animal emissions in the watershed, and share from indirect transport from source through atmosphere to stream.

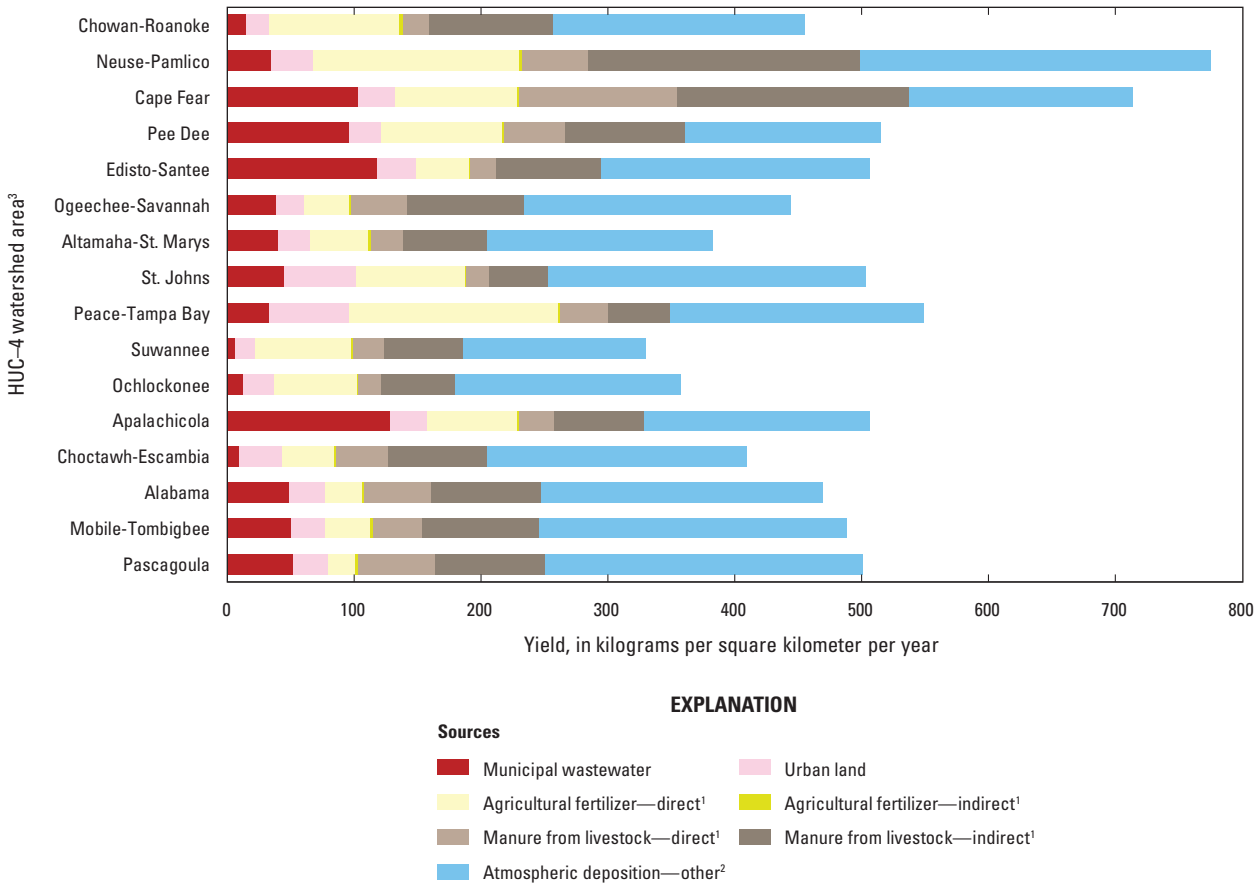

[1]The shares for Agricultural fertilizer and Manure from livestock are divided into two separate components, direct and indirect: the share from direct movement of N to the stream from mass applied in the watershed, and the share from indirect transport from source through atmosphere to stream.

[2]The share attributed to atmospheric deposition includes emissions to the atmosphere (and subsequent deposition) from power plants, other industry, vehicles, and background.

[3]Hydrologic Unit Code–4 watershed areas are shown on figure 2 and listed here in north-south order for watersheds (Chowan-Roanoke through St. Johns) draining to the Atlantic Ocean and in east-west order for watersheds (Peace-Tampa Bay through Pascagoula) draining to the Gulf of Mexico.

Figure 13. Predicted total nitrogen yield delivered to the adjacent stream by source and by HUC–4 watershed area.

Total Phosphorus SPARROW Model

Calibration

Observations of TP loads at 594 monitoring sites in the Southeast (illustrated as yields in figure 14) were used to calibrate the TP SPARROW model. In general, TP yields were smallest (less than 14 [kg/km²]/yr) in South Carolina, southern Virginia, and northern North Carolina and isolated areas in Georgia and Florida. Phosphorus yields exceeding 46 (kg/km²)/yr were observed throughout the Southeast and especially in north-central Georgia and along the western coast of Florida.

Of the 12 attributes tested as source variables (table 9), one variable represented the natural source of phosphorus to streams: *Incremental catchment area* (*P source term in combination with delivery term representing P content of upland soil and parent rock*). The remaining 11 variables evaluated as sources in the TP model represented the spatial distribution of anthropogenic sources.

The four log transformed variables representing P content in soil and parent rock—*P content of bed sediment in small pristine streams* (*national extent*), *P content of bed sediment in small pristine streams* (*Southeast extent*), *P content of soil A horizon*, and *P content of soil C horizon*—are listed as land-to-water delivery variables in table 9 but described as source variables in the Methods section. In previous TP SPARROW models for the Southeast, the variable representing this

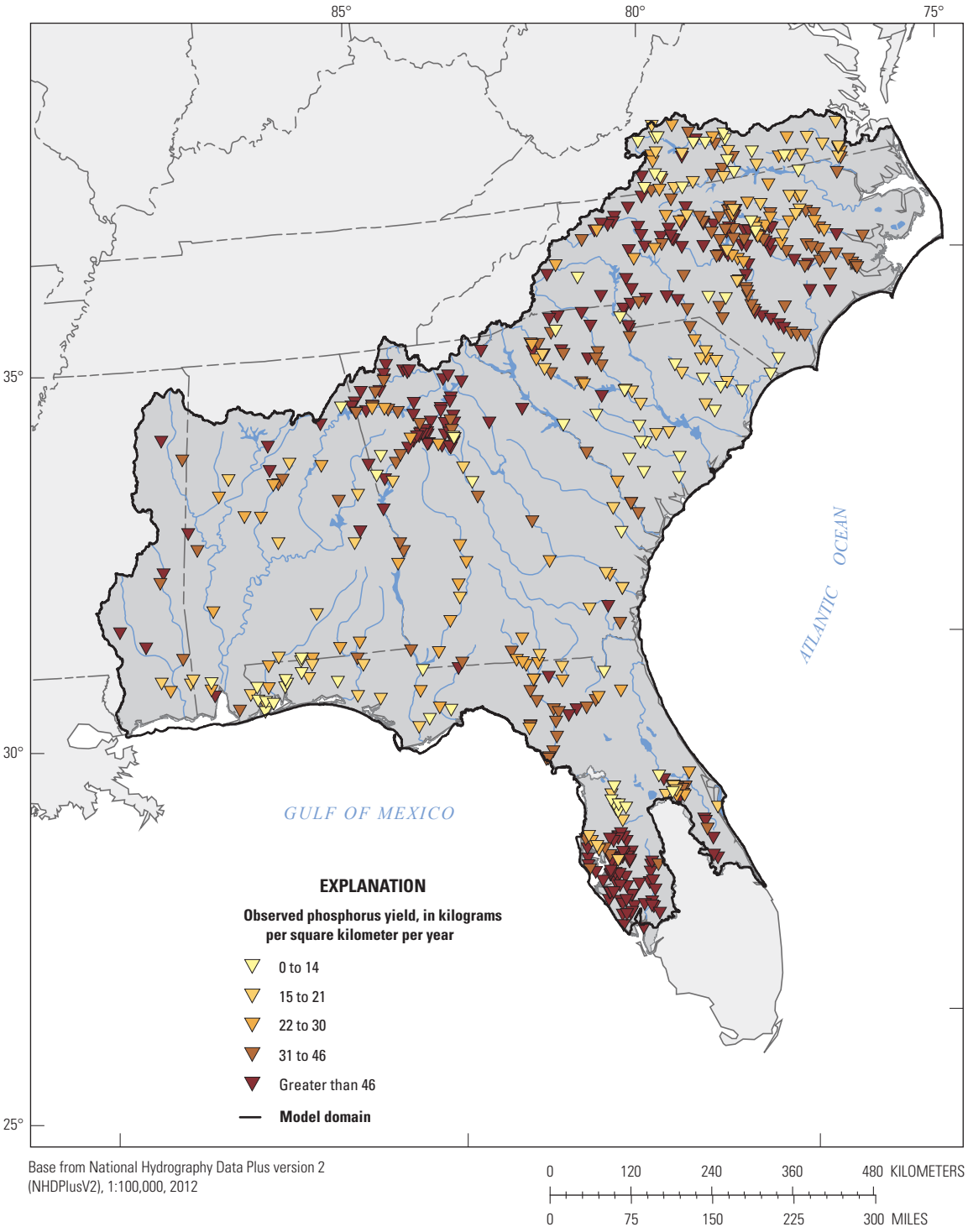

Figure 14. Total phosphorus yield for the base year 2012 estimated from stream monitoring data from 594 sites in the Southeast.

Table 9. Source, delivery, loss, and removal variables evaluated in the total phosphorus SPARROW model for the Southeast.

[SPARROW, SPAtially Referenced Regression On Watershed attributes; Variables retained in the final specification of the model are denoted with an asterisk (*); variables tested but not retained are denoted with grey-shading; additional information (publication references, links for downloading) for each variable is provided in appendix 3; Log, natural logarithm; P, phosphorus; TP, total phosphorus; PPT−AET, precipitation minus actual evapotranspiration; PredQ_SESpar, mean-annual streamflow in the reach, 2000–14, estimated from conditioned predictions of the streamflow SPARROW model; NHD, National Hydrography Dataset; NID, National Inventory of Dams; MAFlowUcfs, mean-annual streamflow in the reach, estimate from enhanced National Hydrography Dataset Plus (NHDPlus) version 2; kg/yr, kilogram per year; km^2, square kilometer; mm/yr, millimeter per year; ppm, part per million; km, kilometer]

Source variable	
*	Incremental catchment area (P source term in combination with delivery term representing P content of upland soil and parent rock)
*	Municipal/domestic wastewater TP discharge to streams, kg/yr, 2012
*	Urban land cover, km^2, 2011
*	Fertilizer TP applied to agricultural land, kg/yr, 2012, national weighted
*	Manure TP from livestock production, kg/yr, 2012
*	Mined area P content, ppm*km^2
*	Mined land permitted TP discharge to streams, kg/yr, 2012
	Length of main channel in catchment, km
	Industrial wastewater TP discharge to streams, kg/yr, 2012
	Fertilizer TP applied to agricultural land (state weighted), kg/yr, 2012
	Fertilizer TP applied to agricultural land, (unconditioned), kg/yr, 2012
	Fertilizer TP applied to agricultural land (Kalman conditioned), kg/yr, 2012
Land-to-water delivery variable	
*	Log of P content of bed sediment in small pristine streams (national extent), interpolated by (in 4 locations) using geologic mapping units
	Log of P content of bed sediment in small pristine streams (regional extent), interpolated using geologic mapping units
	Log of P content of soil A horizon, interpolated using geologic mapping units
	Log of P content of soil C horizon, interpolated using geologic mapping units
*	Log of incremental flow from catchment to stream (streamflow SPARROW model), mean of 2000–14
*	Log of K factor (erodibility index) in upper soil layer
*	Log of depth to water table, feet
*	Log of percent of catchment in no till or conservation tillage, 2012
	Log of percent of catchment in cover crops, 2012
	Log of percent of catchment in conservation easement, 2012
	Log of PPT−AET, mm/yr, detrended to base year 2012; in contrast to PPT−AET used as source term in the streamflow model, this term is normalized by the area of the catchment
Aquatic-loss variable	
*	Reach time of travel (days) per meter of stream depth, where depth is estimated as a continuous function of stream discharge PredQ_SESpar and other channel characteristics (by using the six-parameter regional regression equation)
	Reach time of travel per meter of stream depth, where depth is estimated as a continuous function of stream discharge PredQ_SESpar according to the simple power law formula: depth (meters) = 0.06356 * PredQ_SESpar (ft^3/s) ^ 0.3966
*	Time of travel in intermediate streams (stream discharge 31–100 ft^3/s, or 0.849–2.83 m^3/s
*	Time of travel in large streams (stream discharge > 100 ft^3/s, or > 2.83 m^3/s)
Water-removal variable	
*	Consumptive use at power plants, 2010, expressed as -log(1-fraction of unremoved streamflow)
*	Surface-water withdrawal for municipal water supply based on popn served, 2013, expressed as -log(1-fraction of unremoved streamflow)

property was specified as a source variable; in contrast, the specification for the current model treats these variables as land-to-water delivery terms acting on the source term *Incremental catchment area*. The previous approach, specification as a source variable, forces a linear relation (if land-to-water transport factors are assumed to be equal) between bed sediment or soil P content multiplied by incremental catchment area and the mass of TP exported from catchment to stream. Assumption of a linear relation between source input and export (holding land-to-water variables constant) is reasonable for mass-based source variables such as mass of applied fertilizer but may not be reasonable for surrogate source variables such as bed sediment or soil P content scaled by catchment area. The approach used in the current model quantifies P delivery to streams as proportional to incremental catchment area and also enhanced or mitigated as a function—not constrained to linear—of P content.

Seven source terms were significant in explaining variation in P loads (table 10): *Incremental catchment area (in relation to delivery term P content of bed sediment in small pristine streams)*, *Municipal/domestic wastewater discharge to streams, Urban land cover, Fertilizer TP applied to agricultural land, Manure TP from livestock production, Mined land area P content,* and *Mined land permitted TP discharge to streams*. A coefficient value of 1 is expected for the coefficient for the two sources discharged directly to the stream—*Municipal/domestic wastewater discharge to streams* and *Mined land permitted TP discharge to streams*—because the source inputs were monitored at the point of discharge to the stream. The model-estimated value of 0.997 (table 10) for *Municipal/domestic wastewater discharge to streams* indicates that the input estimates of TP load in municipal/domestic wastewater likely were unbiased and (or) that all of the TP in the effluent from these facilities was accounted for in the monitored stream loads. In contrast, the estimated value of 2.951 for *Mined land permitted TP discharge to streams* is far from 1. This value may reflect either bias (underestimation) in the input estimates or the uncertainty associated with the estimate (standard error was large, 1.170, or 40 percent of the estimated value). The limited spatial extent of this source, mainly in central and east-central Florida, also contributes to its greater uncertainty.

The remaining five sources were applied to the land surface rather than discharged directly to the stream; therefore, they were subject to transformation and attenuation during land-to-water delivery. For these sources, the estimated coefficients represented the mass delivery ratio for a catchment with average land-to-water delivery properties.

Other variables developed to describe P inputs to the watershed were evaluated but not included in the final model (listed in the shaded section of table 9). The variable *Length of main channel in catchment*, *km* was tested to represent streambank erosion (instream P source). The variable *Industrial wastewater TP discharge to streams, kg/yr, 2012* was tested to represent point-source contribution from industrial wastewater discharge. These sources may not have been significant in explaining P inputs at the scale of this analysis, or their contributions may be substantial but accounted for by one or more of the final source terms that covary spatially with these sources. The variables *Fertilizer TP applied to agricultural land* (*state weighted), kg/yr, 2012*; *Fertilizer TP applied to agricultural land* (*unconditioned*)*, kg/yr, 2012*; and *Fertilizer TP applied to agricultural land* (*Kalman conditioned*)*, kg/yr, 2012* were tested as alternative variables representing agricultural fertilizer use.

The land-to-water delivery variables describe processes that increase or decrease P adsorption to soil particles, or that increase or decrease mobilization (erosion) and transport of the soil particles themselves. Eleven watershed attributes were evaluated as delivery variables (table 9); the five included in the final model and their estimated coefficients and associated statistics are presented in table 10. The larger (more different from 0) coefficient values for *Log of K factor* and *Log of the depth to water table* mean that the delivery ratio for the land-applied sources was more sensitive to these two variables than they were to the other delivery variables.

The delivery variable *Log of P content of bed sediment in small pristine streams* was allowed to interact with only the incremental catchment area to represent contribution of P from natural sources. The positive coefficient (0.591) associated with this variable indicated increasing transport of P to streams with increasing P content in watershed surficial geologic materials. The positive coefficient (0.722) associated with *Log of Kfactor* (*erodibility index*) was expected because increasing erodibility of soil increases mobilization and transport of particulate P to streams. Similarly, the positive coefficient (0.530) associated with *Log of incremental flow from catchment to stream* may reflect higher rates of water transport through the catchment generally causing increased erosion and transport of P associated with soils.

The negative coefficient (−0.771) for *Log of depth to water table* may be explained by the effect of soil saturation on mobilization of P sequestered in soils. As depth to water table decreases and soil saturation increases (in wetland areas, for example), the water-soil system may become anaerobic, causing release of P adsorbed to soil particles to pore water and subsequent transport to an adjacent stream. The negative coefficient (−0.135) for *Log of the percent of catchment in no till or conservation tillage* may reflect reduced erosive loss of soils from agricultural lands managed with these tillage practices. Reduced soil loss translates to a reduction in P delivered to the stream. The agricultural best management practices of cover crops and conservation easements were tested but were not significant.

Six physical stream-channel, reservoir, and lake attributes were evaluated to describe aquatic loss or removal of P in the stream network (table 9). The variable representing P loss in free-flowing streams was computed as the ratio of mean water travel time and mean water depth. Loss in streams is most likely caused by trapping of P in bed sediment and was modeled as a first-order decay function. The model-estimated coefficient (0.094 m/d in table 10) can be interpreted as a

Table 10. Model-estimated coefficients and diagnostics for the total phosphorus SPARROW model for the Southeast.

[SPARROW, SPAtially Referenced Regression On Watershed attributes; additional information (publication references, links for downloading) for each variable is provided in appendix 2; *p*-value, probability value; *t*-value, *t*-statistic; PPT−AET, precipitation minus actual evapotranspiration; P, phosphorus; TP, total phosphorus; RMSE, root mean squared error; Log, natural logarithm; R^2, coefficient of determination; proximal, site pairs that are within 5 kilometers distance; --, not estimated because coefficient was fully constrained; kg/km^2/yr; kilogram per square kilometer per year; ppm*km^2, parts per million multiplied by square kilometer; mm/yr, millimeter per year; d/m, day per meter; m/d, meters per day; y/m, meter per year m/yr, meter per year; <, less than]

Variable	Variable unit	Coefficient unit	Model coefficient value	90-percent confidence interval for the model coefficient		Standard error of the model coefficient	*p*-value	*t*-value	Variance inflation factor
				Lower	Upper				
Source (model coefficient = α)									
Incremental catchment area (in relation to delivery term phosphate mineral content of geologic material)	km^2	kg/km^2/yr	19.466	15.647	23.285	2.977	<0.0001	6.540	4.382
Municipal/domestic TP wastewater discharged to streams	kg/yr	Fraction	0.997	0.771	1.223	0.176	<0.0001	5.659	1.214
Urban land cover	km^2	kg/km^2/yr	49.108	37.031	61.185	9.413	<0.0001	5.217	2.192
Fertilizer TP applied to agricultural land	kg/yr	Fraction	0.035	0.016	0.054	0.014	0.0079	2.423	2.801
Manure TP from livestock production	kg/yr	Fraction	0.040	0.028	0.052	0.009	<0.0001	4.258	2.411
Mined land area P content	ppm*km^2	kg/(ppm*km^2)/yr	0.109	0.049	0.169	0.047	0.0102	2.324	1.185
Mined land permitted TP discharge to streams	kg/yr	Fraction	2.951	1.449	4.452	1.170	0.0060	2.521	1.053
Land-to-water delivery									
(Interacts with the source variable Incremental catchment area) log of P content of bed sediment in small pristine streams, in ppm*km^2	Unitless	Unitless	0.591	0.341	0.841	0.152	0.0001	3.899	1.182
Logarithm of incremental flow from catchment to stream (SPARROW streamflow model), in mm/yr	Unitless	Unitless	0.530	0.293	0.768	0.144	0.0003	3.680	1.491
Logarithm of Kfactor (erodibility index)	Unitless	Unitless	0.722	0.499	0.945	0.135	<0.0001	5.332	2.333
Logarithm of depth to water table, in feet	Unitless	Unitless	–0.771	–1.028	–0.513	0.156	<0.0001	–4.936	3.554
Logarithm of percent of catchment in no till or conservation tillage	Unitless	Unitless	–0.135	–0.181	–0.089	0.028	<0.0001	–4.832	1.730
Aquatic loss									
Streams and rivers—Reach time of travel (days) per meter of stream depth[a]	d/m	m/d	0.094	0.044	0.144	0.039	0.0082	2.406	4.444
Reservoirs and lakes—Reciprocal of areal hydraulic load (excludes waterbodies in karst landscape)	yr/m	m/yr	14.633	10.747	18.519	3.029	<0.0001	4.831	1.159

Table 10. Model estimated coefficients and diagnostics for the total phosphorus SPARROW model for the Southeast.—Continued

[SPARROW, SPAtially Referenced Regression On Watershed attributes; additional information (publication references, links for downloading) for each variable is provided in appendix 2; *p*-value, probability value; *t*-value, *t*-statistic; PPT−AET, precipitation minus actual evapotranspiration; P, phosphorus; TP, total phosphorus; RMSE, root mean squared error; Log, natural logarithm; R^2, coefficient of determination; proximal, site pairs that are within 5 kilometers distance; --, not estimated because coefficient was fully constrained; kg/km^2/yr; kilogram per square kilometer per year; ppm*km^2, parts per million multiplied by square kilometer; mm/yr, millimeter per year; d/m, day per meter; m/d, meters per day; y/m, meter per year m/yr, meter per year; <, less than]

Variable	Variable unit	Coefficient unit	Model coefficient value	90-percent confidence interval for the model coefficient		Standard error of the model coefficient	*p*-value	*t*-value	Variance inflation factor
				Lower	Upper				
Removal as water withdrawals									
Consumptive use at power plants, fraction of instream flow	−log(1-fraction of unremoved streamflow)	Unitless	1.282	--	--	--	--	--	--
Surface-water withdrawal for municipal water supply, fraction of instream flow	−log(1-fraction of unremoved streamflow)	Unitless	1.057	--	--	--	--	--	--

Spatial test	Number of sites/site pairs	Test statistic	*p*-value	Number of sites/site pairs	Test statistic	*p*-value
Spatial autocorrelation of residuals from nonproximal sites (Moran's *I* test statistic)	589 sites	0.0262	0.246	589 sites	0.0262	0.246
Spatial autocorrelation of residuals from nonnested proximal site[a] (Pearson's *r* test statistic)	85 site pairs	–0.0789	0.473	85 site pairs	–0.0789	0.473
Spatial autocorrelation of residuals from nested proximal sites (Pearson's *r* test statistic	41 site pairs	–0.1365	0.395	41 site pairs	–0.1365	0.395
Weights—Coefficient for logarithm of nested area share[b]	589 sites	0.547	<0.0001	589 sites	0.547	<0.0001

Model summary statistics				
Conditioned RMSE[c]	In logarithmic space	0.58	In percent[d]	63
Unconditioned RMSE[e]	In logarithmic space	0.59	In percent[d]	65
Mean exponentiated weighted error		1.20		
R^2 of dependent variable (load)		0.92		
R^2 of yield		0.59		
Number of sites used to calibrate the model		589		

[a]Also including nested sites with dissimilar drainage area.

[b]The fraction of the upstream drainage area that is downstream from other monitoring sites.

[c]Conditioned RMSE: the residuals are calculated as the difference between natural log of monitored load and natural log of predicted load, where the prediction has been conditioned on monitored load at the closest upstream site(s).

[d]RMSE in terms of percent in real space units was computed as: $100 \times (\exp[RMSE^2]-1)^{0.5}$; RMSE in this equation is in natural log space.

[e]Unconditioned RMSE: same as conditioned RMSE except the prediction is not conditioned on monitored load for upstream station(s).

first-order loss-rate coefficient. The model-calculated rate of P loss per day of water travel time mostly ranged between 0.94/d (small streams) and 0.094/d (large streams).

The variable representing loss in lakes and reservoirs, *Reciprocal of areal hydraulic load,* was the ratio of lake or reservoir surface area to outflow. A separate aquatic loss-rate coefficient for waterbodies in karst landscape was evaluated to explore whether the processes and rates of SS loss (settling and burial) in these lakes differed from those in the rest of the Southeast. The estimated coefficient for lakes and reservoirs excluding those in karst landscape for the first-order reservoir decay function (14.63 m/yr) can be interpreted as a hypothetical settling velocity that, when multiplied by the reciprocal of areal hydraulic load (in years per meter) and exponentiated, quantifies the proportion of the P mass transported through the lake or reservoir. The settling velocity estimate of 14.63 m/yr was smaller than the estimate (29.6 m/yr) from the 2002 TP model for the Southeast (Hoos and others, 2013) that was based on the NHDPlusv1 stream network (U.S. Environmental Protection Agency and U.S. Geological Survey, 2010). The reservoir loss-rate coefficient estimated for lakes and reservoirs in karst landscapes was not significant and is not reported.

The removal variables used in the TP model to represent withdrawals from the stream were *Consumptive use at power plants* and *Surface-water withdrawal for municipal water supply*. The coefficients for these variables were not estimated in the TP model; rather, they are constrained to equal the estimated coefficient values from the calibrated streamflow model (1.282 and 1.057 for *Consumptive use at power plants* and *Surface water withdrawal for municipal water supply*, respectively).

Goodness of fit between the monitored values of TP load (illustrated as yield in figure 14) and load predicted by the SPARROW TP model is quantified in the calibration statistics reported in table 10 and illustrated by graphs and maps of model error at calibration stations (figs. 15 and 16). The RMSE of conditioned and unconditioned residual, 0.58 and 0.59, respectively (10), are equivalent to a mean error of 63 and 65 percent, respectively. The R^2 of yield for the TP model (0.59; table 10) indicates the TP model explains 59 percent of the variance in log-transformed monitored TP yield.

Residuals were evenly distributed around the 1:1 line throughout the range of the predicted load for both conditioned and unconditioned residuals (figs. 15*A* and 15*B*). Residuals for yields, however, were heteroscedastic (fig. 15 *D*), with a tendency toward overprediction for low yields and underprediction for high yields.

Figures 16*A* and 16*B* show that the conditioned and unconditioned model residuals have similar spatial distributions and appear to be spatially random, with the exception of clusters of overpredictions and underpredictions (of the same magnitude) in northern Georgia and eastern Florida. The Moran's *I* test was used to test for significant spatial autocorrelation. The test statistic of 0.026 and associated *p*-value of 0.246 (table 10) indicated that these patterns were not statistically significant, indicating the model likely was adequately specified. Spatial dependency among site pairs in close proximity was evaluated by Pearson correlation of pairs within 5 km (described in the Methods section). Residuals for close-proximity site pairs (nested and nonnested site pairs less than 5 km apart) were tested for significant and negative correlation. The residuals for both the close-proximity nested site pairs and nonnested site pairs were not statistically correlated, with *p*-values of 0.395 and 0.473, respectively (table 10). Therefore, no sites from the proximal site pairs were removed from the calibration set.

The positive value (0.547) and *p*-value less than 0.0001 for the nested area share (table 10) indicates that calibrating the model without accounting for the effects of nested basins would have underestimated residuals and discounted the effect of downstream sites in model calibration. The final calibrated model reported in table 10 therefore incorporated a re-calibration step in which weighted regression was used to address the unequal effects of nested basins in calibration.

Predictions

The TP SPARROW model was used to predict TP loads and yields for streams throughout the Southeast (fig. 17*A*). Yields for regions of states forming the northern border of the model domain (in Mississippi, Alabama, North Carolina, and Virginia) were large compared to those for the southernmost areas in the model domain, with Florida as an exception. TP load and yield delivered to adjacent streams from all catchments in the Southeast were 35,961,902 kg/yr and 57 (kg/km²)/yr, respectively (table 11).

The pattern of predictions of incremental TP yield delivered to major basin outlets (fig. 17*B*) was greatly different from that of incremental TP yield delivered to the adjacent stream (fig. 17*A*). Areas near the coast delivered about the same amount of TP to the basin outlet at coastal waters as they delivered to adjacent streams (fig. 17*A*); areas farther from the coast contributed much smaller amounts of TP to coastal waters than to adjacent streams, as a result of losses in the stream network associated with reservoir and stream processes or removal by withdrawal. In the Black Belt region of Alabama and Mississippi, there was little difference in pattern between yields because TP contributions both to adjacent streams and to coastal waters in this area were relatively large. TP mass lost in the stream network throughout the Southeast was estimated to be 44 percent of the amount delivered from catchment to adjacent streams.

Model-predicted source shares for stream loads are summarized by HUC4 watershed area in table 11 and figure 18. Background (parent-rock minerals) was the largest source (40.8 percent) of TP in streams, and manure from livestock (18.8 percent) and municipal wastewater (18 percent) were the second largest sources. TP yields to streams were highest in the Peace-Tampa Bay HUC4 watershed area because this area had the highest yield of both agricultural fertilizers and phosphate mining in the Southeast (fig. 18).

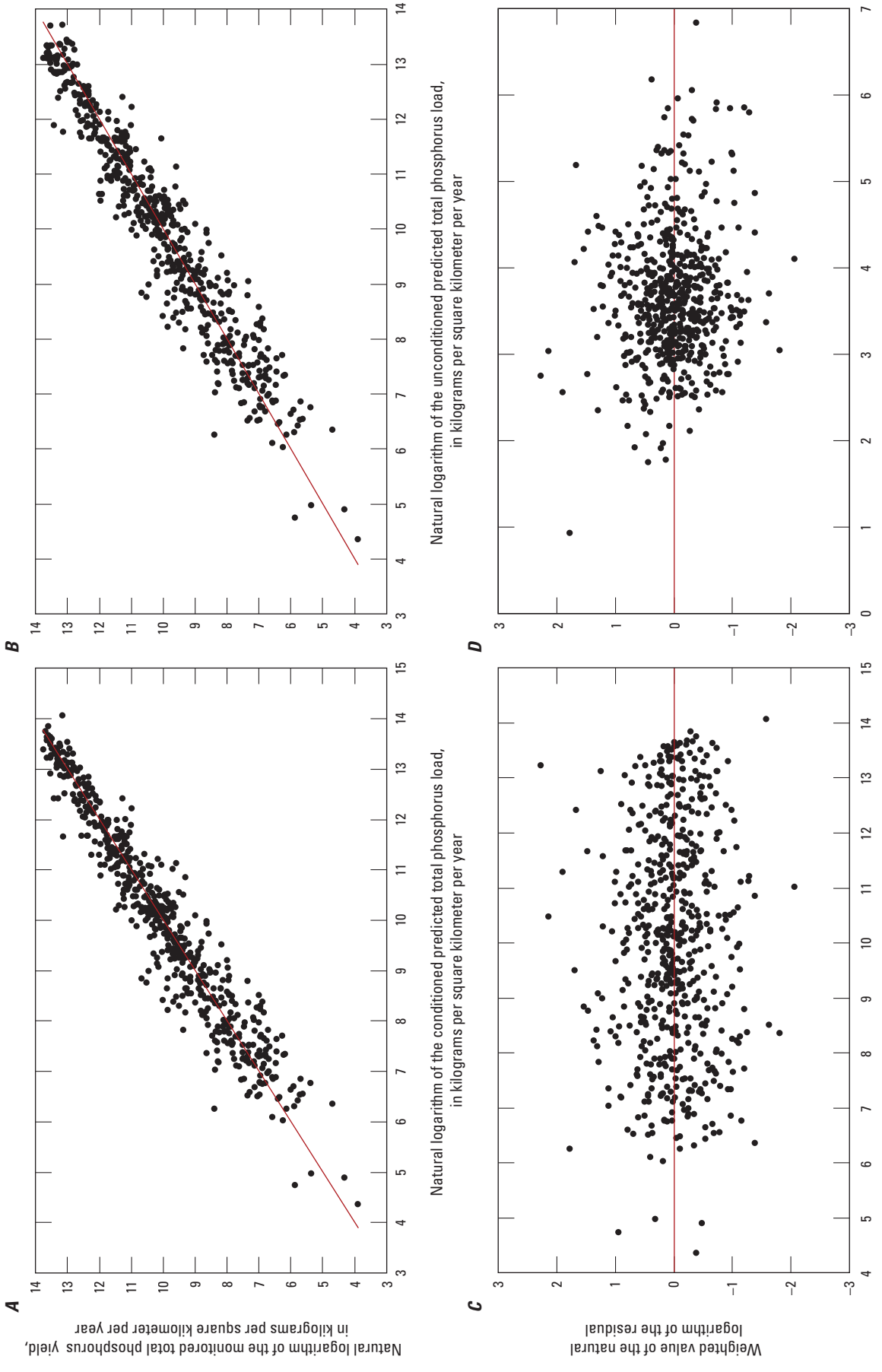

Figure 15. Diagnostic plots for the total phosphorus SPARROW (SPAtially Referenced Regression On Watershed attributes) model for the Southeast: *A*. monitored load versus conditioned predicted load, *B*. monitored load versus unconditioned predicted load, *C*. weighted residuals versus predicted load, and *D*. weighted residuals versus predicted yield, for 589 calibration sites. Conditioned predicted load means that the prediction is conditioned on monitored load for the closest upstream site(s). Unconditioned predicted load means that the prediction is not conditioned on monitored load for upstream site(s).

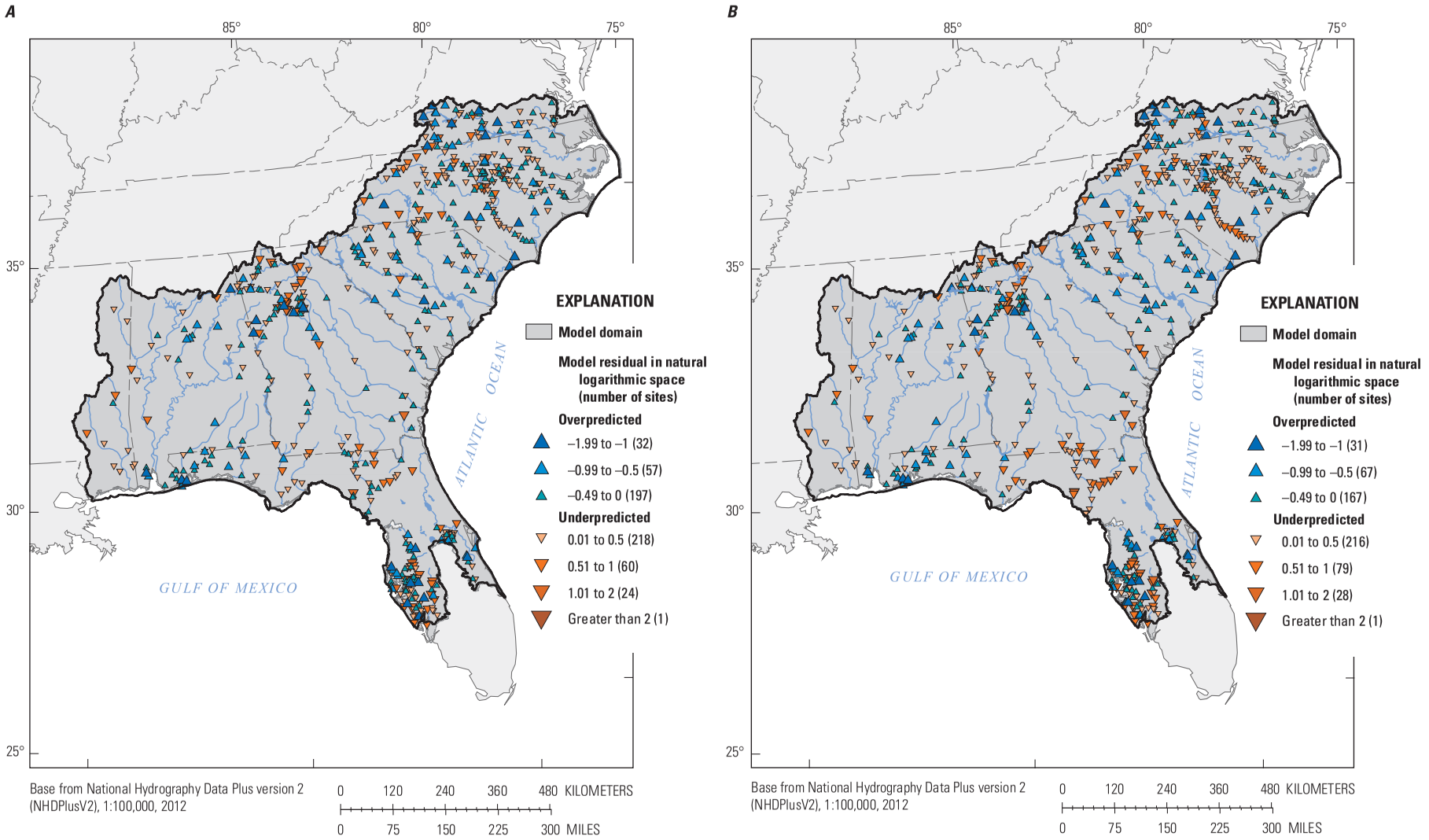

Figure 16. Spatial distribution of *A.* conditioned residuals and *B.* unconditioned residuals from the total nitrogen SPARROW (SPAtially Referenced Regression On Watershed attributes) model for the Southeast. Conditioned residuals are calculated as the difference between natural log of monitored load and natural log of predicted load, where the prediction has been conditioned on the monitored load at the closest upstream site(s). For unconditioned residuals the prediction is not conditioned on monitored load for upstream monitoring site(s).

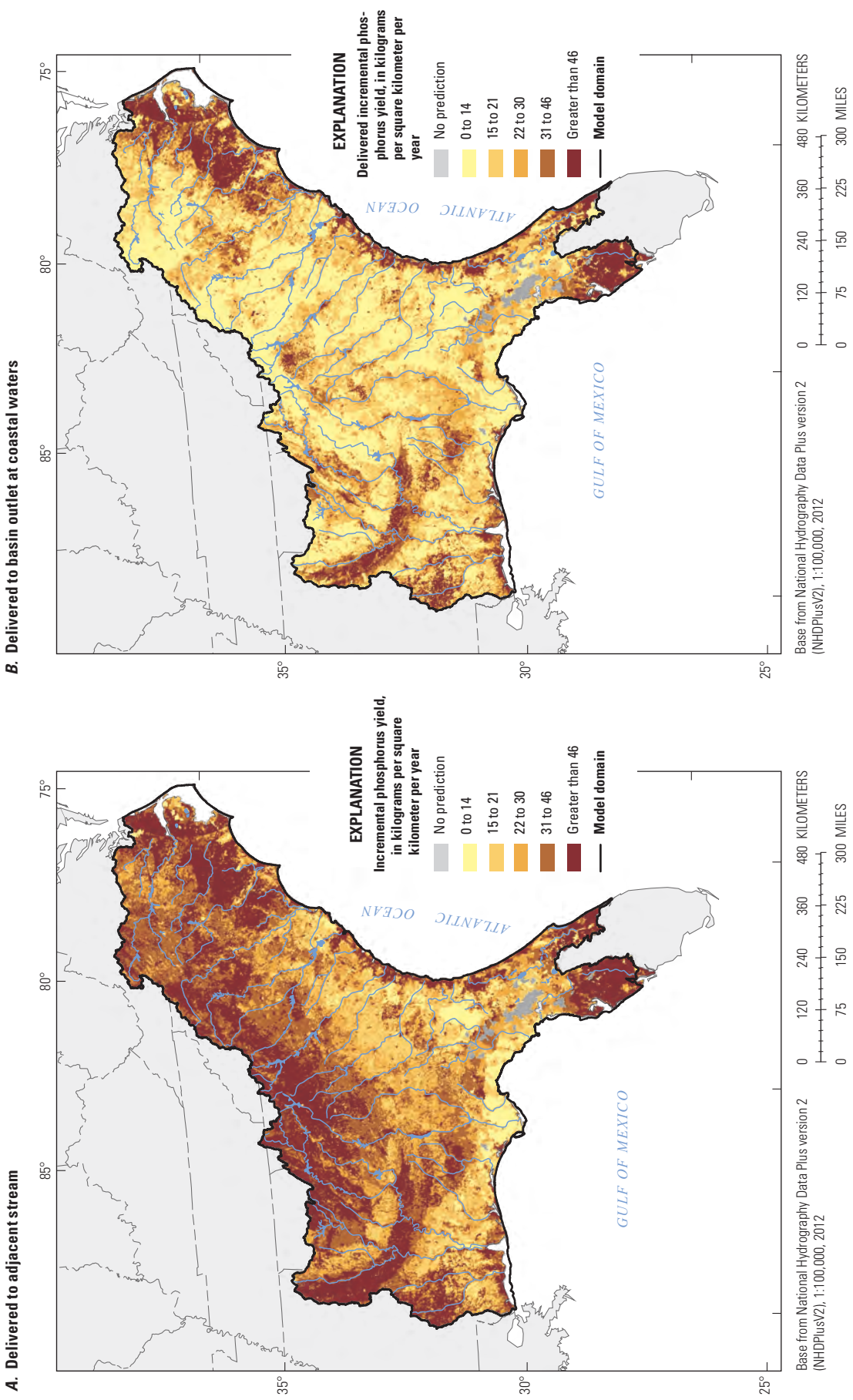

Figure 17. Mean-annual incremental yield of total phosphorus *A*. delivered to the adjacent stream, and *B*. delivered to the basin outlet at coastal waters, predicted from the total phosphorus SPARROW (SPAtially Referenced Regression On Watershed attributes) model for the Southeast.

Table 11. Load, yield, and source shares of total phosphorus delivered from catchment to adjacent stream and summarized by HUC4 watershed area, estimated from the SPARROW total phosphorus model for the Southeast.

[SPARROW, SPAtially Referenced Regression On Watershed attributes; Estimates are based on unconditioned predictions; that is, monitored values are not substituted for simulated values at monitored reaches; Hydrologic Unit Code-4 (HUC4) watersheds are shown in figure 2; National Hydrography Dataset Plus (NHDPlus) version 2; km^2, square kilometers; kg, kilograms; kg/yr, kilogram per year; kg/km^2/yr; kilograms per square kilometer per year]

HUC4 watershed abbreviation[1]	HUC4 watershed name	Basin area, based on NHDPlus network (km^2)	Total phosphorus load delivered to adjacent stream (kg/yr)	Total phosphorus yield delivered to adjacent stream (kg/km^2/yr)	Phosphorus source share (percent of total)					
					Municipal wastewater	Urban land	Agricultural fertilizer	Manure from livestock	Phosphate mining	Background (parent-rock minerals)
Summary for Southeast		**628,346**	**35,961,902**	**57**	**18.0**	**10.4**	**8.2**	**18.8**	**3.8**	**40.8**
CH-RO	Chowan-Roanoke	45,675	2,216,029	49	3.1	10.6	18.8	12.3	0.0	55.1
NE-PA	Neuse-Pamlico	30,893	2,230,405	72	9.3	10.6	17.0	23.9	6.8	32.3
CA-FE	Cape Fear	23,718	2,069,186	87	20.3	6.7	7.4	39.8	0.0	25.7
PE-DE	Pee Dee	47,917	2,942,151	61	27.5	8.4	9.4	19.0	0.0	35.7
ED-SA	Edisto-Santee	59,748	3,377,248	57	31.4	11.0	4.1	7.4	0.0	46.1
OG-SA	Ogeechee-Savannah	42,891	2,203,819	51	20.2	8.9	3.4	18.1	0.0	49.3
AL-SM	Altamaha-St. Marys	53,193	2,091,797	39	14.9	13.0	6.0	15.5	0.0	50.5
ST-JO	St. Johns	26,939	1,720,555	64	25.1	18.7	13.5	21.2	0.0	21.6
PE-TA	Peace-Tampa Bay	22,004	2,747,265	125	7.7	12.1	18.3	18.9	29.6	13.4
SUWA	Suwannee	33,265	1,169,872	35	6.0	7.8	9.8	11.3	33.3	31.7
OCHL	Ochlockonee	9,435	254,763	27	8.5	12.4	9.5	9.2	0.0	60.4
APAL	Apalachicola	52,135	2,360,023	45	17.5	11.4	5.9	12.6	0.0	52.4
CH-ES	Choctawhatchee-Escambia	37,119	1,286,095	35	9.7	12.9	6.2	22.6	0.0	48.6
ALAB	Alabama	58,891	3,739,576	64	18.2	8.2	2.5	20.0	0.0	51.2
MO-TO	Mobile-Tombigbee	55,519	3,552,544	64	18.9	9.2	4.0	15.2	0.0	52.6
PASC	Pascagoula	29,004	2,000,573	69	25.3	9.7	3.1	34.6	0.0	27.3

[1]HUC4 watershed areas are shown in figure 2 and listed here in north-south order for watersheds (Chowan-Roanoke through St. Johns) draining to the Atlantic Ocean and in east-west order for watersheds (Peace-Tampa Bay through Pascagoula) draining to the Gulf of Mexico.

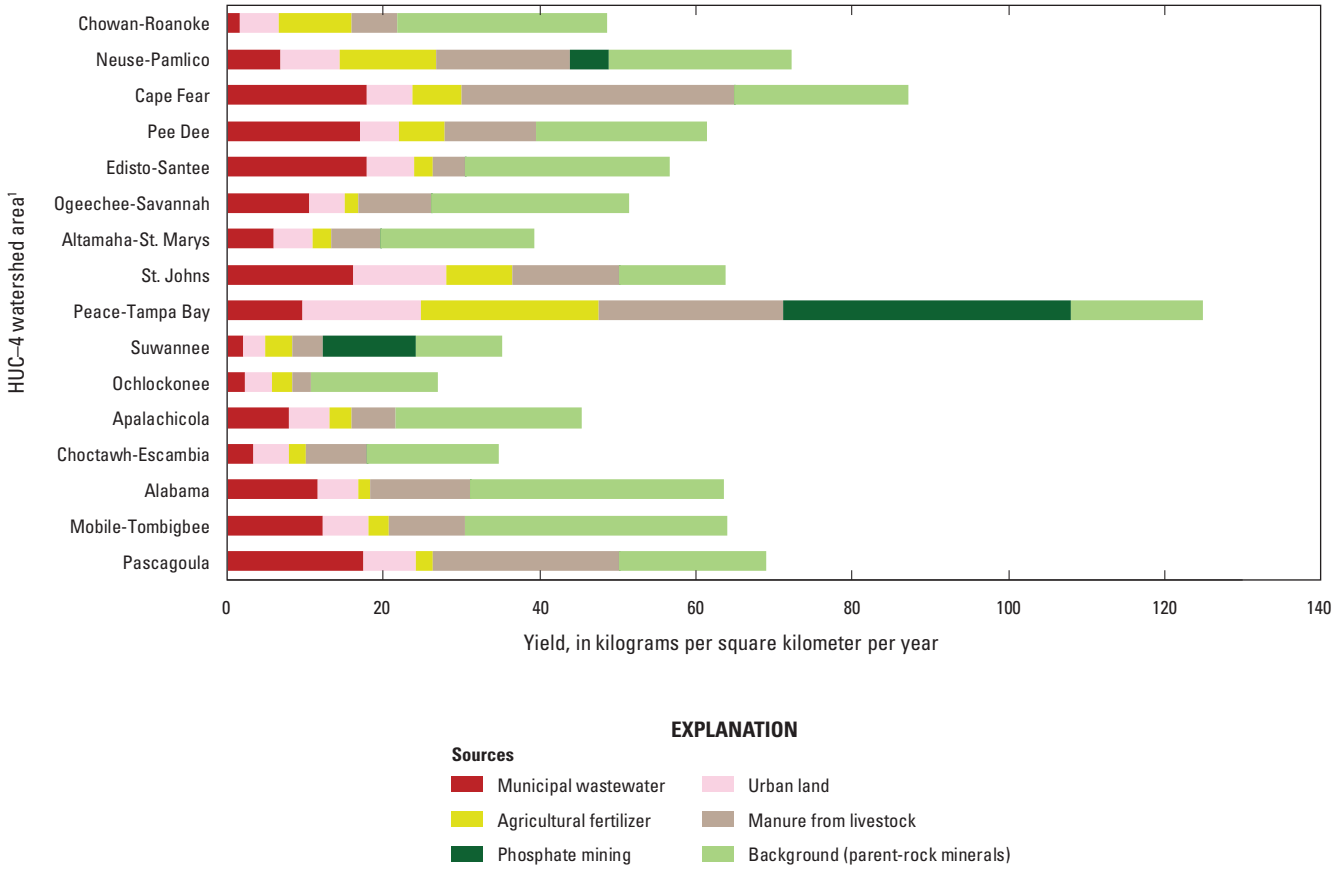

[1]Hydrologic Unit Code–4 watershed areas are shown on figure 2 and listed here in north-south order for watersheds (Chowan-Roanoke through St. Johns) draining to the Atlantic Ocean and in east-west order for watersheds (Peace-Tampa Bay through Pascagoula) draining to the Gulf of Mexico.

Figure 18. Predicted total phosphorus yield delivered to the adjacent stream by source and by HUC4 watershed area.

Suspended-Sediment SPARROW Model

Calibration

Observations of TSS and SS loads at 421 monitoring sites in the Southeast (illustrated as yields in figure 19*A* and 19*B*) were used to calibrate the SS SPARROW model. In general, TSS and SS yields were smallest, less than 14 metric tons per square kilometer per year ([t/km²]/yr), for sites south and east of the Fall Line (location shown in figure 2*B*) except in Mississippi. TSS and SS yields exceeding 48 (t/km²)/yr were observed at scattered monitoring sites north and west of the Fall Line, particularly near urban areas, and south of the Fall Line in Mississippi and Alabama.

The source terms and the transport and delivery factors tested in the SPARROW model are listed in table 12. Three of the 25 attributes tested as source variables represented channel sources; the remainder represented upland sources. Of the attributes representing upland sources, 16 were combination variables (described in the Methods section) that were intended to differentiate the effects of erodibility of native soils (natural sources of sediment) from the effects of land use/land cover (factoring in anthropogenic sources). Attributes representing land-cover change were also examined (for example, *Change in number of housing units between 2000 and 2010* and *Area in catchment that changed to urban from any other land use during 2002-2012*; table 12).

Of the three channel source variables tested, one, *Gain in stream power*, was found to be significant (table 13). Nine of the 16 combination variables representing upland sources were found to be significant. The lack of significance for the other seven can be explained by the small areal extent for the variable, resulting in the number of calibration basins that overlap the areal extent being too small to fit a coefficient value with sufficient precision. From the starting set of 16 combination variables, each of the 7 nonsignificant combination variables

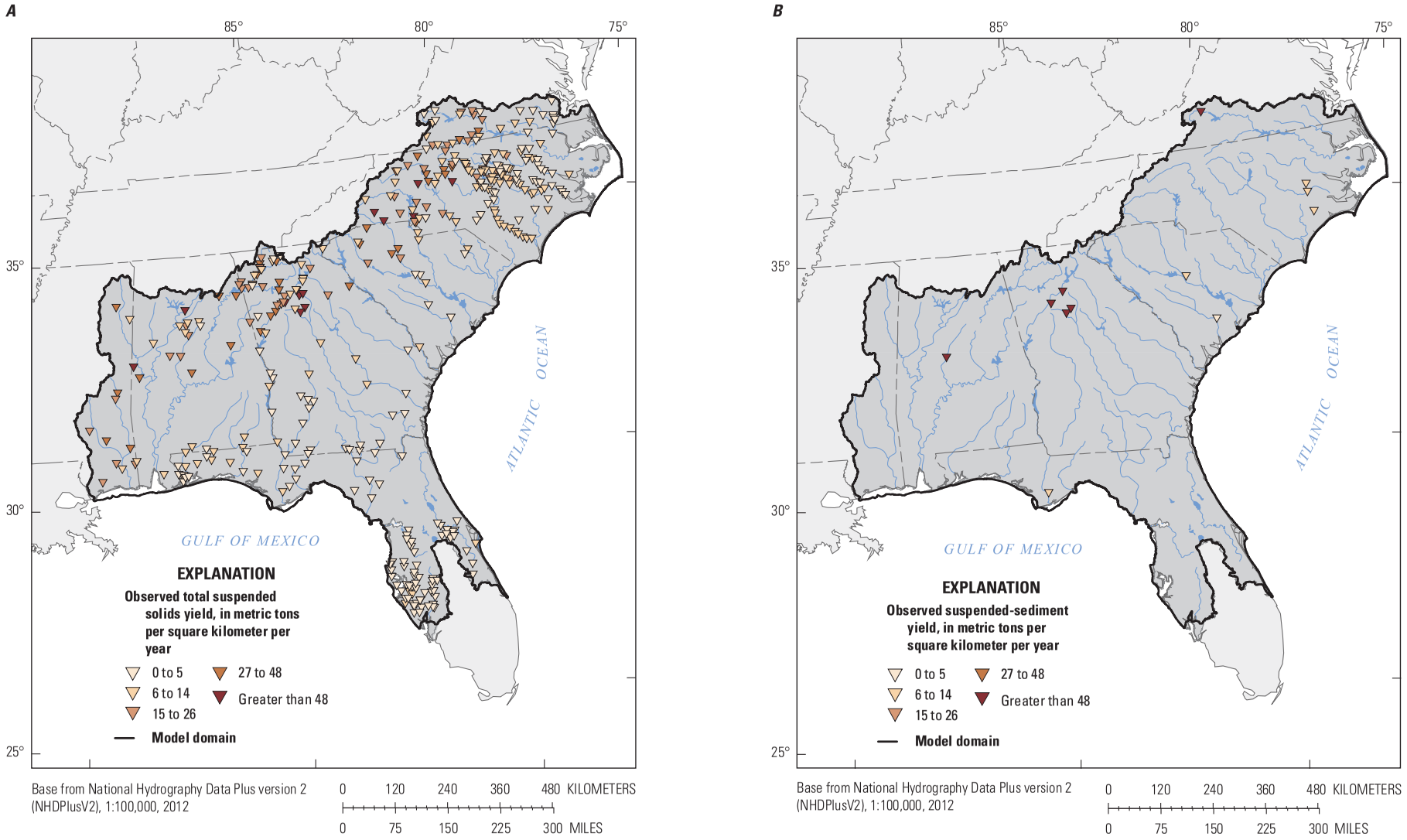

Figure 19. Yield of *A.* total suspended solids and *B.* suspended sediment for the base year 2012 estimated from stream monitoring data from 421 sites in the Southeast.

Table 12. Source, delivery, loss, and removal variables evaluated in the suspended-sediment SPARROW model for the Southeast.

[SPARROW, SPAtially Referenced Regression On Watershed attributes; Variables retained in the final specification of the model or combined with other variables are denoted with an asterisk (*); variables tested but not retained are denoted with grey-shading; additional information (publication references, links for downloading) for each variable is provided in appendix 3; Log, natural logarithm; PPT−AET, precipitation minus actual evapotranspiration; PredQ_SESpar, mean-annual streamflow in the reach, 2000–14, estimated from conditioned predictions of the streamflow SPARROW model; NHD, National Hydrography Dataset; NID, National Inventory of Dams; MAFlowUcfs, mean-annual streamflow in the reach, estimate from enhanced National Hydrography Dataset Plus (NHDPlus) version 2; km, kilometer; ft^3/s, cubic foot per second; mm/yr, millimeter per year; km^2, square kilometer]

	Source variable
*	Channel: Gain in stream power compared to adjacent upstream reach(es), fraction
	Channel: Reciprocal of reach-average sinuosity
	Channel: Stream power, nonzero only for headwater ($Q \leq 10$ ft^3/s) streams, scaled to reach length
*	Upland: Alluvium and residuum in very fine-grained sedimentary rock intersected with Urban
*	Upland: Residuum in igneous and metamorphic rock intersected with Urban
*	Upland: Residuum in sedimentary rocks (discontinuous) intersected with Urban
*	Upland: All other surficial-geology categories (Fine- and medium- grained sediments, also Residuum in alluvium and in carbonate and fine-grained sedimentary rock) intersected with Urban
*	Upland: Alluvium and residuum in very fine-grained sedimentary rock intersected with Forest
*	Upland: Residuum in igneous and metamorphic rock intersected with Forest
*	Upland: Residuum in sedimentary rocks (discontinuous) intersected with Forest
*	Upland: All other surficial geology categories (Fine and medium grained sediments, also Residuum in alluvium and in carbonate and fine-grained sedimentary rock) intersected with Forest
*	Upland: Alluvium and residuum in very fine-grained sedimentary rock intersected with Transitional (Shrub, Scrub, Herbaceous, and Barren)
*	Upland: Residuum in igneous and metamorphic rock intersected with Transitional (Shrub, Scrub, Herbaceous, and Barren)
*	Upland: Residuum in sedimentary rocks (discontinuous) intersected with Transitional (Shrub, Scrub, Herbaceous, and Barren)
*	Upland: All other surficial geology categories (Fine and medium grained sediments, also Residual materials in alluvium and in carbonate and fine-grained sedimentary rock) intersected with Shrub, Scrub, Herbaceous, Barren
*	Upland: Alluvium and residuum in very fine-grained sedimentary rock intersected with Agricultural (Cropland and Pasture)
*	Upland: Residuum in igneous and metamorphic rock intersected with Agricultural (Cropland and Pasture)
*	Upland: Residuum in sedimentary rocks (discontinuous) intersected with Agricultural (Cropland and Pasture)
*	Upland: All other surficial geology categories (Fine and medium grained sediments, also Residuum in alluvium and in carbonate and fine-grained sedimentary rock) intersected with Agricultural (Cropland and Pasture)
	Upland: Number of road crossings, 2018
	Upland: Change in number of housing units between 2000 and 2010
	Upland: Area in catchment that changed from one land use to another land use during 2002–12
	Upland: Area in catchment that changed to urban from any other land use during 2002–12
	Upland: Area in catchment that changed to urban or semideveloped from any other land use during 2002–12
	Upland: Area in catchment that changed from a vegetated land use class to any other class during 2002–12
	Land-to-water delivery variables
*	Log of Kfactor (erodibility index)
*	Log of PPT−AET, mm/yr, detrended to base year 2012; in contrast to PPT−AET used as source term in the streamflow model, this term is normalized by the area of the catchment
*	Log of percent of 100-meter-width buffer in canopy land cover, 2011
*	Log of percent of catchment in no till or conservation tillage, 2012
	Log of basin slope (mean of land-surface elevation slope in catchment)
	Log of channel slope

Table 12. Source, delivery, loss, and removal variables evaluated in the suspended-sediment SPARROW model for the Southeast.—Continued

[SPARROW, SPAtially Referenced Regression On Watershed attributes; Variables retained in the final specification of the model or combined with other variables are denoted with an asterisk (*); variables tested but not retained are denoted with grey-shading; additional information (publication references, links for downloading) for each variable is provided in appendix 3; Log, natural logarithm; PPT−AET, precipitation minus actual evapotranspiration; PredQ_SESpar, mean-annual streamflow in the reach, 2000–14, estimated from conditioned predictions of the streamflow SPARROW model; NHD, National Hydrography Dataset; NID, National Inventory of Dams; MAFlowUcfs, mean-annual streamflow in the reach, estimate from enhanced National Hydrography Dataset Plus (NHDPlus) version 2; km, kilometer; ft^3/s, cubic foot per second; mm/yr, millimeter per year; km^2, square kilometer]

	Log of stream mean velocity (foot per second)
	Log of percent of catchment in cover crops, 2012
	Log of percent of catchment in conservation easement, 2012
	Log of incremental flow from catchment to stream (streamflow SPARROW model), mean of 2000–14
	Log of precipitation intensity, 2000–14
	Change in housing density from 2000 and 2010
Aquatic loss variables	
*	Width (area in catchment divided by channel length) of riparian wetland, scaled to time of travel in reach
	Reciprocal areal hydraulic load for waterbodies in karst landscape (mostly in Florida), surface area from NHD using NID data to supplement, flow from PredQ_SESpar
*	Reciprocal areal hydraulic load for waterbodies not in karst landscape, estimated from NHD (Moore and others), surface area from NHD using NID data to supplement, flow from PredQ_SESpar
	Log of loss in stream power compared to adjacent upstream reach(es)
Removal as water withdrawals	
*	Consumptive use at power plants, 2010, expressed as -log(1-fraction of unremoved streamflow)
Conversion factor	
*	Convert total suspended solids monitored load to suspended-sediment load

was grouped with a significant variable of the same land-use/land-cover classification and with the most similar coefficient estimate, which resulted in 8 combination variables in the final model (table 13).

Coefficients for the eight upland source terms represent the mass delivery ratio for a catchment with average land-to-water delivery properties. The coefficient of the variable *Residuum in sedimentary rocks* (*discontinuous*) *intersected with Urban* (15.34; table 13) means that for a catchment with average delivery properties, 15.34 metric tons (MT) of SS is delivered to the adjacent stream channel for every square kilometer of urban land cover that overlies residuum in sedimentary rock in the catchment. The coefficients for each of the upland source variables are shown in figure 20, and the spatial distribution of each of the surficial-geology categories is shown in figure 21. Transitional land (shrub, scrub, herbaceous, and barren land use/land cover) produced high sediment yields to streams (62.619 [t/km^2]/yr) when combined with all but one category of surficial geology. *Residuum in sedimentary rocks* (*discontinuous*) *intersected with Agricultural* (*Cropland and Pasture*) produced extremely high sediment yields to streams (166.2 [t/km^2]/yr); in the other three geologic settings, average yields from agricultural land were an order of magnitude lower, 14.4 (t/km^2)/yr. Because of these interactions, neither geologic setting nor land use/land cover could be identified as having the greater effect on sediment yield.

The standard errors for the coefficients for almost all the source variables in the SS model were large—greater than 30 percent for all but one coefficient (standard error in percent is computed as the quotient of standard error for the coefficient and the NLLS estimate, from columns 4 and 3 of table 13, respectively, multiplied by 100). This approach is in sharp contrast to the other three SPARROW models, for which standard error was less than 20 percent for most source variables. This level of uncertainty in source coefficients places this model and its predictions in a separate category—a reconnaissance rather than a full assessment model—from the other three models and reduces confidence in the apportionment of stream load among these source shares in the SS model.

The delivery ratios for the upland sources were simulated as varying among catchments according to the model-specified processes of sediment attenuation (settling and burial on land) during land-to-water delivery. Twelve watershed characteristics were evaluated as possible land-to-water delivery variables (table 12). The four land-to-water delivery variables in the final model and their associated estimated coefficients and statistics are presented in table 13. The large coefficient values for *Log of Kfactor* and *Log of PPT–AET* mean that the delivery ratios for the upland sources were most sensitive to these variables.

The positive coefficient (0.982) associated with *Log of PPT–AET* may reflect elevated rates of water transport

Table 13. Model-estimated coefficients and diagnostics for the suspended-sediment SPARROW model for the Southeast.

[SPARROW, SPAtially Referenced Regression On Watershed attributes; additional information (publication references, links for downloading) for each variable is provided in appendix 2; *p*-value, probability value; *t*-value, *t*-statistic; Soller group 1, Alluvium and residuum in very fine-grained sedimentary rock; Soller group 2, Residuum in igneous and metamorphic rock; Soller group 3,Residuum in sedimentary rock (discontinuous); Soller group 4, Soller classes other than 1, 2, and 3, i.e. Fine and medium grained sediments, residuum in alluvium, and residuum in carbonate and fine-grained sedimentary rock; Transitional, land cover classified as Shrub, Scrub, Herbacous, or Barren; PPT−AET, precipitation minus actual evapotranspiration; P, phosphorus; TP, total phosphorus; --, not estimated because coefficient was fully constrained; RMSE, root mean squared error; Log, natural logarithm; R^2, coefficient of determination; proximal, site pairs that are within 5 kilometers distance; t/yr; metric ton per year; km^2, square kilometer; m*d, meter multiplied by day; yr/m, year per meter; m/yr; meter per year; <, less than, TSS, total suspended solids]

Variable	Variable unit	Coefficient unit	Model coefficient value	90-percent confidence interval for the model coefficient		Standard error of the model coefficient	*p*-value	*t*-value	Variance inflation factor
				Lower	Upper				
Source (model coefficient = α)									
Gain in stream power (channel erosion)	Fraction	t/yr	17.197	7.698	26.696	7.399	0.0206	2.324	4.872
Soller groups 1 and 2 and Urban	km^2	$t/km^2/yr$	81.886	58.570	105.201	18.161	<0.0001	4.509	2.503
Soller group 3 and Urban	km^2	$t/km^2/yr$	15.339	4.644	26.034	8.331	0.0664	1.841	1.428
Soller group 4 and Urban	km^2	$t/km^2/yr$	27.219	15.697	38.741	8.975	0.0026	3.033	2.928
All four Soller groups and Forested	km^2	$t/km^2/yr$	15.006	8.040	21.972	5.426	0.0060	2.765	4.144
Soller groups 1, 2, and 3 and Transitional	km^2	$t/km^2/yr$	62.619	21.102	104.135	32.339	0.0536	1.936	2.764
Soller group 4 and Transitional	km^2	$t/km^2/yr$	27.757	8.239	47.275	15.204	0.0687	1.826	2.160
Soller groups 1, 2, and 4 and Agricultural	km^2	$t/km^2/yr$	14.414	5.190	23.638	7.185	0.0456	2.006	3.410
Soller group 3 and Agricultural	km^2	$t/km^2/yr$	166.152	84.616	247.688	63.512	0.0093	2.616	2.657
Land-to-water delivery									
Logarithm of Kfactor (erodibility index)	Unitless	Unitless	2.292	1.767	2.818	0.319	<0.0001	7.197	3.929
Logarithm of PPT−AET, in mm/yr	Unitless	Unitless	0.982	0.619	1.344	0.220	<0.0001	4.465	2.176
Logarithm of percent of 100-meter buffer in canopy land cover	Unitless	Unitless	–0.321	–0.464	–0.177	0.087	0.0003	–3.685	1.708
Logarithm of percent of catchment in no till or conservation tillage	Unitless	Unitless	–0.121	–0.220	–0.022	0.060	0.0444	–2.017	1.864
Aquatic loss									
Streams and rivers—Riparian wetland width scaled to time of travel in reach	m*d	1/(m*d)	0.00016	0.0001	0.0002	0.00006	0.0027	2.794	1.285
Reservoirs and lakes—Reciprocal of areal hydraulic load (excludes waterbodies in karst landscape)	yr/m	m/yr	25.356	20.335	30.377	3.911	<0.0001	6.483	1.435
Reservoirs and lakes—Reciprocal of areal hydraulic load (waterbodies in karst landscape)	yr/m	m/yr	Estimation is forced to zero	--	--	--	--	--	--

Table 13. Model-estimated coefficients and diagnostics for the suspended-sediment SPARROW model for the Southeast—Continued

[SPARROW, SPAtially Referenced Regression On Watershed attributes; additional information (publication references, links for downloading) for each variable is provided in appendix 2; *p*-value, probability value; *t*-value, *t*-statistic; Soller group 1, Alluvium and residuum in very fine-grained sedimentary rock; Soller group 2, Residuum in igneous and metamorphic rock; Soller group 3,Residuum in sedimentary rock (discontinuous); Soller group 4, Soller classes other than 1, 2, and 3, i.e. Fine and medium grained sediments, residuum in alluvium, and residuum in carbonate and fine-grained sedimentary rock; Transitional, land cover classified as Shrub, Scrub, Herbacous, or Barren; PPT−AET, precipitation minus actual evapotranspiration; P, phosphorus; TP, total phosphorus; --, not estimated because coefficient was fully constrained; RMSE, root mean squared error; Log, natural logarithm; R^2, coefficient of determination; proximal, site pairs that are within 5 kilometers distance; t/yr; metric ton per year; km^2, square kilometer; m*d, meter multiplied by day; yr/m, year per meter; meter per year; <, less than, TSS, total suspended solids]

Variable	Variable unit	Coefficient unit	Model coefficient value	90-percent confidence interval for the model coefficient		Standard error of the model coefficient	*p*-value	*t*-value	Variance inflation factor
				Lower	Upper				
Removal as water withdrawals									
Consumptive use at power plants, fraction of instream flow	−log(1−fraction of unremoved streamflow)	Unitless	1.282	--	--	--	--	--	--
Conversion factor									
Binary variable (*Convert*) distinguishing loads estimated from SSC concentration data from loads estimated from TSS concentration data	Unitless	Unitless	–1.174	–1.437	–0.910	0.160	<0.0001	–7.353	13.769

Spatial test	Number of sites/site pairs	Test statistic	*p*-value
Spatial autocorrelation of residuals from nonproximal sites (Moran's *I* test statistic)	395 sites	0.0178	0.567
Spatial autocorrelation of residuals from nonnested proximal site[a] (Pearson's *r* test statistic)	29 site pairs	0.0575	0.767
Spatial autocorrelation of residuals from nested proximal sites (Pearson's *r* test statistic	0 site pairs	(no sites in this category)	(no sites in this category)
Weights—Coefficient for log of nested area share[b]	395 sites	0.306	0.0004

Model summary statistics				
Conditioned RMSE[c]	In logarithmic space	0.62	In percent[d]	68
Unconditioned RMSE[e]	In logarithmic space	0.65	In percent[d]	73
Mean exponentiated weighted error		1.22		
R^2 of dependent variable (load)		0.93		
R^2 of yield		0.76		
Number of sites used to calibrate the model		395		

[a]Also including nested sites with dissimilar drainage area.

[b]The fraction of the upstream drainage area that is downstream from other monitoring sites.

[c]Conditioned RMSE: the residuals are calculated as the difference between natural log of monitored load and natural log of predicted load, where the prediction has been conditioned on monitored load at the closest upstream site(s).

[d]RMSE in terms of percent in real space units was computed as: $100 \times (\exp[RMSE^2]-1)^{0.5}$; RMSE in this equation is in natural log space.

[e]Unconditioned RMSE: same as conditioned RMSE except the prediction is not conditioned on monitored load for upstream station(s).

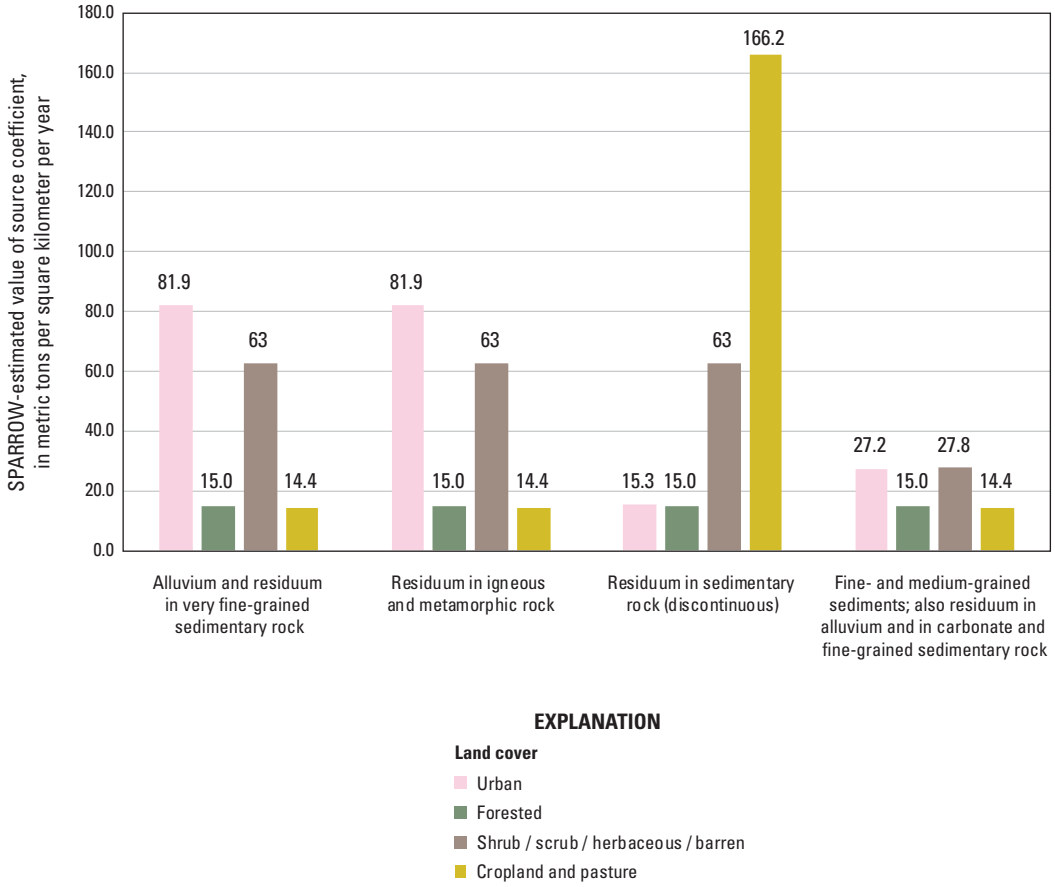

Figure 20. Suspended-sediment delivery ratios (α) for upland sources estimated by the suspended-sediment SPARROW (SPAtially Referenced Regression On Watershed attributes) model, by surficial geology category and land use/land cover category.

through the catchment, causing elevated rates of mobilization and transport of sediment. The positive coefficient (2.292) for *Log of Kfactor* indicates that the surficial-geology source categories likely do not capture all the spatial variability in native erodibility of the soil and that additional variability in soil erodibility is needed to characterize its effect on sediment delivery to stream reaches. The negative coefficient (−0.321) associated with *Log of percent of 100-meter buffer in canopy land cover* indicates that vegetated riparian areas may intercept and immobilize SS. The negative coefficient (−0.121) associated with *Log of percent of catchment in no till or conservation tillage* indicates that these tillage practices likely decrease the loss of sediment from cropland and pasture. The change (reduction) in sediment delivery ratio from a 1-percent change in extent of land in these tillage practices is relatively small (0.121 percent), but in catchments underlain by residuum in sedimentary rock, a 10-percent change in the amount of land in these tillage practices would represent a 0.0121 * 166.2 (t/km^2)/yr = 2.01 (t/km^2)/yr change in sediment delivered to the stream. The agricultural best management practices of cover crops and conservation easements were tested but were not significant.

Four physical stream-channel, reservoir, and lake attributes were evaluated to describe long-term aquatic loss or removal of SS during transport through the stream network (table 13). The attribute selected to represent loss in free-flowing streams, *Riparian wetland width scaled to time of travel in reach* (units of m*d) was computed as the quotient of area of riparian wetland and channel length multiplied by the time of travel in the reach. Loss was modeled as a first-order decay function; therefore, the model-estimated coefficient (0.00016 m/d) can be interpreted as first-order loss-rate coefficient. The small magnitude of this coefficient means that although its effect on spatial distribution of sediment load was significant, the modeled rate of removal (trapping and burial in riparian wetlands) was small.

The variable representing loss in lakes and reservoirs, *Reciprocal of areal hydraulic load*, was computed as the quotient of lake or reservoir surface area and outflow. The estimated coefficient for the first-order reservoir decay function (25.356 m/yr for lakes and reservoirs excluding those in karst landscapes) can be interpreted as a hypothetical settling velocity that, when multiplied by reciprocal of areal hydraulic load (in years per meter) and exponentiated, quantifies the proportion of the SS mass transported through the lake or reservoir.

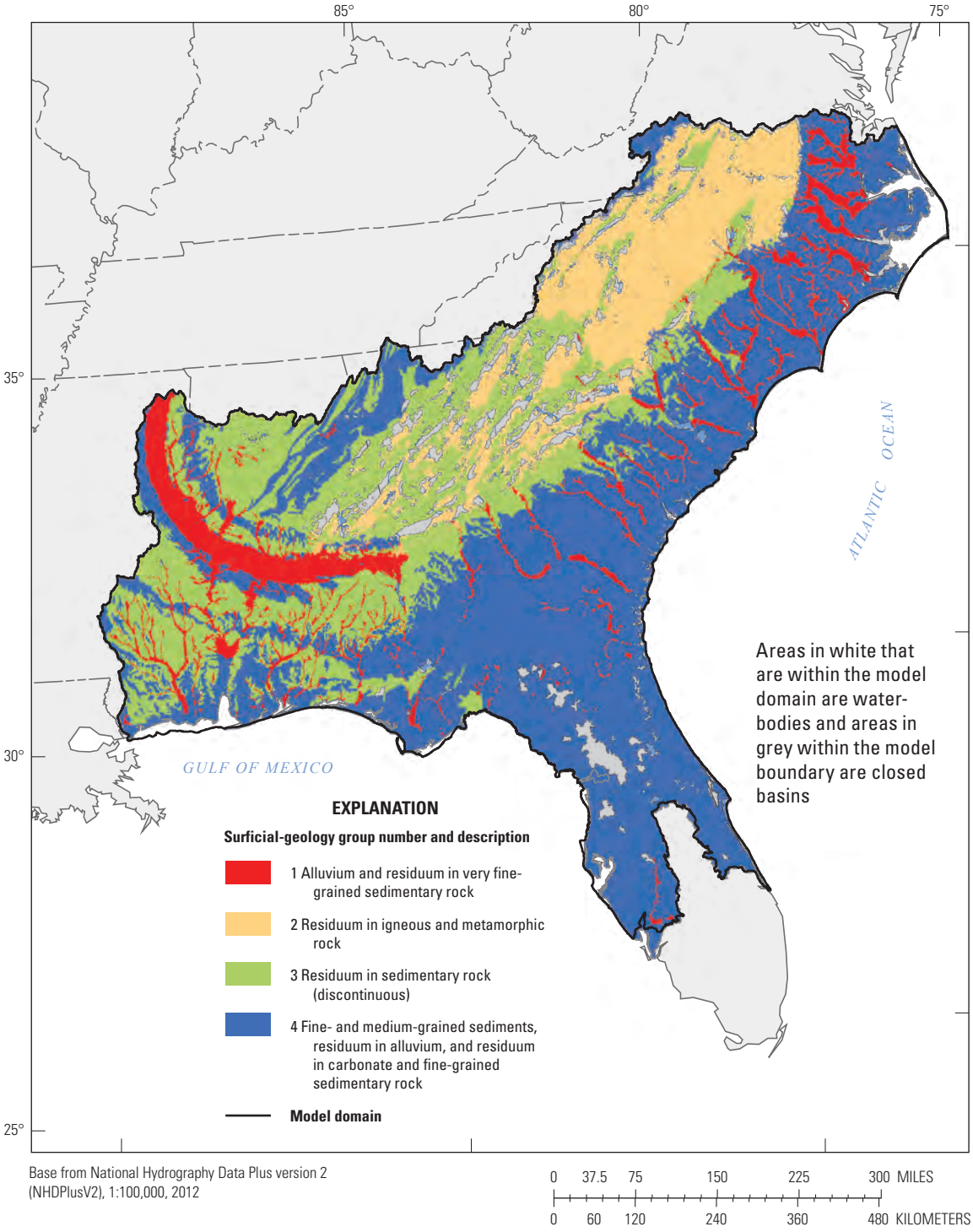

Figure 21. Spatial distribution of the four categories of surficial geology used in the suspended-sediment SPARROW (SPAtially Referenced Regression On Watershed attributes) model specification.

The removal variable *Consumptive use at power plants* was used to represent withdrawals from the stream. The coefficient for this variable was not estimated in the SS model; rather, it was constrained to equal the estimated coefficient value, 1.282, from the calibrated streamflow model. Surface-water withdrawals for municipal water supply were excluded from the model because estimates of discharge from wastewater-treatment plants were not available to balance them (sediment loads in wastewater discharges were not estimated) and consequently the surface-water withdrawal term would have overestimated removal for municipal use.

The variable *Convert,* a binary variable distinguishing between loads estimated from SSC data and loads estimated from TSS concentration data, was tested to evaluate the difference between these two groups of load estimates (described in the Methods section). The model-estimated coefficient, −1.17 (dimensionless), can be used to calculate a scaling factor for converting between the two groups of estimates, given by equation (3) in the Methods section.

The scaling factor determined from this model is 3.23, computed as 1/exp(−1.17). This estimate of scaling factor is higher than expected on the basis of a comparison of the two groups of estimates for streams in Georgia (Aulenbach and others, 2017); the average ratio of mean-annual load of TSS compared to SS for 13 stream sites was 2.14 (minimum and maximum values 1.27 and 4.75). Several studies have reported average ratio of SSC and TSS concentration but scaling factor for concentration is likely different from a scaling factor for mean-annual load estimates.

Goodness of fit between the monitored SS loads (illustrated as yield in figure 19) and those predicted by the SPARROW model is quantified in the calibration statistics reported in table 13 and illustrated by graphs and maps of model error at calibration stations (figs. 22 and 23). The RMSEs of conditioned and unconditioned residuals (see Glossary for definition of these terms), 0.62 and 0.65, respectively, are equivalent to a mean error of 68 and 73 percent, respectively (table 13) and are the largest among the four models. The R^2 of yield for the SS SPARROW model, 0.76 (table 13), indicates that the SS model explains 76 percent of the variance in log-transformed monitored yield.

Conditioned residuals from the sediment model were homoscedastic (fig. 22*A*, *C*, and *D*). The spread of observations around the 1:1 line for predicted against actual SS loads was similar for conditioned and unconditioned residuals (compare figure 22*A* to figure 22*B*) except for a tendency to underpredict loads at large values (fig. 22*B*).

Aside from isolated clusters of underprediction or overprediction related to nested stations and propagation of error from upstream to downstream stations, the spatial distribution of unconditioned residuals (fig. 23*B*) is a scattered pattern of over- and underpredictions with no tendency to predominantly over- or underpredict in specific areas. The *p*-value of 0.567 associated with Moran's *I* test statistic (0.0178, table 13) confirmed that residuals were not spatially autocorrelated.

Residuals for site pairs in close proximity (less than 5 km apart) were tested for significant and negative correlation (described in the Methods section). The residuals for nonnested proximal pairs were not correlated, with a *p*-value of 0.767 (table 13). Therefore, no thinning of nonnested proximal pairs was required. Nested proximal pairs were excluded from the final calibration set when a previous test of an intermediate calibration set showed significant negative correlation among the nested proximal pairs.

The positive value (0.306) and *p*-value less than 0.0004 for the coefficient for nested area share (table 13) indicates that calibrating the model without accounting for the effects of nested basins would have underestimated residuals and discounted the influence of downstream sites in model calibration. The final calibrated model reported in table 13 therefore incorporated a recalibration step in which weighted regression was used to address the unequal effects of nested basins in calibration.

Predictions

The SS SPARROW model was used to estimate SS loads and yields for streams throughout the Southeast (fig. 24). The model-predicted source shares for load and yield are summarized by HUC4 watershed area in table 14 and illustrated in figure 25. These predictions should be considered with caution, however, as a result of the large calibration error for this model (unconditioned RMSE of 73 percent) and the large uncertainty in most of the source coefficients. The pattern of model-predicted sediment yield delivered from the incremental catchment to the adjacent stream (fig. 24*A*) was similar to the pattern of monitored sediment yield (fig. 19). TP load and yield delivered to adjacent streams from all catchments in the Southeast was 22,769,525 t/yr and 36 (t/km²)/yr, respectively (table 14).

SS yields were smallest, less than 14 (t/km²)/yr, for all catchments below the Fall Line, except for catchments in Mississippi and Alabama; this area of small yield corresponds to the areal extent of Soller Group 4 (fine- and medium-grained sediments, residuum in alluvium, and residuum in carbonate and fine-grained sedimentary rock; compare to figure 21; Soller and others, 2009). Sediment yields exceeded 48 (t/km²)/yr in southern Mississippi and in the Black Belt area (Soller Group 1, Alluvium and residuum in very fine-grained sedimentary rock), throughout the Piedmont region of Georgia and Alabama (Soller Group 2, Residuum in igneous and metamorphic rock), and in northern Alabama (Soller Group 3, Residuum in sedimentary rock—discontinuous).

The markedly different patterns in sediment yield delivered from catchment to adjacent stream (fig. 24*A*) and sediment yield delivered from catchment to the basin outlet at coastal waters (fig. 24*B*), especially for catchments at great distance from the coast, illustrates the model finding of substantial losses of sediment during transport through the channel network. Sediment mass lost in the stream network

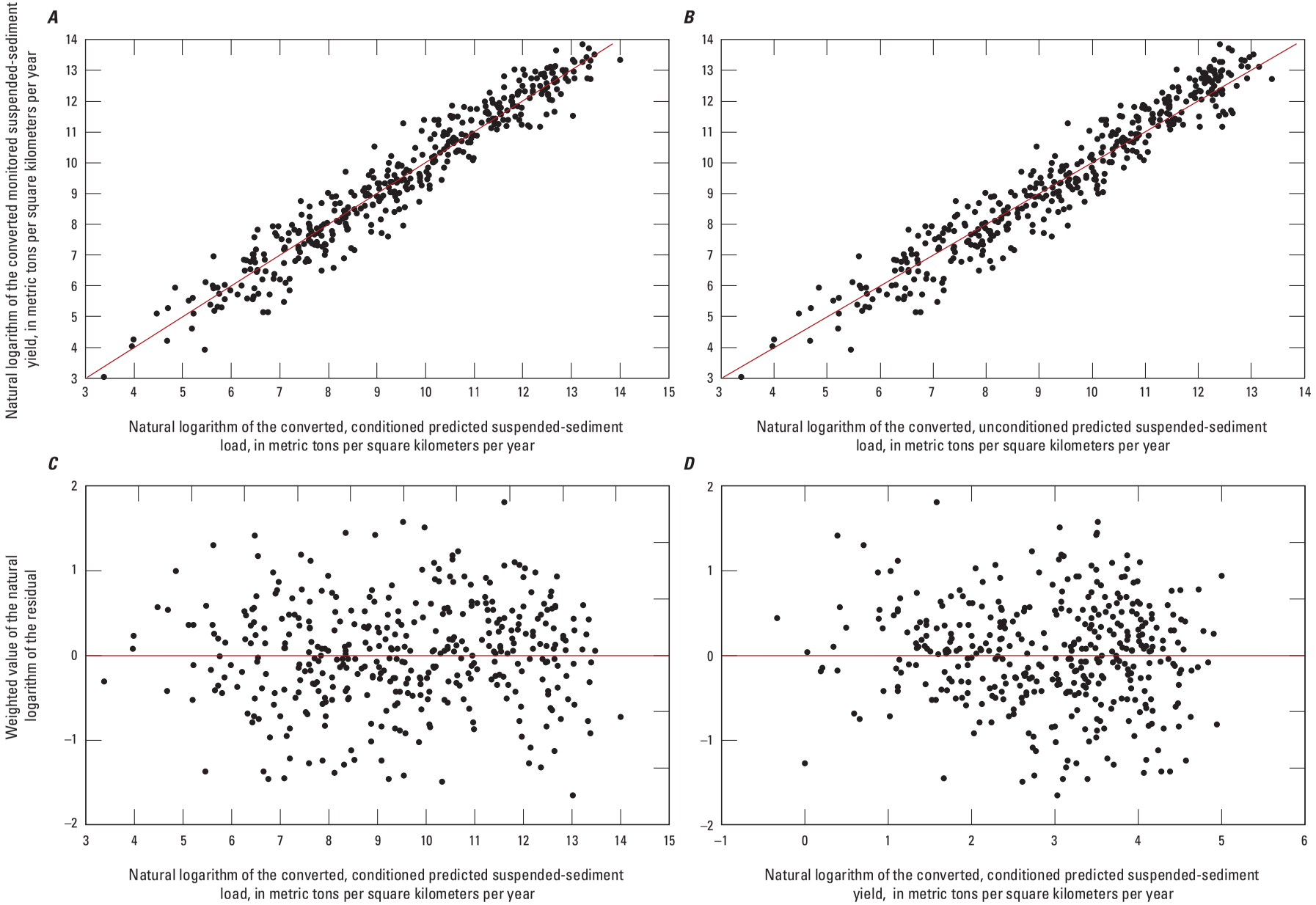

Figure 22. Diagnostic plots for the suspended-sediment SPARROW (SPAtially Referenced Regression On Watershed attributes) model for the Southeast: *A*. monitored load versus converted, conditioned predicted load, *B*. monitored load versus unconditioned predicted load, *C*. weighted residuals versus predicted load, and *D*. weighted residuals versus predicted yield, for 395 calibration sites. Conditioned predicted load means that the prediction is conditioned on monitored load for the closest upstream site(s). Unconditioned predicted load means that the prediction is not conditioned on monitored load for upstream site(s).

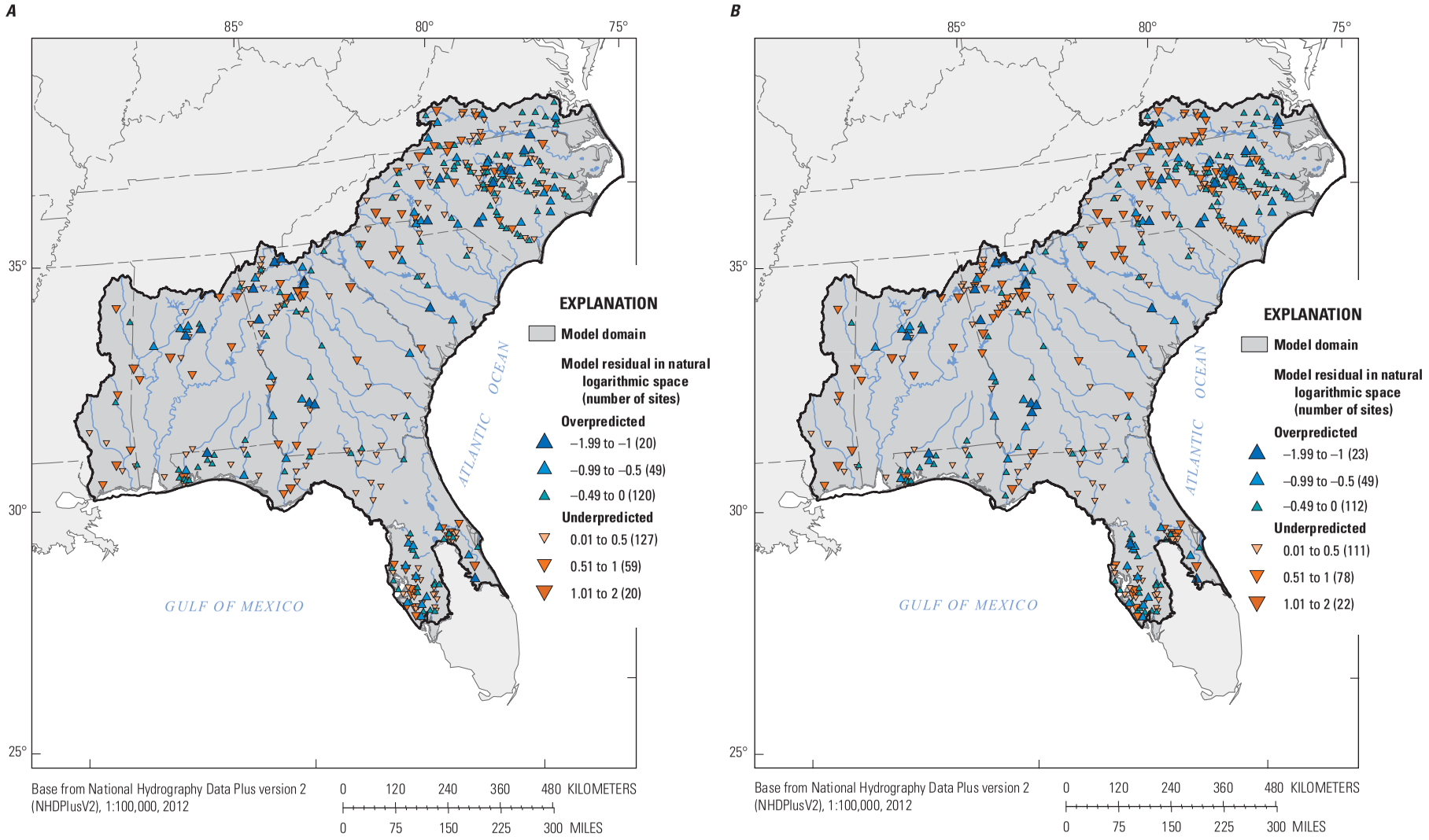

Figure 23. Spatial distribution of *A*. conditioned residuals and *B*. unconditioned residuals from the suspended-sediment SPARROW (SPAtially Referenced Regression On Watershed attributes) model for the Southeast. Conditioned residuals are calculated as the difference between natural log of monitored load and natural log of predicted load, where the prediction has been conditioned on the monitored load at the closest upstream site(s). For unconditioned residuals the prediction is not conditioned on monitored load for upstream monitoring site(s).

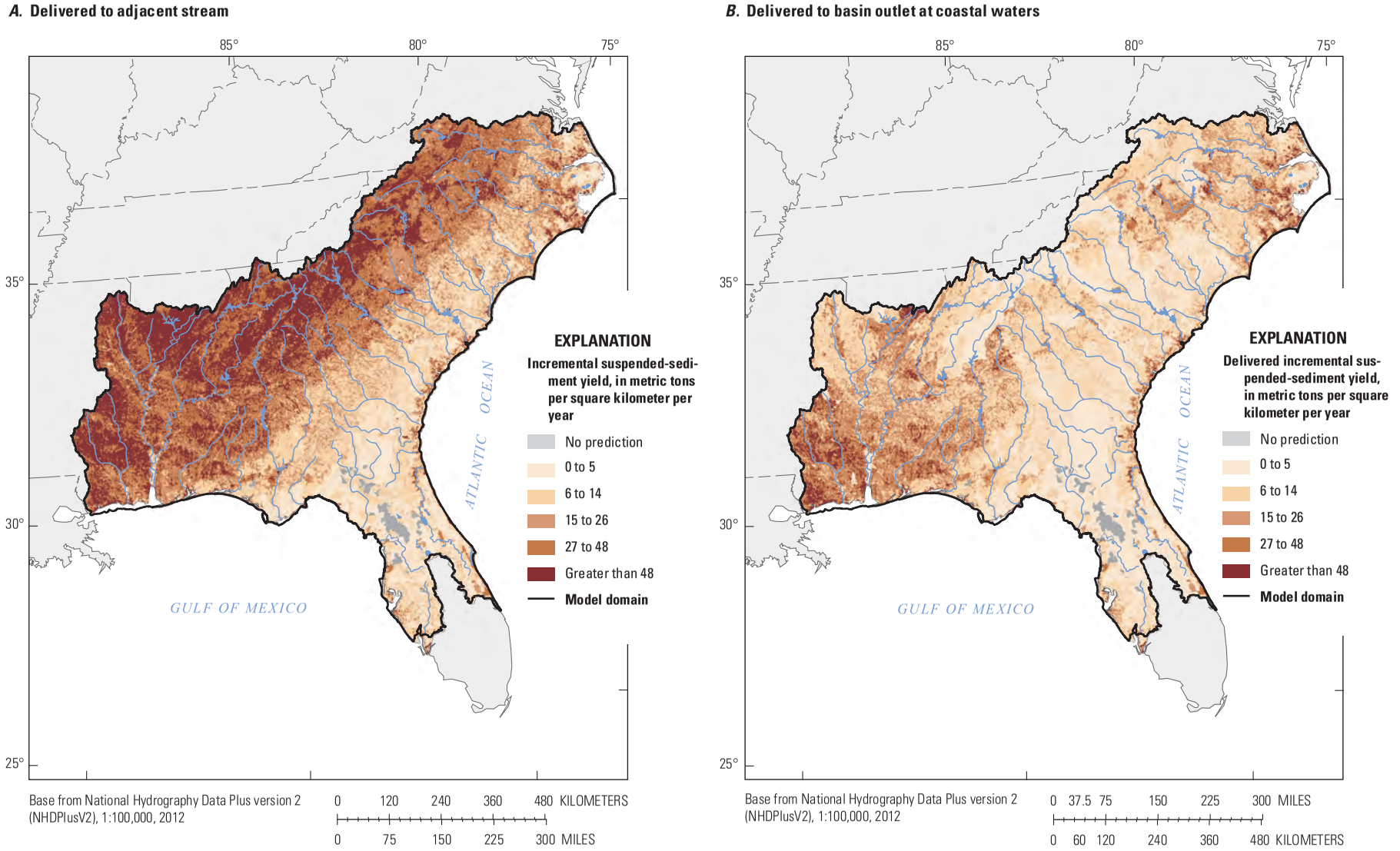

Figure 24. Mean-annual incremental yield of suspended sediment *A.* delivered to the adjacent stream, and *B.* delivered to the basin outlet at coastal waters, predicted from the suspended-sediment SPARROW (SPAtially Referenced Regression On Watershed attributes) model for the Southeast.

Table 14. Load, yield, and source shares of suspended-sediment delivered from catchment to adjacent stream and summarized by HUC4 watershed area, estimated from the suspended-sediment SPARROW model for the Southeast.

[SPARROW, SPAtially Referenced Regression On Watershed attributes; estimates are based on unconditioned predictions, that is, monitored values are not substituted for simulated values at monitored reaches; Hydrologic Unit Code-4 (HUC4) watersheds are shown in figure 2; Soller group 1, Alluvium and residuum in very fine-grained sedimentary rock; Soller group 2, Residuum in igneous and metamorphic rock; Soller group 3, Residuum in sedimentary rock (discontinuous); Soller group 4, Soller classes other than 1, 2, and 3, i.e. Fine- and medium-grained sediments, residuum in alluvium, and residuum in carbonate and fine-grained sedimentary rock; Transitional; land cover classified as Shrub, Scrub, Herbacous and Barren; National Hydrography Dataset Plus (NHDPlus) version 2; kg/yr, kilogram per year; kg/km^2/yr; kilograms per square kilometer per year; km^2, square kilometers; t, metric ton]

HUC4 watershed abbreviation[1]	HUC4 watershed name	Basin area, based on NHDPlus network (km^2)	Suspended-sedment load delivered to adjacent stream (t/yr)	Supended-sediment yield delivered to adjacent stream (t/km^2/yr)	Suspended-sediment source share (percent of total)										
					Channel Erosion	Soller groups 1 and 2 and Urban	Soller group 3 and Urban	Soller group 4 and Urban	All four Soller groups and Forested	Soller groups 1 and 2 and Transitional[2]	Soller group 3 and Transitional[2]	Soller group 4 and Transitional	Soller groups 1 and 2 and Agricultural[3]	Soller group 3 and Agricultural	Soller group 4 and Agricultural[3]
Summary for Southeast		**628,346**	**22,769,525**	**36**	**12.3**	**10.7**	**1.9**	**5.0**	**22.1**	**6.6**	**10.3**	**4.9**	**1.9**	**21.1**	**3.1**
CH-RO	Chowan-Roanoke	45,675	1,475,372	32	15.0	12.9	0.4	5.2	26.3	16.1	1.7	5.1	5.0	7.9	4.4
NE-PA	Neuse-Pamlico	30,893	902,026	29	15.7	20.4	1.1	8.1	16.1	10.1	1.2	13.4	3.2	3.4	7.3
CA-FE	Cape Fear	23,718	625,819	26	19.6	24.6	1.6	3.3	17.9	10.9	4.3	6.0	4.1	5.0	2.9
PE-DE	Pee Dee	47,917	1,256,726	26	18.2	22.9	0.6	3.2	21.0	9.9	3.4	3.9	4.6	9.8	2.5
ED-SA	Edisto-Santee	59,748	2,065,200	35	10.5	27.3	2.1	2.4	22.5	10.0	4.8	2.7	3.3	13.6	0.9
OG-SA	Ogeechee-Savannah	42,891	1,520,700	35	12.7	12.8	2.0	1.8	24.8	10.4	8.0	2.6	2.1	22.2	0.7
AL-SM	Altamaha-St. Marys	53,193	1,431,012	27	14.8	16.2	2.8	2.5	17.7	7.5	7.9	4.4	1.8	23.0	1.5
ST-JO	St. Johns	26,939	233,178	9	20.3	0.0	0.0	44.2	11.3	0.0	0.0	13.5	0.0	0.0	10.7
PE-TA	Peace-Tampa Bay	22,004	183,508	8	27.6	0.4	0.0	39.8	4.2	0.3	0.0	9.9	0.8	0.0	17.0
SUWA	Suwannee	33,265	214,499	6	35.1	0.5	0.0	8.8	21.4	1.7	0.0	21.8	0.2	0.0	10.4
OCHL	Ochlockonee	9,435	104,706	11	30.9	0.6	0.7	11.9	27.0	1.1	3.8	14.2	0.1	2.3	7.4
APAL	Apalachicola	52,135	2,109,847	40	11.5	11.8	4.5	1.3	19.9	4.8	10.2	2.0	1.4	30.5	2.1

Table 14. Load, yield, and source shares of suspended-sediment delivered from catchment to adjacent stream and summarized by HUC4 watershed area, estimated from the suspended-sediment SPARROW model for the Southeast.—Continued

[SPARROW, SPAtially Referenced Regression On Watershed attributes; estimates are based on unconditioned predictions, that is, monitored values are not substituted for simulated values at monitored reaches; Hydrologic Unit Code-4 (HUC4) watersheds are shown in figure 2; Soller group 1, Alluvium and residuum in very fine-grained sedimentary rock; Soller group 2, Residuum in igneous and metamorphic rock; Soller group 3, Residuum in sedimentary rock (discontinuous); Soller group 4, Soller classes other than 1, 2, and 3, i.e. Fine- and medium-grained sediments, residuum in alluvium, and residuum in carbonate and fine-grained sedimentary rock; Transitional; land cover classified as Shrub, Scrub, Herbacous and Barren; National Hydrography Dataset Plus (NHDPlus) version 2; kg/yr, kilogram per year; kg/km^2/yr; kilograms per square kilometer per year; km^2, square kilometers; t, metric ton]

HUC4 watershed abbreviation[1]	HUC4 watershed name	Basin area, based on NHDPlus network (km^2)	Suspended-sedment load delivered to adjacent stream (t/yr)	Supended-sediment yield delivered to adjacent stream (t/km^2/yr)	Suspended-sediment source share (percent of total)										
					Channel Erosion	Soller groups 1 and 2 and Urban	Soller group 3 and Urban	Soller group 4 and Urban	All four Soller groups and Forested	Soller groups 1 and 2 and Transitional[2]	Soller group 3 and Transitional[2]	Soller group 4 and Transitional	Soller groups 1 and 2 and Agricultural[3]	Soller group 3 and Agricultural	Soller group 4 and Agricultural[3]
CH-ES	Choctawhatchee-Escambia	37,119	1,334,527	36	14.2	2.0	1.4	6.8	19.8	3.1	16.5	7.5	0.5	25.7	2.5
ALAB	Alabama	58,891	3,556,820	60	9.7	6.2	2.1	5.3	28.8	4.8	10.7	4.9	1.1	22.7	3.6
MO-TO	Mobile-Tombigbee	55,519	3,776,247	68	8.2	2.6	2.0	4.3	22.2	3.0	17.7	4.5	0.8	30.5	4.2
PASC	Pascagoula	29,004	1,979,337	68	9.1	2.2	1.8	6.8	18.2	3.7	21.3	4.3	0.5	30.7	1.4
						Share of model area occupied by source category[4]									
Summary for Southeast						2.6	2.3	4.9	39	2.8	4.2	7.1	4	3.1	9.7

Upland source shares aggregated by land cover	Urban	Forested	Transitional	Agricultural
	Suspended-sediment source share (percent of total)			
	18	22	22	26
	Share of model area occupied by source category[4]			
	9.9	39	14	17

[1]HUC4 watershed areas are shown in figure 2 and listed here in north-south order for watersheds (Chowan-Roanoke through St. Johns) draining to the Atlantic Ocean and in east-west order for watersheds (Peace-Tampa Bay through Pascagoula) draining to the Gulf of Mexico.

[2]The estimate of the suspended-sediment source share for the source term Soller groups 1, 2, and 3 and Transitional (table 13) is reported as two separate components—Soller groups 1 and 2 and Transitional, and Soller group 3 and Transitional—to parallel the Soller group categories reported for Urban.

[3]The estimate of the suspended-sediment source share for the source term Soller groups 1, 2, and 4 and Agricultural (table 13) is reported as two separate components—Soller groups 1 and 2 and Agricultural, and Soller group 4 and Agricultural—to parallel the Soller group categories reported for Urban.

[4]Open water or wetlands cover the remaining 20 percent of the model area.

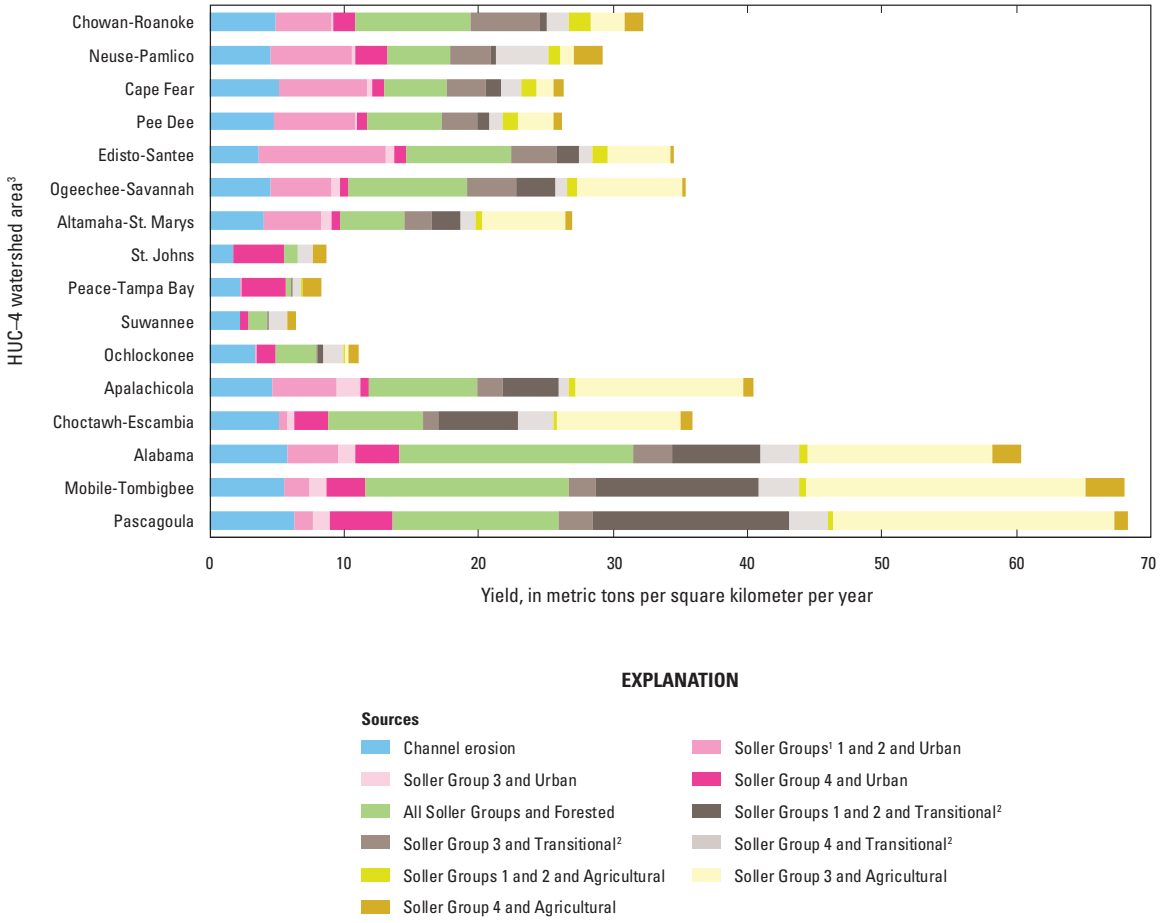

The Soller Group categories for Transitional and Agricultural—Groups 1 and 2, Group 3, and Group 4—are disaggregated from the source terms (table 13) to parallel the Soller Group categories reported for Urban.

[1]Soller group 1, Alluvium and residuum in very fine-grained sedimentary rock; Soller group 2, Residuum in igneous and metamorphic rock; Soller group 3, Residuum in sedimentary rock (discontinuous); Soller group 4, Soller classes other than 1, 2, and 3, i.e. Fine-and medium-grained sediments, residuum in alluvium, and residuum in carbonate and fine-grained sedimentary rock.

[2]Transitional is the combination of shrub/scrubland, herbaceous, and barren land cover.

[3]Hydrologic Unit Code–4 watershed areas are shown on figure 2 and listed here in north-south order for watersheds (Chowan-Roanoke through St. Johns) draining to the Atlantic Ocean and in east-west order for watersheds (Peace-Tampa Bay through Pascagoula) draining to the Gulf of Mexico.

Figure 25. Predicted suspended-sediment yield delivered to the adjacent stream by source and by HUC4 watershed area.

throughout the Southeast was estimated to be 65 percent of the amount delivered from catchment to adjacent streams.

Model-predicted source shares for load and yield delivered from catchment to the adjacent stream are summarized by HUC4 watershed area in table 14 and illustrated in figure 25. Transitional land (shrub, scrub, herbaceous, and barren areas) contributed a disproportionately large amount of SS (22.0 percent summed from all four surficial-geology categories) relative to its area in the model domain (occupying only 14 percent of the model area) because of the large model-estimated coefficients for this land-cover group. In contrast, Forested land contributed a disproportionately small amount relative to its area (22 percent of SS but occupies 39 percent of the model area). Large yields from the Alabama, Mobile-Tombigbee, and Pascagoula River Basin HUC4 watershed areas (fig. 25) were the result of larger values of the land-to-water delivery variable, Kfactor, in these areas and, for the Pascagoula River Basin, were the result of the predominance of the Transitional land-cover category (covering 20 percent of the land in the Pascagoula River Basin, almost twice the average for the Southeast area).

Stream-channel contributions were estimated to account for 12.3 percent of sediment delivered to the adjacent stream throughout the Southeast. In contrast, sediment fingerprinting studies of small streams in the Southeast document much higher contributions from stream channel erosion, particularly from the Piedmont region. As much as 90 percent of the total sediment load for a Piedmont stream in Georgia (Mukundan and others, 2011), and 60 percent of the total sediment load during high-flow events for a Piedmont stream in South Carolina (McCarney-Castle and others, 2017), have been documented. These reported values indicate that the SS SPARROW model may incorrectly attribute a large portion of the channel source to the upland sources. The geomorphic indices evaluated in the model to represent spatial distribution of channel sources—slope changes and sinuosity—were based on data from NHDPlusv2 and therefore represent 1:100,000-scale estimates. A recent SPARROW analysis of SS transport and source apportionment in North Carolina streams (Ana Garcia, U.S. Geological Survey, written commun., 2019) using geomorphic indices derived from 1-meter imagery estimated that channel sources contributed more than 50 percent of stream sediment load. Results from that study indicate that characterizing channel geomorphic features at a finer scale would likely provide meaningful predictors of spatial variability of channel erosion and allow the influence of channel sources to be distinguished from that of upland sources. Estimates of these features derived from 1-meter imagery, when available throughout the Southeast region, could offer substantial improvements in future sediment models.

Comparing Model Calibration Errors and Predicted Yields Between the 2012 and Previously Published SPARROW Models

In this section, model errors and predicted yields from the 2012 SPARROW model are compared with estimates from the previously published 2002 SPARROW models. The 2002 SPARROW models used for this comparison (Hoos and others, 2013) are those developed from a stream network at the same 1:100,000 scale as the stream network in this study, rather than the 2002 SPARROW models developed by using a coarser 1:500,000-scale stream network (Hoos and McMahon, 2009; Garcia and others, 2011).

Comparing Calibration Error

To determine whether the improvements made to the model datasets for the 2012 SPARROW models improved model predictive ability for TN and TP loads, RMSEs were compared between the constituent models for the two different periods (table 15). Two adjustments were made to the model calibrations to ensure a valid comparison between the corresponding models:

1. The 2012 models were calibrated without weighting of residuals by nested area so that weighting would be consistent between the compared models. The 2012 model specifications documented in tables 7 and 10 include nested-area weighting so that least-squares optimization was not biased by systematic smaller error for nested monitoring stations. RMSE from calibration without nested-area weighting, as was done for the 2002 models, is typically smaller than RMSE from calibration with weighting.
2. Only the calibration sites that were in common between the two periods were used to control for the effect of changing the set of calibration sites between the models. There were 257 sites that were in both the 2012 and 2002 TN models (compared to n=603 for the full calibration set for the 2012 model). There were 270 sites that were in common in the 2012 and 2002 TP models (compared to n=594 for the full calibration for the 2012 model). The relatively sparse overlap in sites included in calibration sets for the two periods resulted in part from changes by monitoring agencies to their water-quality sampling networks, and in part from the modified site selection criteria for the 2012 models established to increase the number of calibration sites on small streams to improve characterization of aquatic-loss and removal processes in small streams. SPARROW models generally have a systematic bias to larger residuals for smaller drainage areas than for larger drainage areas, for reasons detailed by Schwarz and others (2006, p. 94).

For both the TN and TP models, the RMSEs of both conditioned and unconditioned residuals (see Glossary for the definition of the terms “conditioned” and “unconditioned”) were smaller for the 2012 model than for the 2002 model. For the TN model, the difference was substantial: 29 percent for the 2012 model compared to 37 percent for the 2002 model for conditioned RMSEs, and 34 percent for the 2012 model compared to 42 percent for the 2002 model for unconditioned RMSEs. For the TP models the difference in RMSE between the two periods was smaller: 51 and 57 percent conditioned RMSE and 55 and 60 percent unconditioned RMSE for the 2012 and 2002 models, respectively.

The greater precision in both the 2012 SPARROW TN and TP models compared to their 2002 counterparts for the shared calibration sites may result from one or many of the revisions and improvements made to procedures for estimating model input, including monitored stream loads, or to the improved flow routing in NHDPlusv2 compared to NHDPlusv1. The smaller improvement for TP model than for the TN model indicates additional work is needed to develop estimates of TP sources and processes, perhaps particularly for

Table 15. Comparison of model error between the 2012 timeframe models and the previously published models.

[ln, natural logarithm; RMSE, root mean squared error of the set of residuals for monitored reaches; conditioned RMSE, residuals are calculated as the difference between natural log (ln) of monitored load and natural log of predicted load, where predicted load has been conditioned on the monitored load at the closest upstream monitoring site(s); unconditioned RMSE, same as conditioned RMSE except the predicted load is not conditioned on monitored load for upstream site(s) (more representative of prediction error); 2002 model for National Hydrography Dataset Plus (NHDPlus) version 2, documented in Hoos and others, 2013]

	Nitrogen		Phosphorus	
	RMSE, in ln space	RMSE, in percent	RMSE, in ln space	RMSE, in percent
Conditioned RMSE				
2012 nested-area-weighted model[1]	0.35	36	0.58	63
2012 model without nested-area weighting[2], evaluated for subset of calibration stations[3]	0.28	29	0.48	51
2002 model (no nested-area weighting), evaluated for subset of calibration stations[3]	0.35	37	0.53	57
Unconditioned RMSE				
2012 nested-area-weighted model[1]	0.36	38	0.59	65
2012 model without nested-area weighting[2], evaluated for subset of calibration stations[3]	0.33	34	0.52	55
2002 model (no nested-area weighting), evaluated for subset of calibration stations[3]	0.40	42	0.56	60

[1]Presented in tables 7 and 10 of this report.

[2]For valid comparison of model calibration error between the 2002 model (no nested-area weighting) and 2012 model, RMSE is evaluated from a model calibration without weighting to correct bias for nested stations.

[3]For valid comparison between the 2002 and 2012 model calibration error RMSE is evaluated from the subset of monitoring stations common between the 2012 and 2002 model calibrations.

the sources and processes related to transport of particulate P, such as streambank erosion and sedimentation.

Comparing Predicted Yield

Predictions of region average yield delivered to the basin outlet were only slightly different between the 2002 and 2012 models: 7 and 13 percent smaller for 2012 for TN and TP, respectively (figs. 26*A* and 26*B*). The difference between 2002 and 2012 was not consistent throughout the region, however. Yields predicted by the 2012 TN model were 30 percent larger for the drainages to the South Atlantic coast and 33 percent smaller for the drainages to the Gulf of Mexico than those predicted by the 2002 model (fig. 26*A*). The pattern was similar for the TP models; yields predicted by the 2012 TP model were 15 percent larger for the drainages to the South Atlantic coast and 31 percent smaller for the drainages to the Gulf of Mexico than those predicted by the 2002 model (fig. 26*B*)

The relative importance of individual sources changed substantially from 2002 to 2012 for both TN and TP models (table 16). These changes could result from actual changes in the source inputs between the two periods or could result instead from the changes (and presumably greater accuracy) in the methods for estimating 2012 model input datasets, including monitored stream loads. For the SPARROW TN model, the predicted yields from Municipal wastewater and Atmospheric deposition (all components) were substantially larger (approximately twice) for the 2012 model than for the 2002 model, whereas the predicted yields from Urban land and Agricultural fertilizer were correspondingly smaller. Predicted TN yield from Manure from livestock from the 2012 model was similar (5 percent smaller) to predicted yield from the 2002 model; however, the relative importance of direct and indirect transport differed widely between the two models. Predicted TP yield from Manure from livestock was 80 percent larger in the 2012 predictions than in the 2002 predictions. For both TN and TP, the yield from Agricultural fertilizer was half as large in the 2012 predictions than in the 2002 predictions; this difference corresponds to the decrease in farm fertilizer use in the Southeast during this period (Falcone and others, 2019).

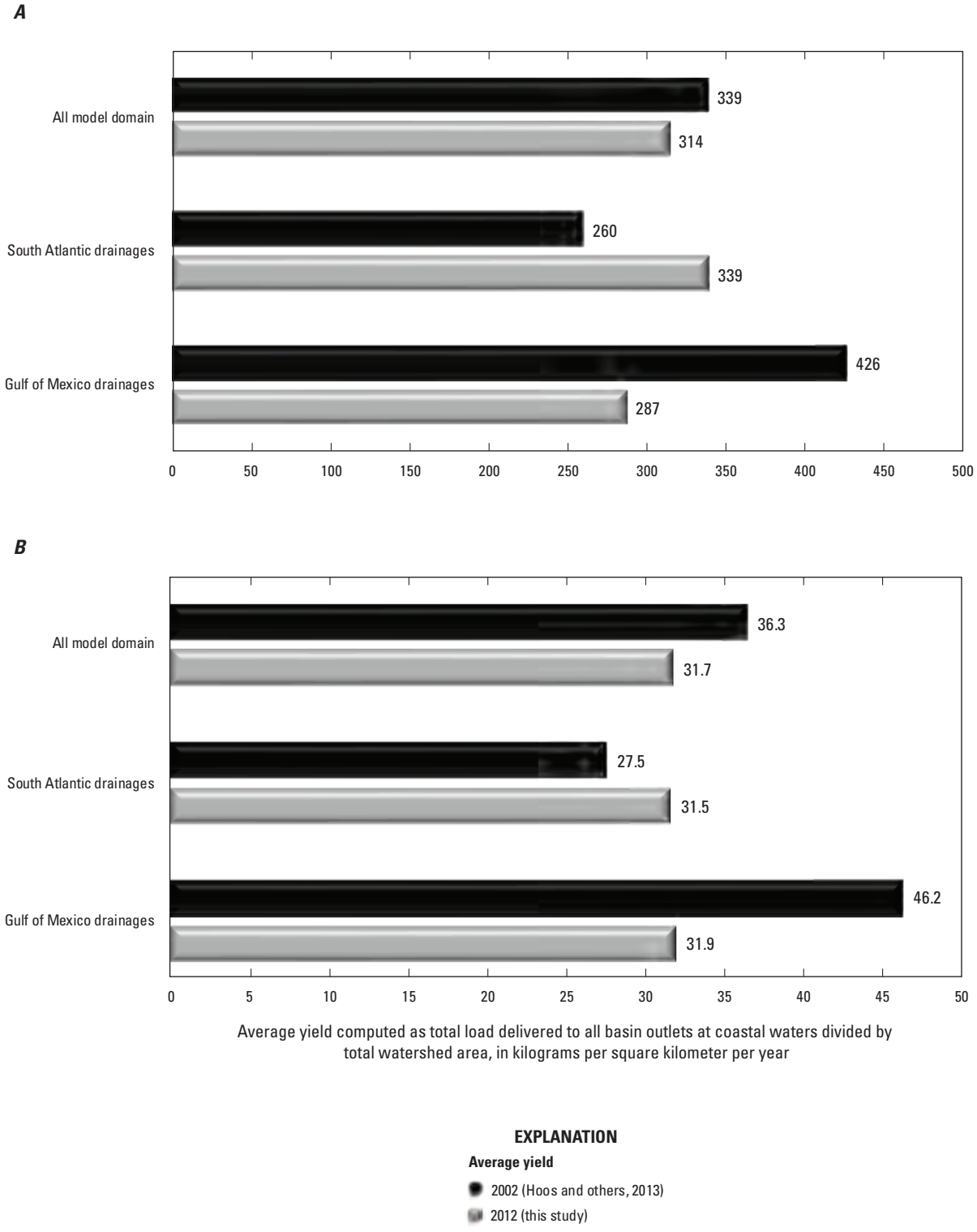

Figure 26. Region and sub-region average yield of *A*. nitrogen and *B*. phosphorus delivered to basin outlet at coastal waters, 2012 (this report) compared to 2002 (previously published models).

Table 16. Comparison between the 2012 and 2002 (previously published) SPARROW models of region-average load, yield, and sources shares for A. nitrogen and B. phosphorus delivered from the catchment to coastal waters.

[SPARROW, SPAtially Referenced Regression On Watershed attributes; estimates are based on unconditioned predictions, that is, predictions that are not conditioned on monitored load for upstream monitoring sites; estimates for 2002 are based on the SPARROW models documented in Hoos and others, 2013; source apportionment of delivered yield is calculated by summing source-share loads delivered to the downstream outlet(s) of each watershed and dividing by the total model area; National Hydrography Dataset Plus (NHDPlus) version 2; kg/yr, kilogram per year; kg/km^2/yr; kilogram per square kilometer per year; km^2, square kilometer]

Model	Basin area, based on NHDPlus network (km^2)	Total nitrogen load delivered to basin outlet at coast (kg/yr)	Total nitrogen yield delivered to basin outlet at coast (kg/km^2/yr)	Source apportionment of delivered nitrogen yield, kg/km^2/yr					
				Municipal wastewater	Urban land	Agricultural fertilizer, including from atmospheric deposition[1]	Manure from livestock, including from atmospheric deposition[2]	Emissions to atmosphere (and subsequent deposition) from power plants, other industry, vehicles, and background	Atmospheric deposition (all components)
Total nitrogen—2002	632,779	214,313,367	339	17.6	66.8	87.6/3.7	61.9/22.1	78.1	104.0
Total nitrogen—2012 (this study)	632,062	198,633,838	314	36.5	18.5	44.1/1.3	22/58.1	133.7	193.1

Model	Basin area, based on NHDPlus network (km^2)	Total phosphorus load delivered to basin outlet at coast (kg/yr)	Total phosphorus yield delivered to basin outlet at coast (kg/km^2/yr)	Source apportionment of delivered phosphorus yield, kg/km^2/yr					
				Municipal wastewater[3]	Urban land	Agricultural fertilizer	Manure from livestock	Phosphate mining	Background (parent-rock minerals)
Total phosphorus—2002	632,778	22,992,652	36	8.3	4.2	7.4	3.1	0.7	12.7
Total phosphorus—2012 (this study)	632,062	20,023,025	32	6.3	3.5	3.0	5.5	1.5	11.9

[1]The estimate for nitrogen source share for "Agricultural fertilizer" is reported as two separate components: share from direct movement of nitrogen to the stream from fertilizer applied in the watershed, and share from indirect transport from source through atmosphere to stream.

[2]The estimate for nitrogen source share for "Manure from livestock" is reported as two separate components: share from direct movement of nitrogen to stream from livestock manure and direct animal emissions in the watershed, and share from indirect transport from source through atmosphere to stream.

[3]Wastewater source term in the 2002 total phosphorus model included industrial wastewater inputs; in the 2012 model, permitted wastewater from phosphate mine facilities is included in the phosphate mining share.

Summary and Conclusions

SPAtially Referenced Regression On Watershed attributes (SPARROW) models were used to explain the spatial distribution of streamflow and stream transport of total nitrogen (TN), total phosphorus (TP), and suspended-sediment (SS) across the Southeast United States as functions of predictor variables that included source terms and physical watershed and channel characteristics. The SPARROW-calibrated regression coefficients and the predictor-variable data were then used to estimate streamflow and constituent load and source shares in 380,000 stream reaches in the Southeast. Load and source contributions for the 2012 TN and TP models were then compared to the 2002 TN and TP SPARROW models to assess differences in model-predicted constituent delivery to basin outlet between the two periods.

Variability in streamflow across the Southeast was explained as a function of precipitation adjusted for evapotranspiration, spring discharge, and municipal and domestic wastewater discharges to streams. Variable rates of water delivery to streams were attributed to variations in vegetative cover, soil texture, land cover, and average distance across the catchment to the stream. In the model, inputs to streams were balanced against removals from the streams by water withdrawals for municipal water supply, irrigation, and power generation and by evaporation from lakes and reservoirs. Model error was small (mean value of 17 percent), and smaller than 35 percent for 539 of the 569 calibration sites. The 30 sites with errors greater than 35 percent were mostly in urban areas and in Florida, which points to the need for improved characterization of the hydrologic manipulations that effectively divert water between urban watersheds and for improved characterization of losses in karst landscapes. Results from the streamflow model were used as inputs to the water-quality models.

Variability in TN transport in Southeast streams was explained by five sources, in decreasing order of mass contribution to streams: atmospheric deposition, agricultural fertilizer, municipal wastewater, manure from livestock, and urban land. Except for the part of atmospheric deposition that is derived from natural sources, all these sources are associated with human activities. Atmospheric deposition contributed an average 60.8 percent of TN to streams, and as much as 69.7 percent in areas with few other sources. The estimated average yield to coastal waters from this source, 193.1 $(kg/km^2)/yr$, was almost twice as large as that estimated with the 2002 SPARROW TN model. Almost one-third of the share from atmospheric deposition, however, is derived from volatilization or emissions and then subsequent deposition of N from manure from livestock; when the contribution along this indirect transport pathway from source through atmosphere to stream was reclassified from the atmospheric deposition source to the manure from livestock source, the latter was the second largest contributor, accounting for 26.3 percent of TN transport in streams. The estimated average yields from manure from livestock were similar to 2002 model estimates, whereas estimated yields from agricultural fertilizer and urban land were substantially smaller than 2002 model estimates.

Variability in TP transport in Southeast streams was explained by six sources, listed in decreasing order of mass contribution to streams: background (parent-rock minerals), urban land, manure from livestock, municipal wastewater, agricultural fertilizer, and phosphate mining. The background source contributed an average 41 percent of TP to streams, and as much as 60.4 percent in areas with few other TP sources. Estimated average yield to coastal waters from agricultural fertilizer was half as large as in the 2002 model, whereas the estimated yield from manure from livestock was 56 percent larger for the 2012 model than for the 2002 model.

Variable rates of TN delivery from source to stream were attributed to variation in climate, soil texture, and vegetative cover, including the extent of the conservation practice of cover cropping in the watershed. Variable rates of TP delivery were attributed to variation in climate, soil erodibility, depth to water table, and the extent of conservation tillage practices in the watershed.

Variability in sediment transport in Southeast streams was explained by variable sediment export rates from different combinations of land cover and geologic setting (for upland sources of sediment) and by gains in stream power caused by longitudinal changes in channel hydraulics (for channel sources of sediment). Sediment yields for the transitional land cover (shrub, scrub, herbaceous, and barren) varied widely depending on geologic setting, and similarly for agricultural land cover. Sediment yield was also affected by the areal extent of conservation tillage practices in the watershed.

Although the SS SPARROW model explained much of the variability in SS transport (77 percent in log space), large uncertainty in estimates for almost all the sediment source coefficients indicates the need for caution in interpreting the estimates of source apportionment. The share assigned to channel sources of sediment, 8.6 percent, was extremely small compared to estimates (in the range of 60 percent) from other studies in the Southeast region. The 1:100,000-scale estimates of channel geomorphic indices used to represent channel source terms in the Southeast SS model may be insufficient to provide meaningful predictors of spatial variability of channel erosion. Estimates derived from 1-meter imagery, which were not available throughout the Southeast region when model input sets were compiled, could offer substantial improvements in future sediment models for this region.

TN and TP and sediment inputs to streams from sources were balanced in the models with losses from physical processes in streams and reservoirs and with water withdrawals. Losses in streams and reservoirs along with withdrawals removed 35, 44, and 65 percent of the TN, TP, and SS loads, respectively, during downstream transport. TN losses in streams were likely the result of denitrification, whereas TP losses likely resulted from trapping in bed sediment. Losses of TN and TP were both modeled as a factor inversely proportional to mean water depth in the stream. The estimated rate of TN loss in streams ranged from 0.83 m/d (small, shallow

streams) to 0.083 m/d (large streams); the estimated rate of TP loss ranged from 0.94 m/d to 0.094 m/d. Sediment loss was statistically significant in streams that were connected to riparian wetlands. The estimated rate of trapping and burial in riparian wetlands was 0.0016 unit/(m*d), where m measures the width transverse to the channel of the riparian wetland. Loss rates in lakes and reservoirs for TN, TP, and SS were 5.036, 14.633, and 25.356 m/yr, respectively, except for lakes in karst landscape regions, where TN and TP losses are statistically insignificant.

Inputs to and outputs from all models are available in a U.S. Geological Survey data release (https://doi.org/10.5066/P9A682GW). Information provided by these models about nutrient and sediment yields, the relative importance of various sources, and specific loss processes and associated loss rates may help in watershed restoration efforts, specifically in selecting the most effective placement of these efforts.

References Cited

American Public Health Association, American Water Words Association, and Water Pollution Control Federation, 2012, Standard methods for the examination of water and wastewater (22d ed.): Washington, D.C., 1496 p.

American Society for Testing and Materials, 2006, Standard test methods for determining sediment concentration in water samples: D 3977–97, v. 11.02, Water (II), p. 395–400.

Appel, K.W., Napelenok, S.L., Foley, K.M., Pye, H.O.T., Hogrefe, C., Luecken, D.J., Bash, J.O., Roselle, S.J., Pleim, J.E., Foroutan, H., Hutzell, W.T., Pouliot, G.A., Sarwar, G., Fahey, K.M., Gantt, B., Gilliam, R.C., Heath, N.K., Kang, D., Mathur, R., Schwede, D.B., Spero, T.L., Wong, D.C., and Young, J.O., 2017, Description and evaluation of the Community Multiscale Air Quality (CMAQ) modeling system version 5.1: Geoscientific Model Development, v. 10, no. 4, p. 1703–1732.

Aulenbach, B.T., Joiner, J.K., and Painter, J.A., 2017, Hydrology and water quality in 13 watersheds in Gwinnett County, Georgia, 2001–15: U.S. Geological Survey Scientific Investigations Report 2017–5012, 82 p., accessed September 27, 2019, at https://doi.org/10.3133/sir20175012.

Bagnold, R.A., 1966, An approach to the sediment transport problem from general physics: U.S. Geological Survey Professional Paper 422–I, 137 p.

Barlow, P.M., and Leake, S.A., 2012, Streamflow depletion by wells—Understanding and managing the effects of groundwater pumping on streamflow: U.S. Geological Survey Circular 1376, 84 p., accessed September 27, 2019, at https://pubs.usgs.gov/circ/1376/.

Beale, E.M.L., 1962, Some uses of computers in operational research: Industrielle Organisation, v. 31, 27–28.

Boyer, E.W., Goodale, C.L., Jaworski, N.A., and Howarth, R.W., 2002, Anthropogenic nitrogen sources and relationships to riverine nitrogen export in the northeastern USA: Biogeochemistry v, 57, no. 1, p. 137–169, accessed September 27, 2019, at https://doi.org/10.1023/A:1015709302073.

Brakebill, J.W., Schwarz, G.E., and Wieczorek, M.E., in press, An enhanced hydrologic network in support of SPARROW modeling: U.S. Geological Survey Scientific Investigations Report 2019–5127.

Bull, W.B., 1979, Threshold of critical power in streams: Geological Society of America Bulletin, v. 90, no. 5, p. 453–464, accessed September 27, 2019, at https://doi.org/10.1130/0016-7606(1979)90%3C453:TOCPIS%3E2.0.CO;2.

Callahan, J.T., 1964, The yield of sedimentary aquifers of the Coastal Plain Southeast River Basins: U.S. Geological Survey Water-Supply Paper 1669W, 56 p., accessed September 27, 2019, at https://doi.org/10.3133/wsp1669W.

Cliff, A.D., and Ord, J.K., 1973, Spatial autocorrelation, London, Pion Limited, 178 p.

Cochran, W.G., 1977, Sampling techniques (3d ed.): New York, Wiley, 428 p.

Falcone, J.A., Murphy, J.C., and Sprague, L.A., 2019, Regional patterns of anthropogenic influences on streams and rivers in the conterminous United States, from the early 1970s to 2012, Journal of Land Use Science, v. 13, no. 6, p. 585–614, accessed September 27, 2019, at https://doi.org/10.1080/1747423X.2019.1590473.

Florida Department of Environmental Protection Water Reuse Program, 2014, 2013 Reuse Inventory: accessed March 14, 2015, at https://floridadep.gov/water/domestic-wastewater/content/reuse-inventory-database-and-annual-report.

Galloway, J.N., Aber, J.D., Erisman, J.W., Weitzinger, S.P., Howarth, R.W., Cowling, E.B., and Cosby, B.J., 2003, The nitrogen cascade: BioScience, v. 53, no. 4, p. 341–356, accessed September 27, 2019, at https://doi.org/10.1641/0006-3568(2003)053[0341:TNC]2.0.CO;2.

Garcia, A.M., Hoos, A.B, and Terziotti, Silvia, 2011, A regional modeling framework of phosphorus sources and transport in streams of the southeastern United States: Journal of the American Water Resources Association, v. 47, no. 5, p. 991–1010, accessed September 27, 2019, at https://doi.org/10.1111/j.1752-1688.2010.00517.x.

Gellis, A.C., Fitzpatrick, F.A., and Schubauer-Berigan, M.K., 2016, A manual to identify sources of fluvial sediment: Washington, D.C., U.S. Environmental Protection Agency, EPA/600/R-16/210, 124 p., accessed September 27, 2019, at https://nepis.epa.gov/Exe/ZyPDF.cgi/P100QVM1.PDF?Dockey=P100QVM1.PDF.

Gray, J.R., Glysson, G.D., Turcios, L.M., and Schwarz, S.E., 2000, Comparability of suspended sediment concentration and total suspended solids data: U.S. Geological Survey Water-Resources Investigations Report 00–4191, 14 p., [Also available at https://doi.org/10.3133/wri004191.]

Gronberg, J.M., and Arnold, T.L., 2017, County-level estimates of nitrogen and phosphorus from animal manure for the conterminous United States, 2007 and 2012: U.S. Geological Survey Open-File Report 2017–1021, 6 p., [Also available at https://doi.org/10.3133/ofr20171021.]

Guy, H.P., 1969, Laboratory theory and methods for sediment analysis: U.S. Geological Survey Techniques of Water-Resources Investigations, book 5, chap. C1, 58 p., [Also available at https://doi.org/10.3133/twri05C1.]

Homer, C.G., Dewitz, J.A., Yang, L., Jin, S., Danielson, P., Xian, G., Coulston, J., Herold, N.D., Wickham, J.D., and Megown, K., 2015, Completion of the 2011 National Land Cover Database for the conterminous United States—Representing a decade of land cover change information: Photogrammetric Engineering and Remote Sensing, v. 81, no. 5, p. 345–354, accessed September 27, 2019, at https://www.ingentaconnect.com/content/asprs/pers/2015/00000081/00000005/art00002.

Hoos, A.B., and McMahon, G., 2009, Spatial analysis of instream nitrogen loads and factors controlling nitrogen delivery to streams in the southeastern United States using Spatially Referenced Regression on Watershed Attributes (SPARROW) and regional classification frameworks: Journal of Hydrological Processes, v. 23, no. 16, p. 2275–2295, [Also available at https://doi.org/10.1002/hyp.7323.]

Hoos, A.B., Moore, R.B., Garcia, A.M., Noe, G.B., Terziotti, S.E., Johnston, C.M., and Dennis, R.L., 2013, Simulating stream transport of nutrients in the eastern United States, 2002, using a spatially-referenced regression model and 1:100,000-scale hydrography: U.S. Geological Survey Scientific Investigations Report 2013–5102, 33 p., [Also available at http://pubs.usgs.gov/sir/2013/5102/.]

Horizon Systems, 2013, NHDPlus Home: accessed March 18, 2019, at http://horizon-systems.com/nhdplus/.

Howarth, R.W., Billen, G., Swaney, D., Townsend, A., Jaworski, N., Lajtha, K., Downing, J.A., Elmgren, R., Caraco, N., Jordan, T., Berendse, F., Freney, J., Kudeyarov, V., Murdoch, P., and Zhao-Liang, Zhu, 1996, Regional nitrogen budgets and riverine N & P fluxes for the drainages to the North Atlantic Ocean—Natural and human influences: Biochemistry, v. 35, no. 1, p. 75–139, accessed September 27, 2019, at https://link.springer.com/article/10.1007/BF02179825.

Katz, B.G., Hornsby, H.D., Bohlke, J.F., and Mokray, M.F., 1999, Sources and chronology of nitrate contamination in spring waters, Suwannee River Basin, Florida: U.S. Geological Survey Water-Resources Investigations Report 99–4952, 59 p., accessed September 27, 2019, at https://doi.org/10.3133/wri994252.

Lee, C.J., Hirsch, R.M., Schwarz, G.E., Holtschlag, D.J., Preston, S.D., Crawford, C.G., and Vecchia, A.V., 2016, An evaluation of methods for estimating decadal stream loads: Journal of Hydrology, v. 54, p. 185–203, accessed September 27, 2019, at https://doi.org/10.1016/j.jhydrol.2016.08.059.

Maupin, M.A., Kenny, J.F., Hutson, S.S., Lovelace, J.K., Barber, N.L., and Linsey, K.S., 2014, Estimated use of water in the United States in 2010: U.S. Geological Survey Circular 1405, 56 p., accessed September 27, 2019, at https://doi.org/10.3133/cir1405.

McCarney-Castle, K., Childress, T.M., and Heaton, C.R., 2017, Sediment source identification and load prediction in a mixed-use Piedmont watershed, South Carolina: Journal of Environmental Management, v. 185, p. 60–69, accessed September 27, 2019, at https://doi.org/10.1016/j.jenvman.2016.10.036.

Mosner, M.S., 2002, Stream-aquifer relations and the potentiometric surface of the Upper Floridan aquifer in the Lower Apalachicola-Chattahoochee-Flint River Basin in parts of Georgia, Florida, and Alabama, 1999–2000: U.S. Geological Survey Water-Resources Investigations Report 2002–4244, 45 p., accessed September 27, 2019, at https://doi.org/10.3133/wri20024244.

Mukundan, R., Radcliffe, D.E., and Ritchie, J.C., 2011, Channel stability and sediment source assessment in streams draining a Piedmont watershed in Georgia, USA: Journal of Hydrological Processes, v. 25, no. 8, p. 1243–1253, accessed September 27, 2019, at https://doi.org/10.1002/hyp.7890.

Mulholland, P.J., Valett, H.M., Webster, J.B., Thomas, S.A., Cooper, L.W., Hamilton, S.K., and Peterson, B.J., 2004, Stream denitrification and total nitrate uptake rates measured using a field 15N tracer addition approach: Limnology and Oceanography, v. 49, p. 809–820, accessed September 27, 2019, at https://doi.org/10.4319/lo.2004.49.3.0809.

Nardi, M.R., 2014, Watershed potential to contribute phosphorus from geologic materials to receiving streams, conterminous United States: accessed August 3, 2018, at https://water.usgs.gov/lookup/getspatial?pmapnatl.

Preston, S.D., Alexander, R.B., and Wolock, D.M., 2011, SPARROW modeling to understand water-quality conditions in major regions of the United States—A featured collection introduction: Journal of the American Water Resources Association, v. 47, no. 5, p. 887–890, also available at https://doi.org/10.1111/j.1752-1688.2011.00585.x.

Preston, S.D., Alexander, R.B., Woodside, M.D., and Hamilton, P.A., 2009, SPARROW modeling—Enhancing understanding of the Nation's water quality: U.S. Geological Survey Fact Sheet 2009–3019, 6 p, [Also available at https://doi.org/10.3133/fs20093019.]

Qian, S.S., Reckhow, K.H., Zhai, J., and McMahon, G., 2005, Nonlinear regression modeling of nutrient loads in streams—A Bayesian approach: Water Resources Research, v. 41 no. 7, W07012, also available at https://doi.org/10.1029/2005WR003986.

Richards, R.P., Akameddine, I., Allan, J.D., Baker, D.B., Bosch, N.S., Confesor, R., DePinto, J.V., Dolan, D.M., Reutter, J.M., and Scavia, D., 2012, Discussion of "Nutrient Inputs to the Laurentian Great Lakes by Source and Watershed Estimated Using SPARROW Watershed Model": Journal of the American Water Resources Association, v. 49, no. 3, p. 715–724, accessed September 27, 2019, at https://doi.org/10.1111/jawr.12006.

Robertson, D.M., and Saad, D.A., 2013, SPARROW models used to understand nutrient sources in the Mississippi/Atchafalaya River Basin: Journal of Environmental Quality, v. 42, p. 1422–1440, accessed September 27, 2019, at https://doi.org/10.2134/jeq2013.02.0066.

Roland, V.L. II, and Hoos, A.B., 2019, SPARROW model inputs and simulated streamflow, nutrient and suspended-sediment loads in streams of the Southeastern United States, 2012 base year: U.S. Geological Survey data release, https://doi.org/10.5066/P9A682GW.

Ruddy, B.C., Lorenz, D.L., and Mueller, D.K., 2006, County-level estimates of nutrient inputs to the land surface of the conterminous United States, 1982–2001: U.S. Geological Survey Scientific Investigations Report 2006–5012, 17 p., accessed September 27, 2019, at https://pubs.usgs.gov/sir/2006/5012/.

Saad, D.A., Schwarz, G.E., Argue, D.M., Anning, D.W., Ator, S.W., Hoos, A.B., Preston, S.D., Robertson, D.M., and Wise, D.R., 2019, Estimates of long-term mean daily streamflow and annual nutrient and suspended-sediment loads considered for use in regional SPARROW models of the conterminous United States, 2012 base year: U.S. Geological Survey Scientific Investigations Report 2019–5069, accessed September 29, 2019, at https://dx.doi.org/10.3133/sir20195069.

Schwarz, G.E., 2008, A preliminary SPARROW model of suspended sediment for the conterminous United States: U.S. Geological Survey Open-File Report 2008–1205, 8 p., accessed September 27, 2019, at http://pubs.usgs.gov/of/2008/1205.

Schwarz, G.E., 2019, E2NHDPlusV2_us: Database of ancillary hydrologic attributes and modified routing for NHDPlus Version 2.1 flowlines: U.S. Geological Survey data release, https://doi.org/10.5066/P986KZEM.

Schwarz, G.E., Hoos, A.B., Alexander, R.B., and Smith, R.A., 2006, The SPARROW surface water-quality model—Theory, applications and user documentation: U.S. Geological Survey Techniques and Methods, book 6, chap. B3, 248 p., accessed September 27, 2019, at http://pubs.usgs.gov/tm/2006/tm6b3/. [Also available on CD-ROM.]

Scott, T.M., Means, G.H., Meegan, R.P., Means, R.C., Upchurch, S., Copeland, R.E., Jones, J., Roberts, T., and Willet, A., 2004, Springs of Florida (v. 1.1): Florida Geological Survey, Bulletin no. 66, accessed September 27, 2019, at http://publicfiles.dep.state.fl.us/FGS/WEB/springs/bulletin_66.pdf.

Simley, J.D., and Carswell, W.J., Jr., 2009, The National Map—Hydrography: U.S. Geological Survey Fact Sheet 2009–3054, 4 p., accessed September 27, 2019, at https://doi.org/10.3133/fs20093054.

Schiffer, Donna M., 1998, Hydrology of Central Florida Lake—A primer: U.S. Geological Survey Circular 1137, 38 p., accessed September 27, 2019, at https://doi.org/10.3133/cir1137.

Seaber, P.R., Kapinos, F.P., and Knapp, G.L., 1987, Hydrologic unit maps: U.S. Geological Survey Water Supply Paper 2294, 63 p., accessed September 30, 2019, at https://doi.org/10.3133/wsp2294.

Skinner, K.D., and Maupin, M.A., 2019, Point-source nutrient loads to streams of the conterminous United States, 2012: U.S. Geological Survey Data Series 1101, 13 p., accessed September 29, 2019, at https://doi.org/10.3133/ds1101.

Smith, D.B., Cannon, W.F., Woodruff, L.G., Solano, Federico, and Ellefsen, K.J., 2014, Geochemical and mineralogical maps for soils of the conterminous United States: U.S. Geological Survey Open-File Report 2014–1082, 386 p., accessed September 27, 2019, at https://dx.doi.org/10.3133/ofr20141082.

Smith, R.A., Schwarz, G.E., and Alexander, R.B., 1997, Regional interpretation of water-quality monitoring data: Water Resources Research, v. 33, no. 12, p. 2781–2798, accessed September 27, 2019, at https://doi.org/10.1029/97WR02171.

Soller, D.R., Reheis, M.C., Garrity, C.P., and Van Sistine, D.R., 2009, Map database for surficial materials in the conterminous United States: U.S. Geological Survey Data Series 425, accessed September 27, 2019, at http://pubs.usgs.gov/ds/425.

Stenback, G.A., Crumpton, W.G., Schilling, K.E., and Helmers, M.J., 2011, Rating curve estimation of nutrient loads in Iowa rivers: Journal of Hydrology, v. 396, no. 1–2, p. 158–169, accessed September 27, 2019, at https://doi.org/10.1016/j.jhydrol.2010.11.006.

Stewart, J.S., Schwarz, G.E., Brakebill, J.W., and Preston, S.D., 2019, Catchment-level estimates of nitrogen and phosphorus agricultural use from commercial fertilizer sales for the conterminous United States, 2012: U.S. Geological Survey Scientific Investigations Report 2018–5145, 52 p., https://doi.org/10.3133/sir20185145.

Swanson, F.J., Gregory, S.V., Sedell, J.R., and Campbell, A.G., 1982, Land-water interactions—The riparian zone, in Analysis of coniferous forest ecosystems in the western United States: Stroudsburg, Pennsylvania, Hutchinson Ross Publishing Company, p. 267–291, accessed September 27, 2019, at https://ir.library.oregonstate.edu/concern/defaults/0c483k64v.

Terziotti, S., Hoos, A.B., Harned, D.A., and Garcia, A., 2009, Mapping watershed potential to contribute phosphorus from geologic materials to receiving streams, southeastern United States: U.S. Geological Survey Scientific Investigations Map 3102, 1 pl., accessed September 29, 2019, at https://pubs.usgs.gov/sim/3102/.]

Upchurch, S.B., Chen, J., and Cain, C.R., 2007, Trends of nitrate concentrations in waters of the Suwannee River Water Management District, 2007: Tampa. Florida, SDII Global Corporation, prepared for Suwannee River Water Management District, Live Oak, Florida, accessed February 18, 2019, at http://www.srwmd.state.fl.us/DocumentCenter/Home/View/130.

U.S. Army Corps of Engineers, 2011, National inventory of dams, accessedSeptember 27, 2019, at http://nid.usace.army.mil/cm_apex/f?p=838:12.

U.S. Department of Agriculture, 2015, 2012 Cropland data layer: USDA-NASS, Washington, D.C., U.S. Department of Agriculture, National Agricultural Statistics Service – Web interface, accessed April 22, 2015, at https://nassgeodata.gmu.edu/CropScape/.

U.S. Department of Agriculture, 1986, Urban hydrology for small watersheds-Technical Release 55 (TR55): U.S. Department of Agriculture, Natural Resources Conservation Service, Washington, D.C., accessed November 1, 2019, at https://www.nrcs.usda.gov/Internet/FSE_DOCUMENTS/stelprdb1044171.pdf.

U.S. Environmental Protection Agency, 2016, ATTAINS, accessed December 1, 2018, at https://www.epa.gov/waterdata/attains.

U.S. Environmental Protection Agency and U.S. Geological Survey, 2010, NHDPlus user guide: accessed May 8, 2011, at ftp://ftp.horizonsystems.com/NHDPlus/documentation/NHDPLUS_UserGuide.pdf.

U.S. Geological Survey, 2015, USGS water data for the Nation: U.S. Geological Survey National Water Information System database, accessed February 28, 2018, at http://dx.doi.org/10.5066/F7P55KJN.

U.S. Office of Management and Budget, 2017, North American Industry Classification System: Executive Office of the President, accessed September 30, 2019, at https://www.census.gov/eos/www/naics/2017NAICS/2017_NAICS_Manual.pdf.

Wellen, C., Arhonditis, G.B., Labencki, T., and Boyd, D., 2014, Application of the SPARROW model in watersheds with limited information—A Bayesian assessment of the model uncertainty and the value of additional monitoring: Hydrological Processes, v. 28, no. 3, p. 1260–1283, [Also available at https://doi.org/10.1002/hyp.9614.]

Wieczorek, M.E., Jackson, S.E., and Schwarz, G.E., 2019, Select Attributes for NHDPlus Version 2.1 Reach Catchments and Modified Network Routed Upstream Watersheds for the Conterminous United States (ver 2.0, October 2019): U.S. Geological Survey data release, https://dx.doi.org/10.5066/F7765D7V.

Wiegner, T.N., and Seitzinger, S.P., 2004, Seasonal bioavailability of dissolved organic carbon and nitrogen from pristine and polluted freshwater wetlands: Limnology and Oceanography, v. 49, p. 1703–1712, accessed September 29, 2019, at https://doi.org/10.4319/lo.2004.49.5.1703.

Williams, L.J., and Dixon, J.F., 2015, Digital surfaces and thicknesses of selected hydrogeologic units of the Floridan aquifer system in Florida and parts of Georgia, Alabama, and South Carolina: U.S. Geological Survey Data Series 926, 24 p., accessed September 29, 2019, at https://dx.doi.org/10.3133/ds926.

Wilson, B.T., Lister, A.J., Riemann, R.I., and Griffith, D.M., 2013, Live tree species basal area of the contiguous United States (2000–09): Newtown Square, Pennsylvania: U.S. Department of Agriculture, Forest Service, Rocky Mountain Research Station, accessed September 29, 2019, at https://doi.org/10.2737/RDS-2013-0013.

Wolock, D.M., and McCabe, G.J., 2018, Water balance model inputs and outputs for the conterminous United States, 1900–2015: U.S. Geological Survey data release, https://dx.doi.org/10.5066/F71V5CWN.

Zhang, W., Capps, S.L., Hu, Y., Nenes, A., Napelenok, S.L., and Russell, A.G., 2012, Development of the high-order decoupled direct method in three dimensions for particulate matter—Enabling advanced sensitivity analysis in air quality models: Geoscientific Model Development, v. 5, no. 2, p. 355–368, accessed September 29, 2019, at https://doi.org/10.5194/gmd-5-355-2012.

Zhang, Y., Foley, K.M., Schwede, D.B., Bash, J.O., Pinto, J.P., and Dennis, R.L., 2019, A measurement-model fusion approach for improved wet deposition maps and trends: Journal of Geophysical Research Atmospheres, v. 124, no. 7, p. 4237–4251, accessed September 29, 2019, at https://doi.org/10.1029/2018JD029051.

Glossary

Catchment The incremental drainage area associated with a reach segment in the digital stream network. See the entry for 'Reach' below for definition of a reach segment.

Conditioned prediction The SPARROW model prediction that is conditioned on the monitored value of the dependent variable (load or streamflow) for the closest upstream calibration stations.

Conditioned residual Calculated for monitored reaches, the difference between the monitored value of the dependent variable (load or streamflow) and the conditioned prediction, calculated for monitored reaches.

HUC4 4-digit hydrologic unit code, from the hierarchical classification system developed by the U.S. Geological Survey. The Southeast SPARROW model area contains 16 HUC4 units, also known as subregions.

Reach The segment of stream channel that extends between nodes in the digital stream network. Nodes are located at tributary junctions and where streams enter lakes, reservoirs, or coastal waters.

Unconditioned prediction The SPARROW model prediction that is not conditioned on monitored load for upstream monitoring stations.

Unconditioned residual Calculated for monitored reaches, the difference between the monitored value of the dependent variable (load or streamflow) and the conditioned prediction. The unconditioned residual is more representative of prediction error than the conditioned residual for reaches where calibration data at upstream locations are not available, for example in watersheds or subregions of the model domain without calibration data.

Appendixes 1, 2, and 3

Appendix 1. The SPARROW Model Equation

For each reach in a hydrologic network, the SPAtially Referenced Regression On Watershed attributes (SPARROW) model predicts mean-annual instream constituent load as a function of sources, land-to-water attenuation rates, and aquatic attenuation rates. Conceptually, the instream load or flux at the downstream node of a reach can be expressed as the sum of two components:

$$Log\ (instream)_i = Log\ (catchment)_i + Log\ (upstream)_i \quad (1.1)$$

where

$instream_i$ is the instream load at the downstream node of reach i;

$catchment_i$ is the load originating within the catchment for reach i and delivered to the downstream node of reach i; and

$upstream_i$ is the load generated within catchments for upstream reaches and transported to the downstream node of reach i by means of the stream network.

The load originating within the catchment for reach i ($catchment_i$) is determined by

$$Log(catchment_i) = \sum_{n=1}^{N_S} S_{n,i}\alpha_n D_n\left(Z_i^D;\theta_D\right)A\left(Z_i^S, Z_i^R;\theta_S,\theta_R\right) \quad (1.2)$$

where

n, N_s is the source index (N_s is the total number of individual sources);

$\sum$ represents summation across all individual sources;

$S_{n,i}$ is the vector of source variables for reach i (for example, a measurement of mass placed in the watershed, or the area of a particular land cover);

α_n is the vector of coefficients, estimated by the model, in units that convert source variable units to flux units. For land-applied sources, α_n is the model estimate of the average land-to-water delivery ratio across all catchments in the model area. For land-applied sources represented by characteristics other than mass input (for example, area of developed land), α expresses the conversion of source units to mass applied to the watershed, as well as the average land-to-water delivery ratio for the source;

$D_n(\cdot)$ is the delivery variation factor, defining the variation among catchments in land-to-water attenuation processes and, therefore, in the land-to-water delivery ratio. The delivery variation factor is modeled as a series of exponential functions of physical landscape characteristics that affect nutrient attenuation;

Z_i^D is the vector of physical landscape variables for reach i (for example, measured landform or soil characteristics, area of long-hydroperiod wetlands, and so forth);

θ_D is the vector of coefficients, *estimated by the model*, for the physical landscape variables;

$A(\cdot)$ is the aquatic delivery function, representing the result of attenuation processes acting on mass as it travels along the stream channel. Modeled as first-order decay, the aquatic delivery function defines the fraction of flux originating in, and delivered to, reach i that is transported to the reach's downstream node;

Z_i^S, Z_i^R are vectors of measured stream and reservoir variables, respectively, for reach i (examples include streamwater depth or velocity, width of riparian corridor, and reservoir areal hydraulic loading); and

θ_s, θ_R are vectors of coefficients, estimated by the model, for the stream and reservoir variables, respectively.

The delivery variation factor $D_n(\cdot)$ allows the model to estimate variation in land-to-water transport rates among catchments. Values of $D_n(\cdot)$ greater than 1 for a catchment indicate a larger fraction of nutrient reaching streams than the median for the model area; values of $D_n(\cdot)$ less than 1 indicate a smaller fraction of nutrient reaching streams than the median for the model area.

The second component in equation 1.2, the flux entering reach i from upstream reaches, is the sum of the flux from any upstream catchment ($catchment_{i-1}$, $catchment_{i-2}$, and so forth) adjusted for losses caused by stream and reservoir attenuation processes acting on flux along the reach pathway to and including reach i. For headwater reaches, equation 1.2 is simplified to include only the $catchment_i$ term. More information about the model form and assumptions is available in Schwarz and others (2006).

Reference Cited

Schwarz, G.E., Hoos, A.B., Alexander, R.B., and Smith, R.A., 2006, The SPARROW surface water-quality model—Theory, applications and user documentation: U.S. Geological Survey Techniques and Methods, book 6, chap. B3, 248 p., accessed September 27, 2019, at http://pubs.usgs.gov/tm/2006/tm6b3/.

Appendix 2. Calculation of Model Error as Percent from Model Error in Natural Log Space

Root Mean Square Error (RMSE) as percent error (pctRMSE) of predicted load or yield in real space can be calculated from RMSE in natural log space (*ln*RMSE, as reported from SPAtially Referenced Regression On Watershed attributes (SPARROW) model calibration), as

$$\text{pctRMSE} = 100\sqrt{\exp(ln\text{RMSE}^2) - 1} \tag{2.1}$$

Mathematical derivation of this formula, given below, was provided by Gregory Schwarz (U.S. Geological Survey, written commun., 2017). pctRMSE can also be approximated (Schwarz and others, 2006, p. 97), but the approximation is valid only for small values (less than 0.4) of *ln*RMSE, whereas equation 2.1 is valid over a wide range of *ln*RMSE values and will be exact if the model residuals are truly normally distributed.

Let $\tilde{y}$ denote the natural log of the actual load, let $\hat{\tilde{y}}$ denote the predicted value of the natural log of load, let y be the actual load in real space and let $\hat{y}$ be the predicted load in real space, inclusive of the retransformation bias correction. Now pctRMSE is the square root of the ratio of the expected value E of the variance of y to the squared predicted load, the result being multiplied by 100, implying

$$\text{pctRMSE} = 100\sqrt{\frac{E[(y-\hat{y})^2]}{\hat{y}^2}} = 100\sqrt{E[(\frac{y}{y})^2] - 1} \tag{2.2}$$

where the second equality follows if $\hat{y}$ is unbiased.

If we assume that $\hat{\tilde{y}} - \tilde{y}$ is normally distributed with mean zero and variance of $\tilde{\sigma}^2$, that is, *ln*RMSE^2, then it is a well-known property of log-normally distributed variables that

$$E[y] = \hat{y} = e^{\hat{\tilde{y}} + \tilde{\sigma}^2/2} \tag{2.3}$$

Then, we have

$$\frac{y}{\hat{y}} = e^{(\tilde{y}-\hat{\tilde{y}}) - \tilde{\sigma}^2/2}. \tag{2.4}$$

Squaring both sides and taking expectations, we have

$$E\left[\left(\frac{y}{\hat{y}}\right)^2\right] = E\left[e^{2\left(\tilde{y}-\hat{\tilde{y}}\right)-\tilde{\sigma}^2}\right] = e^{2\tilde{\sigma}^2-\tilde{\sigma}^2} = e^{\tilde{\sigma}^2}, \tag{2.5}$$

where the last equality follows from the assumption that $\hat{y} - \hat{\tilde{y}}$ is normally distributed (that is, if x is normally distributed then $E\left[e^x\right] = e^{\sigma_x^2/2}$).

Substitution of this last result into equation 2-2 gives

$$\text{pctRMSE} = 100\sqrt{e^{\tilde{\sigma}^2} - 1}, \tag{2.6}$$

which is the desired result.

For residuals, the percent residual, pctRESID, is given by

$$\text{pctRESID} = 100\,(\frac{y-\hat{y}}{\hat{y}}) = 100(e^{(\tilde{y}-\hat{\tilde{y}})-\tilde{\sigma}^2/2} - 1) = (e^{ln\text{RESID}-lnMSE/2} - 1) \tag{2.7}$$

where the second equality follows from equation 2.4, and where *ln*MSE is (*ln*RMSE)^2.

Reference Cited

Schwarz, G.E., Hoos, A.B., Alexander, R.B., and Smith, R.A., 2006, The SPARROW surface water-quality model—Theory, applications and user documentation: U.S. Geological Survey Techniques and Methods, book 6, chap. B3, 248 p., accessed September 27, 2019, at http://pubs.usgs.gov/tm/2006/tm6b3/.

Appendix 3. Supplemental Description of Data Compilation

Attribution for all the variables tested in the streamflow, total nitrogen, total phosphorus, and suspended-sediment SPAtially Referenced Regression On Watershed attributes (SPARROW) models is provided in table 3.1.

References Cited

Hoos, A.B., Moore, R.B., Garcia, A.M., Noe, G.B., Terziotti, S.E., Johnston, C.M., and Dennis, R.L., 2013, Simulating stream transport of nutrients in the eastern United States, 2002, using a spatially-referenced regression model and 1:100,000-scale hydrography: U.S. Geological Survey Scientific Investigations Report 2013–5102, 33 p., [Also available at http://pubs.usgs.gov/sir/2013/5102/.]

Roland, V.L. II, and Hoos, A.B., 2019, SPARROW model inputs and simulated streamflow, nutrient and suspended-sediment loads in streams of the Southeastern United States, 2012 base year: U.S. Geological Survey data release, https://doi.org/10.5066/P9A682GW.

Saad, D.A., Schwarz, G.E., Argue, D.M., Anning, D.W., Ator, S.W., Hoos, A.B., Preston, S.D., Robertson, D.M., and Wise, D.R., 2019, Estimates of long-term mean daily streamflow and annual nutrient and suspended-sediment loads considered for use in regional SPARROW models of the conterminous United States, 2012 base year: U.S. Geological Survey Scientific Investigations Report 2019–5069, https://dx.doi.org/10.3133/sir20195069.

Schwarz, G.E., 2019, E2NHDPlusV2_us: Database of Ancillary Hydrologic Attributes and Modified Routing for NHDPlus Version 2.1 Flowlines: U.S. Geological Survey data release, https://dx.doi.org/10.5066/P9PA63SM.

Schruben, P.G., Arndt, R.E., and Bawiec, W.J. 1998, Geology of the conterminous United States at 1:250,000 scale; a digital representation of the 1974 P.B. King and H.M. Beikman map: U.S. Geological Data Series 11, also available at https://doi.org/10.3133/ds11.

Skinner, K.D., and Maupin, M.A., 2019, Point-source nutrient loads to streams of the conterminous United States, 2012: U.S. Geological Survey Data Series 1101, 13 p., accessed September 29, 2019, at https://doi.org/10.3133/ds1101.

Stewart, J.S., Schwarz, G.E., Brakebill, J.W., and Preston, S.D., 2019, Catchment-level estimates of nitrogen and phosphorus agricultural use from commercial fertilizer sales for the conterminous United States, 2012: U.S. Geological Survey Scientific Investigations Report 2018–5145, 52 p., https://doi.org/10.3133/sir20185145.

Terziotti, S., Hoos, A.B., Harned, D.A., and Garcia, A., 2009, Mapping watershed potential to contribute phosphorus from geologic materials to receiving streams, southeastern United States: U.S. Geological Survey Scientific Investigations Map 3102, 1 pl. [Also available at https://pubs.usgs.gov/sim/3102/.]

U.S. Department of Agriculture, 1986, Urban hydrology for small watersheds-Technical Release 55 (TR55): U.S. Department of Agriculture, Natural Resources Conservation Service, Washington, D.C., accessed November 1, 2019, at https://www.nrcs.usda.gov/Internet/FSE_DOCUMENTS/stelprdb1044171.pdf.

Wieczorek, M.E., Jackson, S.E., and Schwarz, G.E., 2019, Select Attributes for NHDPlus Version 2.1 Reach Catchments and Modified Network Routed Upstream Watersheds for the Conterminous United States (ver 2.0, October 2019): U.S. Geological Survey data release, https://dx.doi.org/10.5066/F7765D7V.

Williams, L.J., and Dixon, J.F., 2015, Digital surfaces and thicknesses of selected hydrogeologic units of the Floridan aquifer system in Florida and parts of Georgia, Alabama, and South Carolina: U.S. Geological Survey Data Series 926, 24 p., accessed September 29, 2019, at https://dx.doi.org/10.3133/ds926.

Table 3.1. Attribution for all the variables tested in the streamflow, total nitrogen, total phosphorus, and suspended-sediment 2012 southeastern United States (SPARROW) models.

[SPARROW, SPAtially Referenced Regression On Watershed attributes; TN, total nitrogen; TP, total phosphorus; PPT–AET, difference of precipitation and actual evapotranspiration; PredQ_SESpar, Mean-annual streamflow in the reach, 2000–14, estimated from conditioned predictions of the streamflow SPARROW model; NHD, National Hydrography Dataset; NID, National Inventory of dams; ft^3/s, cubic foot per second; km^2, square kilometer; kg/yr, kilogram per year; mm/yr, millimeter per year; ppm, parts per million; >, greater than; <, less than; log, natural logarithm]

Description of variable	Source of dataset: dataset name
Mean streamflow (no detrending) from period of record 2000–14 at streamgage, ft^3/s	Saad and others, 2019: flow_est.txt
Mean-annual (for the decade centered on 2012) TN load at monitoring sites, kg/yr	Saad and others, 2019: load_est_tn.txt
Mean-annual (for the decade centered on 2012) TP load at monitoring sites, kg/yr	Saad and others, 2019: load_est_tp.txt
Mean-annual (for the decade centered on 2012) sediment load at monitoring sites, megagrams/yr; load is for suspended sediment at sites where available, otherwise is for total suspended solids	Saad and others, 2019: load_est_tss.txt and load_est_ssc.txt
Transfer of water from outside model domain (one case, from Tennessee River to a tributary of the Tombigbee River), ft^3/s	Wieczorek and others, 2019: e2nhdplusv2_us
PPT–AET from water–balance model, ft^3/s, mean of 2000–14	Wieczorek and others, 2019: WBM_CAT_CONUS.txt
Municipal/domestic wastewater discharge to streams, ft^3/s, 2012	Skinner and Maupin, 2019: SPARROW_PtSrcLoad_summary_SE_11082017.xlsx; then geoprocessed to assign COMID based on most accurate/current location information to produce the file SE_NPDESLoad_QALoc_IntsctCatch_20171211.dbf (during data1 building records for municipal/domestic wastewater facilities only were selected, and sum_ave was summed)
Spring (1st and 2nd magnitude) discharge to streams, ft^3/s	Roland and Hoos, 2019: springq_sumbycomid_20171003
PPT–AET from water–balance model, cfs, detrended to 2012	Wieczorek and others, 2019: WBM_DT_2012_CAT_CONUS.txt
Municipal wastewater applied to land (irrigation, infiltration basin), ft^3/s, 2013	Roland and Hoos, 2019: landphase_sumbycomid_20150803
Area of land in irrigated agriculture, km^2, 2012	Wieczorek and others, 2019: MIRAD_2012_CONUS.txt
Log of percent clay	Wieczorek and others, 2019: STATSGO_LAYER_CAT_CONUS.txt
Log of average travel distance across catchment to stream, km	Wieczorek and others, 2019: DIST_TO_ST.txt
Log of annual mean Enhanced Vegetation Index (EVI), 2012	Wieczorek and others, 2019: EVI_OND_2011_CONUS.txt, etc.
Log of impervious surface area, 2011	Wieczorek and others, 2019: IMPV11_CONUS.txt
Log of percent agricultural land, 2011	Wieczorek and others, 2019: NLCD11_CAT_CONUS.txt
Log of percent urban land, 2011	Wieczorek and others, 2019: NLCD11_CAT_CONUS.txt
Log of wetland evaporation deficit (percent of catchment in wetland area conditioned by the difference term potential evapotranspiration minus actual evapotranspiration), mm/yr	Wieczorek and others, 2019: NLCD11_CAT_CONUS.txt, WBM_CAT_CONUS.txt
Curve number, calculated by using empirical formula for hydrologic soil group B	Wieczorek and others, 2019: NLCD11_CAT_CONUS.txt, and empirical formula from U.S. Department of Agriculture Natural Resource Conservation Service, 1986, table 2-2a
Log of percent of catchment in each hydrologic soil group	Wieczorek and others, 2019: STATSGO_HYDGRP_CAT_CONUS.txt
Log of percent irrigated agriculture, 2012	Wieczorek and others, 2019: MIRAD_2012_CONUS.txt
Log of percent tile drains, 1992	Wieczorek and others, 2019: TILES92_CONUS.txt

Table 3.1. Attribution for all the variables tested in the streamflow, total nitrogen, total phosphorus, and suspended-sediment 2012 southeastern United States (SPARROW) models.—Continued

[SPARROW, SPAtially Referenced Regression On Watershed attributes; TN, total nitrogen; TP, total phosphorus; PPT–AET, difference of precipitation and actual evapotranspiration; PredQ_SESpar, Mean-annual streamflow in the reach, 2000–14, estimated from conditioned predictions of the streamflow SPARROW model; NHD, National Hydrography Dataset; NID, National Inventory of dams; ft^3/s, cubic foot per second; km^2, square kilometer; kg/yr, kilogram per year; mm/yr, millimeter per year; ppm, parts per million; >, greater than; <, less than; log, natural logarithm]

Description of variable	Source of dataset: dataset name
Log of air temperature from water–balance model, degrees Celsius, mean of 2000–14	Wieczorek and others, 2019: WBM_CAT_CONUS
Log of soil permeability, inches per hour	Wieczorek and others, 2019: STATSGO_LAYER_CAT_CONUS.txt
Lake/reservoir evaporation, expressed as –ln[1–(product of reciprocal areal hydraulic load and potential evapotranspiration)], unitless, mean of 2000–14	Schwarz and others, 2019: e2nhdplusv2_us; and Wieczorek and others, 2019: NID.txt and WBM_CAT_CONUS.txt
Consumptive use at power plants, 2010, expressed as –ln(1–fraction of unremoved streamflow)	Wieczorek and others, 2019: POWERPLANTS.dbf (some comid assignments were shifted downstsream from minor tribs to the mainstem that provides the flow)
Groundwater withdrawal (county level) from unconfined aquifer, 2010, expressed as, expressed as –ln(1–fraction of unremoved streamflow)	Wieczorek and others, 2019: WGW2010_CV.txt
Surface–water withdrawal for municipal water supply based on population served, 2013, expressed as –ln(1–fraction of unremoved streamflow)	Wieczorek and others, 2019: pop_serve_with.csv (some comid assignments were shifted downstsream from minor tribs to the mainstem that provides the flow)
Lake/reservoir and wetland evaporation (surface area of open waterbodies and wetlands conditioned by potential evapotranspiration), cubic meters per year, mean of 2000–14	Wieczorek and others, 2019: NLCD11_CAT_CONUS.txt, WBM_CAT_CONUS.txt
Atmospheric deposition of TN, kg/yr, mean of 2010–12	Wieczorek and others, 2019: CMAQ10_CONUS.txt, CMAQ11_CONUS.txt, CMAQ12_CONUS.txt
Fertilizer TN applied to agricultural land, kg/yr (national weighted), kg/yr, 2012	Stewart and others, 2019: 2012_catchment_fert_use_estimates_N_P.txt
Urban land cover, km^2, 2011	Wieczorek and others, 2019: NLCD11_CAT_CONUS.txt
Manure TN from livestock production, kg/yr, 2012	Wieczorek and others, 2019: TN2012.txt
Fertilizer TN applied to agricultural land (state weighted), kg/yr, 2012	Stewart and others, 2019: 2012_catchment_fert_use_estimates_N_P.txt
Municipal/domestic wastewater TN discharge to streams, kg/yr, 2012	Skinner and Maupin, 2019: SPARROW_PtSrcLoad_summary_SE_11082017.xlsx; then geoprocessed to assign COMID based on most accurate/current location information to produce the file SE_NPDESLoad_QALoc_IntsctCatch_20171211.dbf (during data1 building records for municipal/domestic wastewater facilities only were selected, and kg_00600 was summed)
Spring (1st and 2nd magnitude) discharge to streams, ft^3/s	Roland and Hoos, 2019: springq_sumbycomid_20171003
Fertilizer TN applied to agricultural land (Kalman conditioned), kg/yr, 2012	Stewart and others, 2019: 2012_catchment_fert_use_estimates_N_P.txt
Cropland area of N–fixing cultivated crops, km^2, 2012	Wieczorek and others, 2019: CDL12_CAT_CONUS.txt
Density of N–fixing tree species, 2010	Roland and Hoos, 2019: Basal_Area_PU03.dbf
Spring (1st and 2nd magnitude) TN discharge to streams, kg/yr	Roland and Hoos, 2019: springq_sumbycomid_20171003
Spring (1st magnitude) TN discharge to streams, kg/yr	Roland and Hoos, 2019: springq_sumbycomid_20171003
Population on septic system, 2010 (estimated by using 1990 percent of population served by septic system)	Wieczorek and others, 2019: Septic2010.dbf, and back calculate population served from N load
Fertilizer TN applied to agricultural land (unconditioned), kg/yr, 2012	Stewart and others, 2019: 2012_catchment_fert_use_estimates_N_P.txt

Table 3.1. Attribution for all the variables tested in the streamflow, total nitrogen, total phosphorus, and suspended sediment 2012 southeastern United States (SPARROW) models.—Continued

[SPARROW, SPAtially Referenced Regression on Watershed attributes; TN, total nitrogen; TP, total phosphorus; PPT–AET, difference of precipitation and actual evapotranspiration; PredQ_SESpar, Mean-annual streamflow in the reach, 2000–14, estimated from conditioned predictions of the streamflow SPARROW model; NHD, National Hydrography Dataset; NID, National Inventory of dams; ft^3/s, feet cubed per second; km^2, square kilometer; kg/yr, kilogram per year; mm/yr, millimeters per year; ppm, parts per million; >, greater than; <, less than; log, natural logarithm]

Description of variable	Source of dataset: dataset name
Industrial wastewater TN discharged to streams, kg/yr, 2012	Skinner and Maupin, 2019: SPARROW_PtSrcLoad_summary_SE_11082017.xlsx; then geoprocessed to assign COMID based on most accurate/current location information to produce the file SE_NPDESLoad_QALoc_IntsctCatch_20171211.dbf (during data1 building records for facilities other than municipal/domestic were selected, and kg_00600 was summed)
Log of percent of catchment in cover crops, 2012	Wieczorek and others, 2019: CPRAC16_CONUS.txt
Log of summer mean Enhanced Vegetation Index (EVI), 2012	Wieczorek and others, 2019: EVI_JAS_2012_CONUS.txt
Log of soil organic–matter content	Wieczorek and others, 2019: STATSGO_LAYER_CAT_CONUS.txt
Log of PPT–AET, mm/yr, detrended to base year 2012; in contrast to PPT–AET used as source term in the streamflow model, this term is normalized by the area of the catchment	Wieczorek and others, 2019: WBM_CAT_CONUS.txt
Log of soil clay content	Wieczorek and others, 2019: STATSGO_LAYER_CAT_CONUS.txt
Log of annual mean Enhanced Vegetation Index (EVI), 2012	Wieczorek and others, 2019: EVI_OND_2011_CONUS.txt, etc.
Log of soil permeability, inches per hour	Wieczorek and others, 2019: STATSGO_LAYER_CAT_CONUS.txt
Log of depth to bedrock, inches	Wieczorek and others, 2019: STATSGO_LAYER_CAT_CONUS.txt
Log of incremental flow from catchment to stream (streamflow SPARROW model), mean of 2000–14	Roland and Hoos, 2019: SPARROW streamflow model predict file (conditioned predictions)
Reach time of travel per meter of stream depth, where depth is estimated as a continuous function of stream discharge PredQ_SESpar according to the simple power law formula: depth (meters) = 0.06356 * PredQ_SESpar (ft^3/s) ^ 0.3966	Wieczorek and others, 2019: e2nhdplusv2_us
Reach time of travel (days) per meter of stream depth, where depth is estimated as a continuous function of stream discharge PredQ_SESpar and other channel characteristics (using the six–parameter regional regression equation)	Wieczorek and others, 2019: several data sets, except PredQ_SESPAR, which is from the SPARROW streamflow model predict file; formula for computing stream depth is from Roland and Hoos (2019)
Reciprocal areal hydraulic load for waterbodies in karst landscape (mostly in Florida), calculated by using surface area from NHD or NID and stream discharge PredQ_SESpar	Schwarz, 2019: e2nhdplusv2_wbvars; Wieczorek and others, 2019: NID_2013_CONUS.txt; areal boundary of karst landscape defined as where Floridan aquifer system is unconfined or thinly confined in Florida, Georgia, and Alabama, as delineated by Williams and Dixon, 2013, figure 21
Reciprocal areal hydraulic load for waterbodies not in karst landscape, calculated by using surface area from NHD or NID and stream discharge PredQ_SESpar	same as for rhload_withNID_ypm_KL
Time of travel in small streams (stream discharge <30 ft^3/s, or <0.849 m^3/s)	Schwarz, 2019: e2nhdplusv2_us
Time of travel in intermediate streams (stream discharge 31–100 ft^3/s, or 0.849–2.83 m^3/s)	Schwarz, 2019: e2nhdplusv2_us
Time of travel in large streams (stream discharge > 100 ft^3/s, or > 2.83 m^3/s)	Schwarz, 2019: e2nhdplusv2_us
Incremental catchment area (P source term in combination with delivery term representing P content of upland soil and parent rock)	Schwarz, 2019: e2nhdplusv2_us

Table 3.1. Attribution for all the variables tested in the streamflow, total nitrogen, total phosphorus, and suspended sediment 2012 southeastern United States (SPARROW) models.—Continued

[SPARROW, SPAtially Referenced Regression on Watershed attributes; TN, total nitrogen; TP, total phosphorus; PPT–AET, difference of precipitation and actual evapotranspiration; PredQ_SESpar, Mean-annual streamflow in the reach, 2000–14, estimated from conditioned predictions of the streamflow SPARROW model; NHD, National Hydrography Dataset; NID, National Inventory of dams; ft^3/s, feet cubed per second; km^2, square kilometer; kg/yr, kilogram per year; mm/yr, millimeters per year; ppm, parts per million; >, greater than; <, less than; log, natural logarithm]

Description of variable	Source of dataset: dataset name
Municipal/domestic wastewater TP discharge to streams, kg/yr, 2012	Skinner and Maupin, 2019: SPARROW_PtSrcLoad_summary_SE_11082017.xlsx; then geoprocessed to assign COMID based on most accurate/current location information to produce the file SE_NPDESLoad_QALoc_IntsctCatch_20171211.dbf (during data1 building records for municipal/domestic facilities were selected, and kg_00665 was summed)
Industrial wastewater TP discharge to streams, kg/yr, 2012	Similar to previous, except during data1 building records for facilities other than municipal/domestic and other than phosphate mining were selected, and kg_00665 was summed
Mined land permitted TP discharge to streams, kg/yr, 2012	Similar to previous, except during data1 building records for phosphate mining facilities were selected, and kg_00665 was summed
Urban land cover, km^2, 2011	Wieczorek and others, 2019: NLCD11_CAT_CONUS.txt
Manure TP from livestock production, kg/yr, 2012	Wieczorek and others, 2019: TP2012.txt
Fertilizer TP applied to agricultural land, kg/yr, 2012, national weighted	Stewart and others, 2019: 2012_catchment_fert_use_estimates_N_P.txt
Mined area P content, ppm*km^2	Terziotti and others, 2009 : mrb2_nhd_phos_actmines_110209.csv and mrb2_nhd_phos_inactmines_110209.csv, allocated to NHDPlusv1 and crosswalked to NHDPlusv2
Log of P content of soil A horizon, interpolated by using geologic mapping units	Wieczorek and others, 2019: SOILS_GMU_A_P_CONUS.txt
Log of P content of soil C horizon, interpolated by using geologic mapping units	Wieczorek and others, 2019: SOILS_GMU_C_P_CONUS.txt
Fertilizer TP applied to agricultural land (Kalman conditioned), kg/yr, 2012	Stewart and others, 2019: 2012_catchment_fert_use_estimates_N_P.txt
Length of main channel in catchment, km	Schwarz, 2019: e2nhdplusv2_us
Log of P content of bed sediment in small pristine streams (regional extent), interpolated by using geologic mapping units	Terziotti and others, 2009: mrb2_nhd_phos_backg_110209.csv, allocated to NHDPlusv1 and crosswalked to NHDPlusv2
Fertilizer TP applied to agricultural land (state weighted), kg/yr, 2012	Stewart and others, 2019: 2012_catchment_fert_use_estimates_N_P.txt
Fertilizer TP applied to agricultural land, (unconditioned), kg/yr, 2012	Stewart and others, 2019: 2012_catchment_fert_use_estimates_N_P.txt
Log of percent of catchment in no till or conservation tillage, 2012	Wieczorek and others, 2019: CPRAC7_CONUS.txt and CPRAC13_CONUS.txt
Log of P content of bed sediment in small pristine streams (national extent), interpolated by using geologic mapping units	Wieczorek and others, 2019: NATL_P_CONUS.txt
Log of Kfactor (erodibility index) in upper soil layer	Wieczorek and others, 2019: STATSGO_LAYER_CAT_CONUS.txt
Log of depth to water table, feet	Wieczorek and others, 2019: STATSGO_LAYER_CAT_CONUS.txt
Upland: Alluvium and residuum in very fine–grained sedimentary rock intersected with Urban	Wieczorek and others, 2019: lusoller.txt, except altered for the class residuum in very fine–grained sedimentary class using outcrop of chalky formations as delineated by Schruben and others, 2005
Upland: Alluvium and residuum in very fine–grained sedimentary rock intersected with Forest	similar to above description for Alluvium and residuum in very fine–grained sedimentary rock intersected with Urban

Table 3.1. Attribution for all the variables tested in the streamflow, total nitrogen, total phosphorus, and suspended sediment 2012 southeastern United States (SPARROW) models.—Continued

[SPARROW, SPAtially Referenced Regression on Watershed attributes; TN, total nitrogen; TP, total phosphorus; PPT–AET, difference of precipitation and actual evapotranspiration; PredQ_SESpar, Mean-annual streamflow in the reach, 2000–14, estimated from conditioned predictions of the streamflow SPARROW model; NHD, National Hydrography Dataset; NID, National Inventory of dams; ft^3/s, feet cubed per second; km^2, square kilometer; kg/yr, kilogram per year; mm/yr, millimeters per year; ppm, parts per million; >, greater than; <, less than; log, natural logarithm]

Description of variable	Source of dataset: dataset name
Upland: Alluvium and residuum in very fine–grained sedimentary rock intersected with Transitional (Shrub, Scrub, Herbaceous, and Barren)	similar to above description for Alluvium and residuum in very fine–grained sedimentary rock intersected with Urban
Upland: Alluvium and residuum in very fine–grained sedimentary rock intersected with Agricultural (Cropland and Pasture)	similar to above description for Alluvium and residuum in very fine–grained sedimentary rock intersected with Urban
Upland: Residuum in igneous and metamorphic rock intersected with Urban	Wieczorek and others, 2019: lusoller.txt
Upland: Residuum in igneous and metamorphic rock intersected with Forest	Wieczorek and others, 2019: lusoller.txt
Upland: Residuum in igneous and metamorphic rock intersected with Transitional (Shrub, Scrub, Herbaceous, and Barren)	Wieczorek and others, 2019: lusoller.txt
Upland: Residuum in igneous and metamorphic rock intersected with Agricultural (Cropland and Pasture)	Wieczorek and others, 2019: lusoller.txt
Upland: Residuum in sedimentary rock (discontinuous) intersected with Urban	Wieczorek and others, 2019: lusoller.txt
Upland: Residuum in sedimentary rock (discontinuous) intersected with Forest	Wieczorek and others, 2019: lusoller.txt
Upland: Residuum in sedimentary rock (discontinuous) intersected with Transitional (Shrub, Scrub, Herbaceous, and Barren)	Wieczorek and others, 2019: lusoller.txt
Upland: Residuum in sedimentary rock (discontinuous) intersected with Agricultural (Cropland and Pasture)	Wieczorek and others, 2019: lusoller.txt
Upland: All other surficial–geology categories (Fine– and medium–grained sediments, also Residuum in alluvium and in carbonate and fine–grained sedimentary rock) intersected with Urban	Wieczorek and others, 2019: lusoller.txt
Upland: All other surficial–geology categories (Fine– and medium–grained sediments, also Residuum in alluvium and in carbonate and fine–grained sedimentary rock) intersected with Forest	Wieczorek and others, 2019: lusoller.txt
Upland: All other surficial–geology categories (Fine– and medium–grained sediments, also Residual materials in alluvium and in carbonate and fine–grained sedimentary rock) intersected with Transitional (Shrub, Scrub, Herbaceous, and Barren)	Wieczorek and others, 2019: lusoller.txt
Upland: All other surficial–geology categories (Fine– and medium–grained sediments, also Residuum in alluvium and in carbonate and fine–grained sedimentary rock) intersected with Agricultural (Cropland and Pasture)	Wieczorek and others, 2019: lusoller.txt
Upland: Residuum in igneous, metamorphic, and very fine–grained sedimentary rock, and alluvium, intersected with Urban	Wieczorek and others, 2019: lusoller.txt
Upland: Residuum in igneous, metamorphic, sedimentary (discontinuous), and very fine–grained sedimentary rock, and alluvium, intersected with Transitional (Shrub, Scrub, Herbaceous, and Barren)	Wieczorek and others, 2019: lusoller.txt
Upland: All surficial–geology categories except Residuum in sedimentary rock (discontinuous) intersected with Agricultural (Cropland and Pasture)	Wieczorek and others, 2019: lusoller.txt

Table 3.1. Attribution for all the variables tested in the streamflow, total nitrogen, total phosphorus, and suspended sediment 2012 southeastern United States (SPARROW) models.—Continued

[SPARROW, SPAtially Referenced Regression on Watershed attributes; TN, total nitrogen; TP, total phosphorus; PPT–AET, difference of precipitation and actual evapotranspiration; PredQ_SESpar, Mean-annual streamflow in the reach, 2000–14, estimated from conditioned predictions of the streamflow SPARROW model; NHD, National Hydrography Dataset; NID, National Inventory of dams; ft^3/s, feet cubed per second; km^2, square kilometer; kg/yr, kilogram per year; mm/yr, millimeters per year; ppm, parts per million; >, greater than; <, less than; log, natural logarithm]

Description of variable	Source of dataset: dataset name
Upland: All surficial–geology categories intersected with Forest (in other words, all Forested land)	Wieczorek and others, 2019: lusoller.txt
Channel: Gain in stream power compared to adjacent upstream reach(es), fraction	Schwarz, 2019: e2nhdplusv2_us
Upland: Number of road crossings, 2018	Wieczorek and others, 2019: RDX_CONUS.txt
Upland: Change in number of housing units from 2000 to 2010	Wieczorek and others, 2019: HDENS10_CONUS.txt and HDENS00_CONUS.txt
Upland: Area in catchment that changed to urban from any other land use during 2002–12	Wieczorek and others, 2019: NWALT02_CAT_CONUS and NWALT12_CAT_CONUS (then calculate difference between 2002 and 2012 values of urban class)
Upland: Area in catchment that changed to urban or semideveloped from any other land use during 2002–12	Wieczorek and others, 2019: NWALT02_CAT_CONUS and NWALT12_CAT_CONUS (then calculate difference between 2002 and 2012 values of sum of urban and suburban class)
Upland: Area in catchment that changed from one land use to another during 2002–12	Wieczorek and others, 2019: NWALT02_CAT_CONUS and NWALT12_CAT_CONUS (then calculate difference between 2002 and 2012 values of all classes and sum)
Upland: Area in catchment that changed from a vegetated land use class to any other class during 2002–12	Wieczorek and others, 2019: NWALT02_CAT_CONUS and NWALT12_CAT_CONUS (then calculate difference between 2002 and 2012 values for vegetative classes: i.e. 2 through 11)
Channel: Reciprocal of reach–average sinuosity	Wieczorek and others, 2019: sinuousity_CONUS.txt
Channel: Stream power, nonzero only for headwater ($Q < 10$ ft^3/s) streams, scaled to reach length	Schwarz, 2019: e2nhdplusv2_us
Log of Kfactor (erodibility index)	Wieczorek and others, 2019: STATSGO_LAYER_CAT_CONUS.txt
Log of basin slope (mean of land surface–elevation slope in catchment)	Wieczorek and others, 2019: BASIN_CHAR_CAT_CONUS.txt
Log of percent of 100–meter width buffer in canopy land cover, 2011	Wieczorek and others, 2019: CNPY11_BUFF100_CONUS.txt
Change in housing density from 2000 to 2010	Wieczorek and others, 2019: HDENS10_CONUS.txt and HDENS00_CONUS.txt
Log of percent of catchment in conservation easement, 2012	Wieczorek and others, 2019: CPRAC19_CONUS.txt
Log of stream mean velocity (foot per second)	Schwarz, 2019: e2nhdplusv2_us
Log of precipitation intensity, 2000–14	Wieczorek and others, 2019: WBM_CAT_CONUS.txt, WDANN_CONUS.txt
Log of channel slope	Schwarz, 2019: e2nhdplusv2_us
Width (area in catchment divided by channel length) of riparian wetland, scaled to time of travel in reach	Riparian wetland area delineated U.S. Geological Survey, 2010; further described in Hoos and others, 2013
Loss in stream power compared to adjacent upstream reach(es), fraction	Calculate from variables from Schwarz, 2019: e2nhdplusv2_us (streamflow at upstream and downstream node and channel slope)
Binary variable distinguishing loads estimated from SSC concentration data from loads estimated from TSS concentration data	Saad and others, 2019: load_est_tss.txt and load_est_ssc.txt
Mean-annual streamflow in the reach, 2000–14, estimated from conditioned predictions of the streamflow SPARROW model	Roland and Hoos, 2019: SPARROW streamflow model predict file (conditioned predictions)

For additional information, contact:

NAWQA Science Team
U.S. Geological Survey
12201 Sunrise Valley Drive
Reston, VA 20192
Or visit our website at:
https://ms.water.usgs.gov/
Email: gs-w_opp_nawqa_science_team@usgs.gov

Publishing support provided by the
West Trenton Publishing Service Center

ISSN 2328-0328 (online)
https://doi.org/10.3133/sir20195135